Tectonic Geography of the lower Roper Group, McArthur Basin, Northern Australia using detrital geochronology and shale geochemistry

Thesis submitted in accordance with the requirements of the University of Adelaide for an Honours Degree in Geology/Geophysics

Eilidh Cassidy

November 2018

THE UNIVERSITY of ADELAIDE

TECTONIC GEOGRAPHY OF THE LOWER ROPER GROUP, MCARTHUR BASIN, NORTHERN AUSTRALIA USING DETRITAL GEOCHRONOLOGY AND SHALE GEOCHEMISTRY

TECTONIC GEOGRAPHY OF THE LOWER ROPER GROUP

ABSTRACT

The informally termed greater McArthur basin, covers a wide extent of Northern Australia. The basin spans the Mesoproterozoic and preserves within its sedimentology, evidence for the tumultuous events that surround the basin during its formation. LA-ICP-MS detrital zircon U–Pb, Lu–Hf and REE data presented here provide new constrains on the lower Roper Group and reveal temporal, provenance variations that illustrate the evolution of the basin. Here we attempt to elucidate the rifting of Laurentia from the Australian cratons and identify a provenance change as a consequence.

The maximum depositional age of the Munyi Member of the upper Roper Group has been constrained to 1530 ± 45 Ma. Whereas grains of the Hodgson Sandstone, Jalboi Formation and Arnold Sandstone of the lower Roper Group suggest a maximum depositional age of 1591±90 Ma, 1580±66 Ma and 1633±89 Ma, respectively. The Crawford Sandstone preserved an age of 1766 ± 82 Ma. As well as using U–Pb in zircon, we also look at Rb–Sr isotopes within glauconite to further constrain the deposition history of the Crawford sandstone. These data yielded an age of 1284 ± 51 Ma, too young to reflect a depositional age and we therefore suggest these instead reflect a resetting event; the intrusion of the Derim Derim dolerite (ca. 1313 Ma).

Age variations up-stratigraphy propose a subtle change from older, Paleoproterozoic sources to additional input from younger sources, as we transition from the lower Roper into the Upper Roper. Older formations record age peaks that are consistent with rocks of the Tanami Region and Aileron Province. Overlying Crawford and Jalboi Formations show derivation from a ca. 1700 Ma source, with a minor 2500 Ma peak, both which are consistent with southern sources, specifically Aileron and Arunta Region. The Arnold and Hodgson both show detritus with dominant ca. 1780 Ma age peaks, consistent with southern sources.

We suggest that provenance variation initially records the exhumation and exposure of the Tanami Region as a result of intracratonic rifting and widespread 1.5–1.4 Ga magmatism. The increase in 1860–1650 Ma detritus suggests uplift of the Arunta region.

KEYWORDS

Geochronology, Shale geochemistry, McArthur Basin, lower Roper Group

TABLE OF CONTENTS

LIST OF FIGURES

LIST OF TABLES

INTRODUCTION

The Proterozoic Eon forms a vital time in Earth's history; a period that includes the amalgamation and breakup of supercontinents, (Merdith *et al*., 2017) in conjunction with dramatic, redox shifts resulting in changes in atmospheric and ocean chemistry (Planavasky *et al*., 2018). Cratonic basins, have long been a subject of interest, they record a prolonged history whereby their formation, distribution and sedimentation are linked to the framework of the plates. Uncertainty surrounds how these cratonic basins remain depocentres over extended periods of time, which span the breakup, dispersal and amalgamation of supercontinents (Yang *et al*. 2018).

One of the more studied and accessible of these cratonic basins is the McArthur Baisn, which records nearly a billion years of Earth history (ca. 1.82 Ma to the Tonian). This time period includes extensive periods of uplift, with minimal deposition and therefore understanding the evolution of the basin using detrital chronology can link provenance changes in the McArthur Basin to changes in major tectonic boundaries during the Mesoproterozoic (Sandiford *et al*. 2001; Allen *et al*., 2015; Saha, 2017; Yang *et al*., 2018). The variations in provenance recorded in the successions of McArthur Basin can provide insight in to the evolving tectonic forces and therefore the palaeogeography at the time.

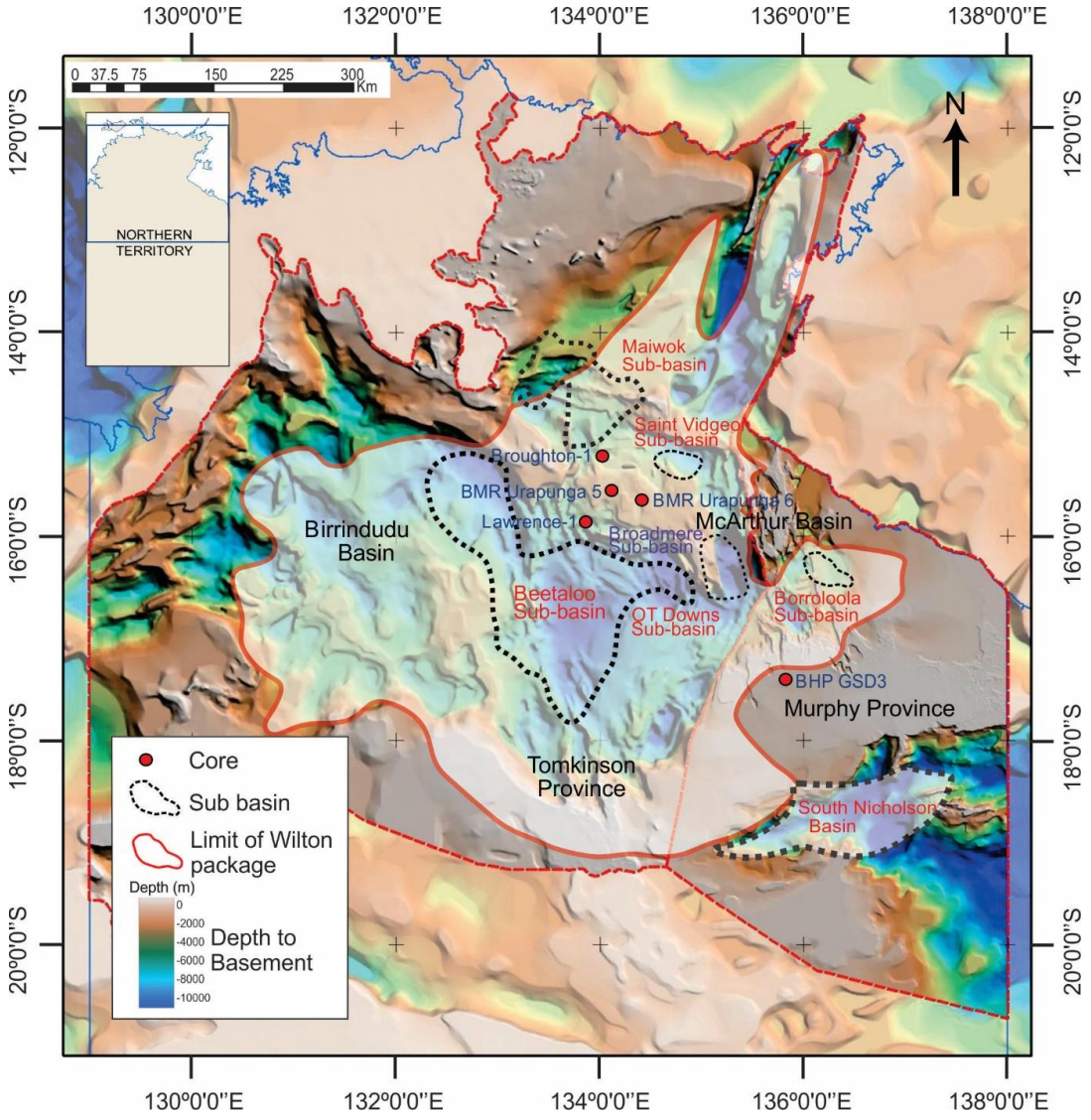

Figure 1. Location map of the Wilton Package showing the top-to-basement (SEEBASE™ basement surface image after Frogtech Geoscience 2018) and locations of cores used in this study. Modified after Yang et al. 2018.

The stratigraphic successions of the McArthur Basin have been subdivided into five, basin-wide, non-generic depositional packages, which have been further divided into associated groups (Munson, 2017). The focus of this study is the shallow-water and principally marine, Collara Subgroup, which forms the lower Roper Group within the Mesoproterozoic Wilton Package (Fig 1) (Munson 2017; Yang *et al*., 2018). The lower Roper Group, is proximal to the oldest, commercial, hydrocarbon-bearing sediments known and is therefore of

considerable economic interest (Close *et al*., 2017; Yang *et al*., 2018). The Roper Group is a silliclastic succession, with alternating cross bedded sands and mudrock layers (Munson 2016) and forms the basis for this study.

Detrital zircons contain crucial information about the source of the Roper Group sedimentary rocks. This due to their resilience and ability to preserve their radiometric clocks. These minerals are vital in understanding the source and age of the Roper sediments that have experienced extensive periods of uplift and deformation during deposition. The sediments that feed into the McArthur Basin to form the lower Roper group can be interrogated using multiple isotopic proxies, namely: U–Pb and Lu–Hf isotopes in zircon, and Rb–Sr isotopes on shale units and glauconite bearing sands to constrain depositional age.

Here we present detrital U–Pb (LA-ICP-MS) age data on samples throughout the lower Roper Group succession. This will allow for a maximum depositional age to be determined for associated sand units, as well as providing an insight into the potential source for these zircons. However, U–Pb dating techniques are not definitive of sources on their own (Lloyd *et al*., 2016) and therefore other isotopic and geochemical techniques can be used as fingerprints. Hafnium isotopes have been analysed along with REE's of the same detrital zircons to better constrain the sediment source regions. Rb–Sr isotopes on a subset of glauconite bearing samples and shales, as well as Sm–Nd isotopes on interbedded shale units throughout the succession have also been analysed. The data constrained will be used to isolate the paleogeography of the Lower Roper group as well as correlating the sediments across all basins within the Greater McArthur Basin.

GEOLOGICAL SETTING/BACKGROUND

The greater McArthur Basin (Close 2014) is an informally termed, Proterozoic basin consisting of five, coherent basin phases which have been subdivided into five stratigraphic sedimentary packages. These packages, formerly known as supersequences, include the Redbank, Goyder, Glyde, Favenc and Wilton Packages. They unconformably lie on top of the North Australian Craton (NAC), which consists of Archean to Palaeproterozoic crystalline basement rocks that are highly metamorphosed and deformed (Munson 2016).

The Wilton package (Rawlings, 1999) comprises several Mesoproterozoic successions that form the upper part of the greater McArthur Basin. The subgroup extends across a vast area in the northeastern Northern Territory (Munson, 2016) with a preserved outcrop extent similar to that of the whole Roper Group at around 145 000 km^2 (Abbott *et al.* 2001; Munson, 2016). The extensive Wilton package contains four sedimentary groups, these include: the Roper Group (McArthur Basin), Tijunna Group (Birrindudu Basin), Renner Group (Tomkinson Province) and the South Nicholson Group (South Nicholson Basin). Recent findings (Munson 2016) have suggested that the four sedimentary groups can be correlated across the greater McArthur Basin, however this study will focus on the Roper Group within the McArthur Basin.

The Roper Group is a siliciclastic succession that is lithologically and laterally continuous (Munson, 2017). The group can be subdivided into the upper Roper Group and the lower Roper Group, which are dominated by mudrock and sandstones, respectively (Fig 2) (Munson, 2017).

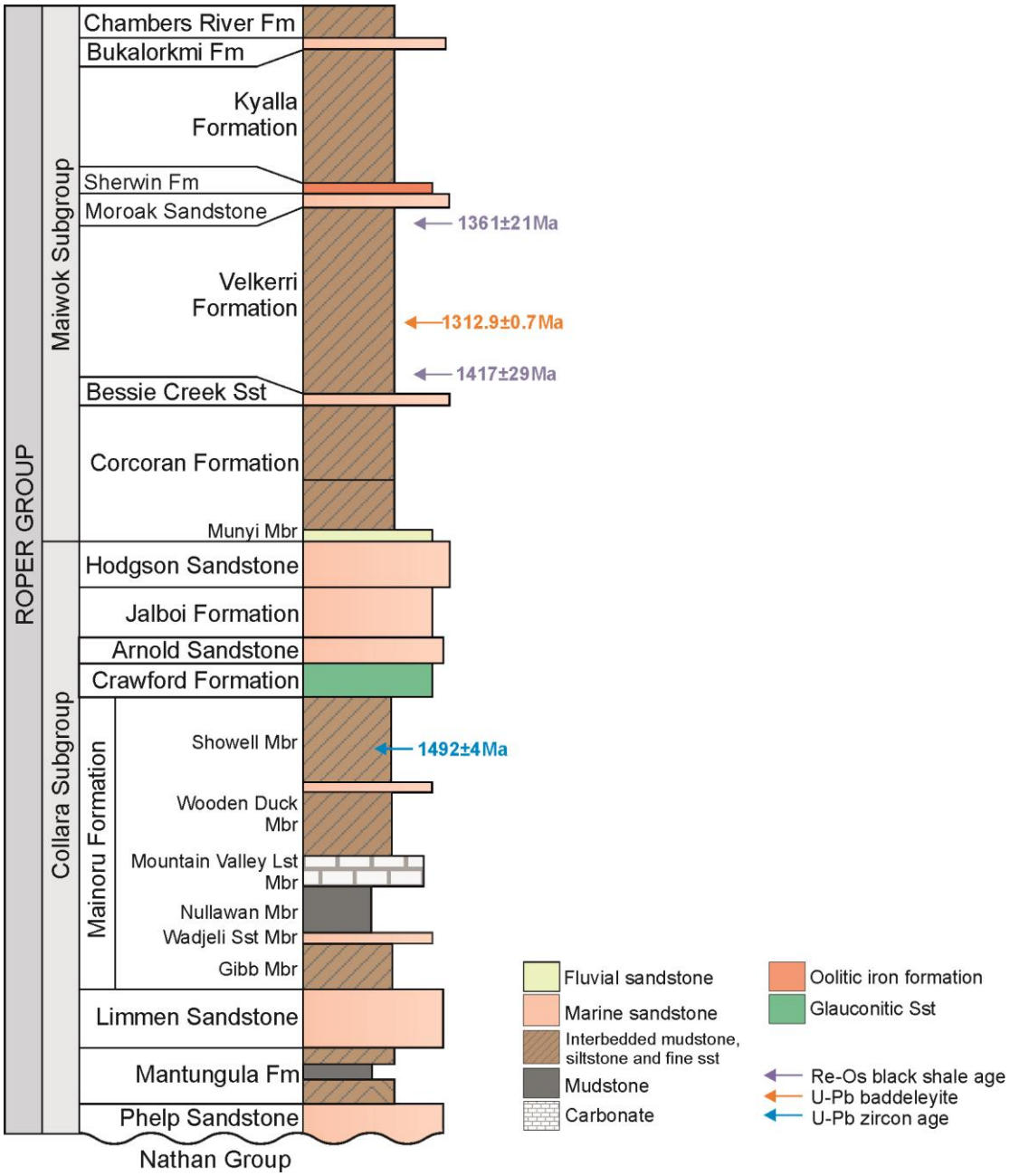

Figure 2. Composite stratigraphic log of the Roper Group modified after Cox et al. (2016) and Yang et al. (2018). SHRIMP U–Pb zircon ages from Abbott et al. (2001) and Jackson et al. (1999). Re-Os ages for the Velkerri Formation from Kendall et al. (2009). Derim Derim Dolerite U–Pb baddeleyite age reported in Cox et al. (2018).

Depositional environment for the Roper Group is often identified as an enclosed sea basin, similar to the modern day Black Sea (Abbott & Sweet 2000; Mukherjee & Large 2016; Cox *et al*. 2016; Munson 2016, Revie 2017; Munson & Revie 2018; Yang et al. 2018).

The transition from dominantly sands in the lower Roper to muds in the upper Roper have been interpreted to represent a change in environment, from a shallow marine shelf into a deeper, shale-rich shelf environment during deposition of the upper Roper Group (Jackson *et al*. 1988; Abbott & Sweet 2000; Abbott *et al*. 2001; Ahmad & Munson 2013, Yang *et al*. 2018). The lower Roper Sub-group is unconformable, with slight angular difference between the beds (Munson 2016). Depending on the location, the base of the subgroup is either the Phelp Sandstone, Mantungula Formation, or Limmen Sandstone. The remaining stratigraphy has been summarised in Fig 2.

Within the Urapunga region, the Collara subgroup is up to 1000m thick. The age of the Roper Group, particularly within the Urapunga region is constrained by the intrusion of the Derim-Derim dolerite, with a U–Pb baddeleyite age of 1314 ± 1 Ma (MSWD = 0.49) (Cox *et al*. 2018). The dolerite sill intrudes the Jalboi Formation in Urapunga 5, which is where majority of the sandstone and shale samples have been sourced from.

The first attempt to constrain the age of the Roper Group was undertaken by McDougall *et al*. (1965) who dated glauconites from the Crawford Formation using Rb–Sr and K–Ar dating techniques. The outcome was seven Rb–Sr ages from 1370–1243 Ma and six K–Ar ages, which provided a significantly younger age range of 1270–1095 Ma.

A regional unconformity marks the base of the Roper Group and its boundary with the underlying Nathan Group. This has been interpreted to be the product of the ca. 1580–1500 Mt Isan Orogeny (Jackson, 1999; Ahmad *et al*., 2013).

METHODS

Selection and drill core sampling

Sandstone and shale samples were obtained from five drillcores; Urapunga 5, Urapunga 6, GSD3, Broughton and Lawrence that were stored in the Geoscience Australia Core Library, Canberra, Australia and the NTGS Darwin Core Library, Northern Territory, Australia (Table. 1). The location of these samples, within McArthur Basin, can be seen in Figure 1. Sandstone samples range from 25cm to 1.3m, while shale units were generally 2cm-15cm.

Formation	Sample	Core	Depth (m)	
Munyi	L04	Lawrence	478.9	479.1
	BR04	Broughton	79	79.3
Hodgson	U501	BMR Urapunga 5	46	47
	L02	Lawrence	505.4	505.6
Jalboi	U503	BMR Urapunga 5	143.2	144.5
Arnold	U505	BMR Urapunga 5	286.2	286.8
	U506	BMR Urapunga 5	309.5	310.1
Crawford	U507	BMR Urapunga 5	328.4	328.9
Limmen	GSD3-01	GSD 3	210.5	211
	GSD3-02	GSD 3	150.5	151
	U602	BMR Urapunga 6	327.9	328.6
	U603	BMR Urapunga 6	412.1	412.7

Table 1. List of samples taken for U–Pb and REE analysis. Samples were taken from upper and lower parts of the Formations and from different cores where possible to allow for the identification of spatial and lateral differences in the data. Age peaks in bold are identified as being major.

U–Pb zircon geochronology

Zircon grains were separated from the host sandstones via crushing and milling and then refined using standard magnetic techniques. Mineral separates were handpicked and mounted in epoxy resin, without preference to size, colour or shape. The polished mounts were carbon coated and zircon grains were imaged using cathodoluminescence (CL) on a FEI Quanta 600 SEM Scanning Electron Microscope (SEM) with attached Gatan CL

detector to identify suitable domains for further analysis (Adelaide Microscopy, The University of Adelaide). Zircon U–Pb isotope analysis were conducted on a New Wave 213nm Nd-YAG laser coupled with an Agilent 7500cs Inductively Coupled Plasma Mass Spectrometer (ICP–MS) at Adelaide Microscopy, The University of Adelaide. A 30 μm spot size was used with a typical pit depth of 30–50 μm. laser frequency was 5Hz with an intensity at 70% and ablation period of 30 seconds targeting principally zircon cores.

The GEMOC GJ-1 zircon (TIMS normalising data $^{207}Pb/^{206}Pb$ = 607.7 ± 4.3 Ma, $^{206}Pb/^{238}U$ = 600.7 ± 1.1 Ma and $^{207}Pb/^{235}U$ = 602.0 ± 1.0 Ma; Jackson *et al*., 2004) was used to correct for U–Pb mass bias and laser induced fractionation. The Plešovice zircon internal standard (ID TIMS $^{206}Pb/^{238}U$ age = 337.13 ± 0.37 Ma; Sláma *et al*., 2008) was used to assess accuracy before and during analysis of the unknowns. Plešovice analyses yield a weighted average mean $^{206}Pb/^{238}U$ age of 338.49 ± 0.70 (n=160, MSWD = 1.2) and a $^{207}Pb/^{206}Pb$ age of 341 ± 10 (MSWD = 01.5 and n=160). Data were processed in the software package Iolite version 3.0 (Chew *et al*. 2014). Concordia diagrams and weighted means were calculated using ISOPLOT 4.15 for Excel (Ludwig, 2009). Multidimensional Scaling (MDS) plots and Kernel Density Estimate (KDE) distributions were calculated using R software package (Vermeesch, 2013), for statistical analysis.

Hafnium Isotope determination

Analytical methods for zircon Lu–Hf isotope analysis follow Payne *et al*. (2013). Analyses were undertaken using a New Wave UP-193 ArF excimer laser attached to a Thermo-Scientific Neptune Multi-Collector ICP-MS at the University of Adelaide. The bulk of analyses were carried out using a beam diameter of ~50 μm, with a beam diameter of

35μm used for smaller grains. Typical ablation times were 40–100 s using a 5 Hz repetition rate, a 4 ns pulse rate, and an intensity of ~4–6 J/cm^2. Zircons were ablated in a helium atmosphere, which was then mixed with Ar and N_2 upstream of the ablation cell. Reduction of zircon data were undertaken using a macro-driven Hf isotope data reduction Excel spreadsheet, HfTRAX (Payne *et al*., 2013). The data were normalised to $^{179}Hf/^{177}Hf = 0.7325$, using an exponential correction for mass bias. Yb and Lu isobaric interferences on ^{176}Hf were corrected following the methods of Woodhead *et al*. (2004).

The accuracy of the Yb and Lu corrections has been demonstrated by repeated analysis of standard zircons with a range in $^{176}Yb/^{177}Hf$ and $^{176}Lu/^{177}Hf$ values (Griffin *et al*., 2006). Before and during the analysis of unknowns, standards were analysed to check instrument performance and stability. The primary zircon standard used was Mudtank, which yielded a mean $^{176}Hf/^{177}Hf$ ratio of 0.282507 ± 0.000006. This compares to the published value of 0.282482 ± 0.000013 (2SD) by Sláma *et al*. (2008). Values for $\varepsilon Hf(t)$, and TDMc were calculated using ^{176}Lu decay constant after Scherer *et al*. (2001). TDMc was calculated using the two stage methods of Griffin *et al*. (2002) with an average crustal composition of $^{176}Lu/^{177}Hf = 0.015$.

Zircon REE Analysis

In addition to the collection of U–Pb masses for zircon age constrains, the abundance of 21 elemental masses were measured: ^{31}P, ^{49}Ti , ^{89}Y ,^{90}Zr , ^{139}La, ^{140}Ce, ^{141}Pr, ^{146}Nd, ^{147}Sm, ^{153}Eu, ^{157}Gd, ^{159}Tb, ^{163}Dy, ^{165}Ho, ^{166}Er, ^{169}Tm, ^{172}Yb, ^{175}Lu, ^{178}Hf, ^{202}Hg and ^{232}Th.

Trace element abundances were collected concurrently with U–Pb isotopic ratios. Trace element data collected were standardised to the primary standard, NIST610 with a

secondary standard 91500. REE data was normalised to chondrite values taken from Taylor and McLennan (1985). Data was plotted in excel using spider plots to identify any changes in in REE trends in each of the Formations.

Insitu Rb–Sr dating of shales and Glauconites

A total of six shale samples throughout the lower Roper group and a glauconitic sandstone sample from the Crawford Formation were sampled for in-situ Rb–Sr dating, a technique currently in development (Zack & Hogmalm, 2016). Age data were collected using the LA-QQQ-ICP-MS at Adelaide Microscopy where ^{87}Rb is separated from ^{87}Sr in the mass spectrometer using N_2O gas. The reaction cell that sits between two quadrapoles allows mass 67 to be isolated (^{87}Rb and ^{87}Sr), followed by a reaction with N_2O to produce $^{87}Sr^{16}O$, making a total mass of 103 and therefore allowing it to be identified from ^{87}Sr. Analyses consisted of ~90 x 75µm laser spots along a single lamination (where available) for each sample. Data were processed in the software package Iolite version 3.0 (Chew *et al*. 2014). Concordia diagrams were calculated using ISOPLOT 4.15 for Excel (Ludwig, 2009).

A nano-powder (MicaMg) and a phlogopite crystal (MDC) were used as standards. An average (or median) spline through MicaMg was used when processing in iolite to avoid introducing any false drift correction. A systematic error has also been discovered in the nano-powder. To cover for this, we have added an arbitrary 5% error to the results (Sarah Gilbert, pers comm. 2018).

Formation	Sample	Core	Depth (m)
Jalboi Fm.	U5-139.9	BMR Urapunga 5	139.9
Derim Derim Dolerite	U5-229.6	BMR Urapunga 5	229.6
Crawford Fm.	U5-329	BMR Urapunga 5	329
Mainorou (Wooden Duck)	U5-578.7	BMR Urapunga 5	578.7
Mainorou (Gibb Mbr)	U6-269.3	BMR Urapunga 6	269.3
Mantungula Fm	U6-422.1	BMR Urapunga 6	422.1

Table 2. Shale samples from Urapunga 5 and Urapunga 6 that were used for Rb–Sr dating

Sm and Nd isotope shale analysis

A total of 10 shale samples throughout the lower Roper group were sampled from Urapunga 5 and Urapunga 6 for Sm/Nd isotopic analysis. Samples were previously crushed and milled at The University of Adelaide. The rock powder (ca. 0.05g) combined with a mixed spike ($^{147}Sm+^{150}Nd$, ca. 0.5g) was dissolved in a solution of nitric acid (2mL, 7M) and hydrofluoric acid (4mL, 48wt.%). The sample was then left on a hot plate at 140°C overnight to evaporate, it was then reconcentrated using hydrochloric acid (6mL, 6M). Using ion chromatography in polyprep columns contains AG 50W-X8 200-400 mesh resin, the rare earth element fraction was concentrated. The successive isolation of Sm and Nd isotopes were carried out in quartz glass columns using Eichrom Ln ion exchange resin.

The isolated Sm and Nd fractions were loaded onto previously prepared outgasses rhenium filaments where the analysis was then carried out on an Isotopx Phoenix TIMS. Machine fractionation was corrected for normalisations to a $^{146}Nd+^{144}Nd$ value of 0.721903. The error in the data did not fall below 2se = 0.000004 excluding two samples that had an error of 0.00002. The standard used in this method was Sco-1. A thorough extended method is found in Appendix B, which includes specifications of the experimental method in isolating Sm/Nd.

RESULTS

U–Pb Detrital Zircon Geochronology

U–Pb detrital zircon geochronology was undertaken on 12 samples from six Formations throughout the lower Roper Group. Sandstone samples are listed below in stratigraphic order, from the deepest Formation through to the shallowest (Table 3). A concordance cut off of 10% was used on all samples except two samples of low zircon yield (U602, BR04) where a 15% cut-off was used. All U–Pb geochronology results are plotted on Wetherill plots with their respective kernel density estimate. Due to the discordant nature of these zircons, where possible discordia lines were calculated to help identify main peaks in the data. Both the youngest zircon analysis and the youngest population (n >3) have been quoted. However, we interpret the maximum depositional age to be best represented by the youngest near-concordant grain (Spencer and Kirkland 2016).

Formation	Sample	Core	Depth		No. concordant grains	Age Peaks (Ma)
Munyi	L04	Lawrence	478.9	479.1	41	1560, **1779**
	BR04	Broughton	79	79.3	6	1781, 1954
Hodgson	U501	BMR Urapunga 5	46	47	27	1645, **1785**, 1914, 2530
	L02	Lawrence	505.4	505.6	76	**1754**, 1973, 2379, 2517
Jalboi	U503	BMR Urapunga 5	143.2	144.5	23	**1764**, 1973, 2555
Arnold	U505	BMR Urapunga 5	286.2	286.8	56	**1764**, 1918, 2453
	U506	BMR Urapunga 5	309.5	310.1	17	**1746**, 2171, 2524
Crawford	U507	BMR Urapunga 5	328.4	328.9	13	**1799**, 1946, 2595
Limmen	GSD3-01	GSD 3	210.5	211	15	**1831**, 2401, 2627
	GSD3-02	GSD 3	150.5	151	27	**1827**, 2081, 2554
	U602	BMR Urapunga 6	327.9	328.6	9	**1838**, 2288, 2911, 3377
	U603	BMR Urapunga 6	412.1	412.7	17	**1794**, 1961, 2025

Table 3. List of samples taken for U–Pb and REE analysis. Samples were taken from upper and lower parts of the Formations and from different cores where possible to allow for the identification of spatial and lateral differences in the data. Age peaks in bold are identified as being major while others age peaks are considered minor.

LIMMEN SANDSTONE

SAMPLE: GSD3-02

Detrital zircons in sample GSD3-01 were generally elongated to well-rounded shape (Fig 3). The grains varied from 50 to 200μm in length with well-defined oscillatory zonation for the majority (Fig 3). Seventy one analyses were undertaken targeting zircon cores with some rim analyses, though there was no discernible age difference. Of these 71 analyses, only 16 lie within 10% of concordance with these grains yielding a range of $^{207}Pb/^{206}Pb$ ages between 2622 Ma and 1676 Ma (Fig 5c). The youngest, concordant grain returned a $^{207}Pb/^{206}Pb$ age of 1676 ± 82 Ma, while the youngest population as calculated by the weighted average is 1706 ± 44 Ma (n=3, MSWD=0.53) (Fig 5c). The four oldest grains provided ages between 2622 Ma and 1876 Ma, these formed a minor peak in the KDE plot as observed in Figure 6f.

SAMPLE: GSD3-02

The zircons from sample GSD3-02 were morphologically characterised by elongated grains that varied in size from 50 to 250μm (Fig 3). There were some grains that appeared featureless under CL. Of the 173 analyses undertaken, 28 were within 10% concordance and had an age range of 2567 Ma to 1726 Ma (Fig 5d). The youngest, concordant single grain was 1745 ± 78 Ma ($^{207}Pb/^{206}Pb$ age). A weighted average of the six youngest grains yield a weighted average of 1761 ± 33 Ma (n=6, MSWD=0.40) (Fig 5d). It can been seen in Figure 6f that there is also a small peak at ~2500 Ma.

SAMPLE: U602

The zircons in sample U602 were quite consistent in size (100–150μm) with the majority being elongated to sub-rounded (Fig 3). Due to a low zircon yield, only 45 analyses were undertaken on zircons of which nine were within 15% concordance. The range of $^{207}Pb/^{206}Pb$ ages was

3378–1692 Ma (Fig 6f). The youngest, concordant grain had a $^{207}Pb/^{206}Pb$ age of 1692 ± 43 Ma. The youngest population was 1829 ± 23 Ma (MSWD=1.2, n=4) (Fig 5e) while the oldest grains returned Palaeoarchaean to Palaeoproterozoic ages of 3378 Ma, 2914 Ma, 2285 Ma and 2042 Ma. Figure 6f suggests a young, bimodal peak at 1700–2000 Ma, however, this interpretation is limited by the number of analyses in this sample (n=18).

SAMPLE: U603

The zircon yield from sample U603 had 70 analyses, however similar to U602, only 30 were zircons. Zircons ranged significantly in size (100–400μm) and have elongated to sub-rounded grain shapes (Fig 3). The youngest concordant grain had a $^{207}Pb/^{206}Pb$ age of 1694 ± 40 Ma while the youngest population gave a weighted average of 1774 ± 37 Ma (MSWD=0.23, n=4). The oldest concordant grain, recorded an age of 2496 ± 73 Ma with a minor peak was identified at ca. 2025 Ma (Table 3, Fig 6f).

CRAWFORD FORMATION

SAMPLE: U507

Sample U507 from the Crawford Formation had a low detrital zircon yield, with 36 analyses, of which 19 were concordant. Zircon grain size were consistent, and were generally rounded and <80μm (Fig 3). The youngest concordant zircon had a $^{207}Pb/^{206}Pb$ age of 1766 ± 82 Ma while the youngest peak had an age of 1835 Ma, as per the KDE plot (Fig 6e). Investigating this peak further, it appears that there are two statistically significant, young populations. One at 1782 ± 37 Ma (MSWD=0.079, n=4) and another population at 1851 ± 35 (MSWD=0.66, n=6). This can be seen in the Figure 6e where a major and minor peak can be observed at 1750–1850 Ma.

ARNOLD SANDSTONE

SAMPLE: U506

Zircon grains derived from sample U506 of the Arnold Sandstone varied from well-rounded to elongated with oscillatory zonation present in some grains and featureless in others (Fig 3). Like shape, the size of the grains also varied from 100 to 200μm. A total of 36 analyses were undertaken, with 22 grains with a concordance of 90% of more. These had an age range of 1696–2521 Ma. The youngest concordant grain recorded a $^{207}Pb/^{206}Pb$ age of 1696 ± 100 Ma. The youngest age cluster of zircons gave a weighted average of $^{207}Pb/^{206}Pb$ age of 1723 ± 23 Ma (MSWD=0.072, n= 8) (Fig 6c). It is evident from Figure 5b that while there appears to be one major peak at 1700 Ma, there is spread in the concordant grains from 1650-1850 Ma.

SAMPLE: U505

Sample U505 returned a detrital zircon yield of 49, of which 37 were within 10% concordance. Similar to U506, grains were found to be well rounded with some preserving their prismatic shape (Fig 3). There were some grains that appeared featureless under CL. Both rims and cores were targeted in the larger grains (>300μm). Zircons range in age from 1560–2449 Ma with the youngest near-concordant grain recorded a $^{207}Pb/^{206}Pb$ age of 1560 ± 66 Ma. A weighted average of the youngest population recorded a $^{207}Pb/^{206}Pb$ age of 1733 ± 14 Ma (MSWD=0.83, n=13) (Fig 6b).

JALBOI FORMATION

SAMPLE: U503

Fifty three analyses were conducted on zircons from sample U503 and of these 24 were concordant. Zircons were found to be small in size (50–100μm). The youngest concordant grain recorded a $^{207}Pb/^{206}Pb$ age of 1633 ± 89 Ma. A broad, young age peak was identified at ca. 1798 Ma (Fig 6d). By looking at the weighted mean of this age peak it was evident there were two, statistically significant populations within this peak. The youngest weighted average recorded an age of 1706 ± 40 Ma (MSWD=1.3, n=5) and the second at 1815 ± 27 Ma (MSWD=0.55, n=11), which is also evident from the KDE (Fig 4e). There is also a minor peak at 2500 Ma, which is evident from both the Concordia and KDE (Fig 4e and Fig 6d).

HODGSON SANDSTONE

SAMPLE: U501

One hundred and twenty six zircons were analysed from sample U501 (Hodgson Sandstone), with 27 of those analyses sitting within 10% concordance. These produced an age range of 3194–1591 Ma. Grains ranged from stubby and well rounded, to elongated (Fig 3). Grain size ranges from 100–200μm (Fig 3). The youngest near-concordant grain had a $^{207}Pb/^{206}Pb$ age of 1591 ± 90 Ma. The youngest age peak, as defined by a kernel density plot was recorded as ca. 1776 Ma (Fig 4c and Fig 6b). Though there is an analyses at 1606 ± 100 Ma, the youngest population (n>3) has a weighted average at 1740 ± 25 Ma (MSWD=0.63, n=5).

SAMPLE: L02

A total of 117 analyses were undertaken for sample L02, of which a yield of 80 grains were > 90% concordant. These gave an age range of 1570–2526 Ma. Grains were found to be elongated with their prismatic shape preserved to well-rounded with variable size (50–350μm) (Fig 3). The youngest near-concordant grain provided a $^{207}Pb/^{206}Pb$ age of 1595± 53 Ma, while the youngest population gave a weighted average age of 1637 ± 23 Ma (n=6, MSWD=1.8). The KDE plot (Fig 6b) suggests one major peak at ca. 1800 Ma, however it can be seen from the Concordia plot (Fig 4d) that there is significant spread in age from 1600–1850 Ma.

MUNYI MEMBER

SAMPLE: L04

One hundred and twelve zircons were analysed from sample L04 from the Munyi Member, of which forty one were concordant. These provided an age range of 1530–1847 Ma. The two, youngest grains recorded $^{207}Pb/^{206}Pb$ ages of 1580 ± 66 Ma and 1665 ± 52 Ma. However, the youngest population (n>3) gave a weighted average of 1734 ± 18 Ma (MSWD=0.23, n=8). This is a significant jump in age between the youngest population and the youngest grain and can be observed in the Concordia plot for this sample (Fig 4b).

SAMPLE: BR04

Detrital zircon yield and concordant grains output from sample BR04 of the Munyi Member was poor, with only 33 analyses and eight concordant grains, therefore any ages will be statistically insignificant by themselves. The concordant grains provided an age range of 1946–1736 Ma. The youngest concordant grain had a $^{207}Pb/^{206}Pb$ age of 1736 ±

75 Ma, while the youngest population returned an age of 1774 ± 41 Ma (n=4, MSWD=0.54). It can be seen in Figure 6a and 4a that there appears to be a bimodal peak in the KDE, however this is again limited by the number of analyses.

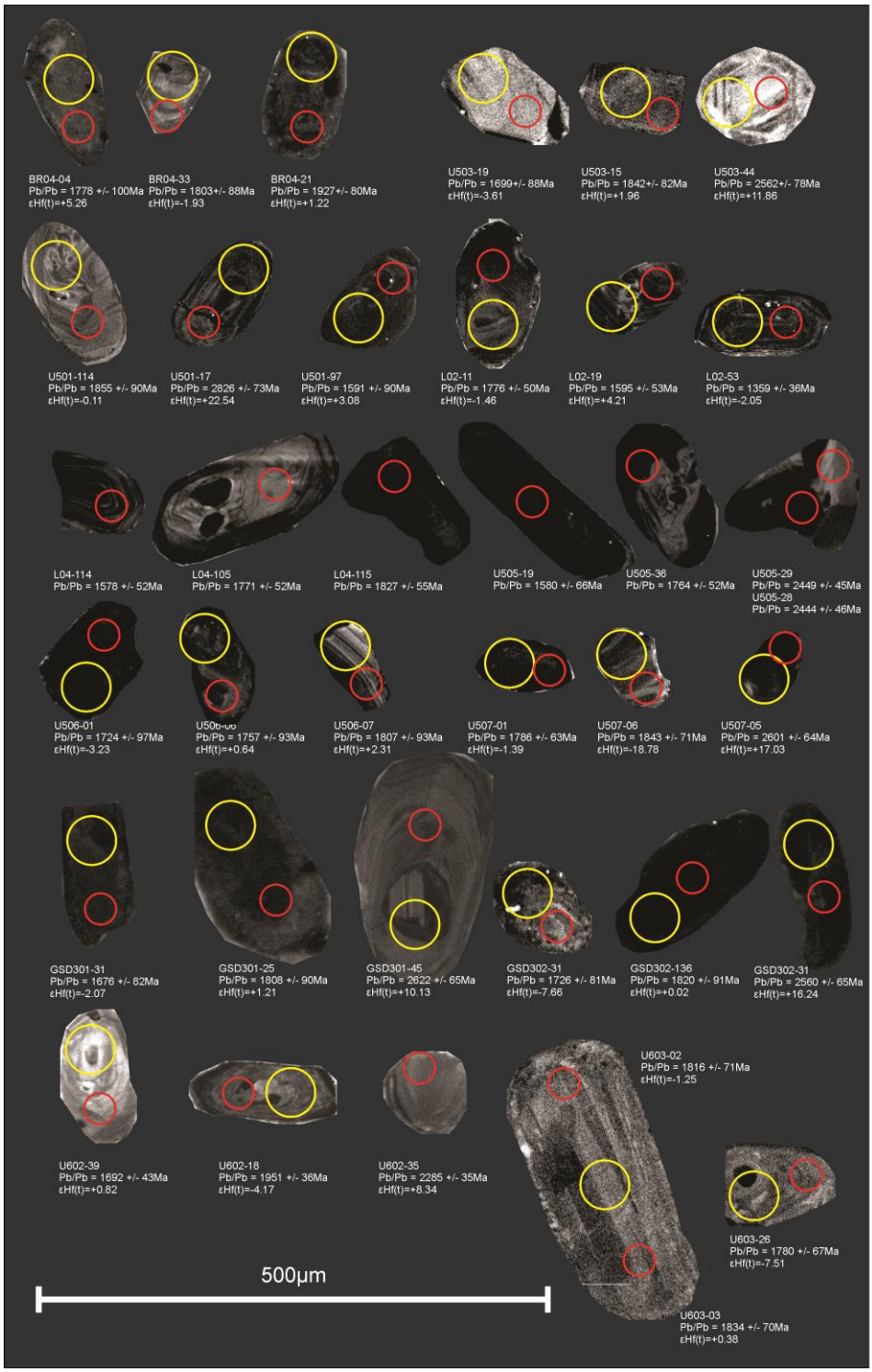

Figure 3. Cathodoluminescence (CL) images of zircons from the lower Roper with their associated207Pb/206Pb age (red dot identifies U–Pb analysis) and εHf(t) value (yellow dot represents Hafnium analysis).

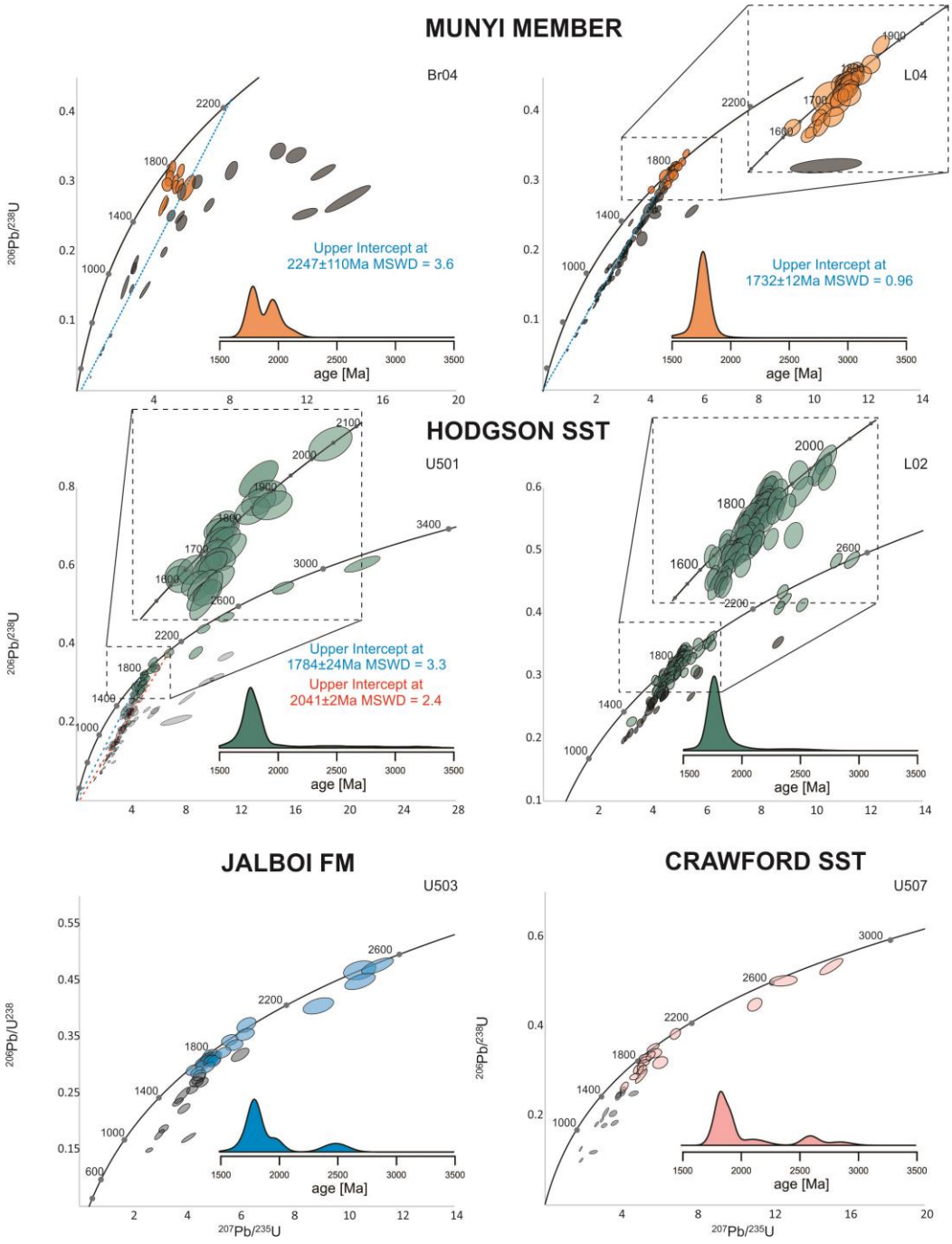

Figure 4. U–Pb Wetherill Concordia plots of detrital zircon grains (10% concordance grains highlighted in colour) from McArthur Basin Urapunga 5, Lawrence and Broughton-1 drill cores. Associated Kernel density estimation (KDE) plots are presented here showing detrital zircon age peaks from the Munyi Member (Maiwok), Hodgson Sandstone, Jalboi Formation and the Crawford Formation. Age clusters have been blown up to show spread in data where necessary. Discordia's were calculated due to the abundance of discordant grains. Upper intercepts and MSWDs have been quoted for each discordia where lower intercepts are statistically valid. With the assumption that no two grains in a sedimentary rock are the same, these discordias are used to further elucidate major peaks within the data.

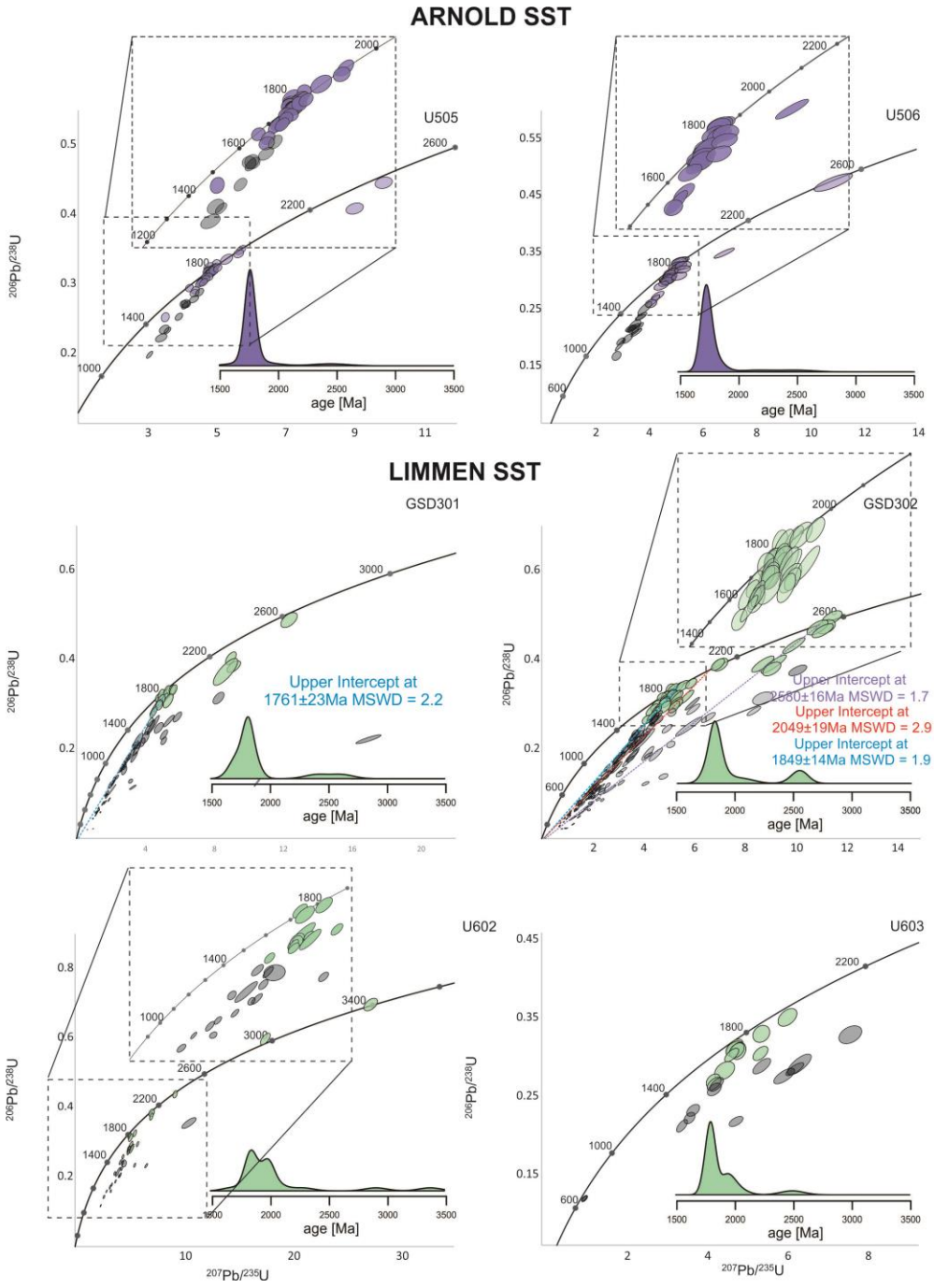

Figure 5. U–Pb Wetherill Concordia plots of detrital zircon grains (10% concordance grains highlighted in colour) from McArthur Basin Urapunga 5, GSD-3 and Urapunga 6 drill cores. Associated kernel density estimation (KDE) plots are presented here showing detrital zircon ages from the Arnold Sandstone and the Limmen Sandstone. Age clusters have been blown up to show spread in data where necessary. Discordia's were calculated due to the abundance of discordant grains. Upper intercepts and MSWDs have been quoted for each discordia where lower intercepts are statistically valid. With the assumption that no two grains in a sedimentary rock are the same, these discordias are used to further elucidate major peaks within the data.

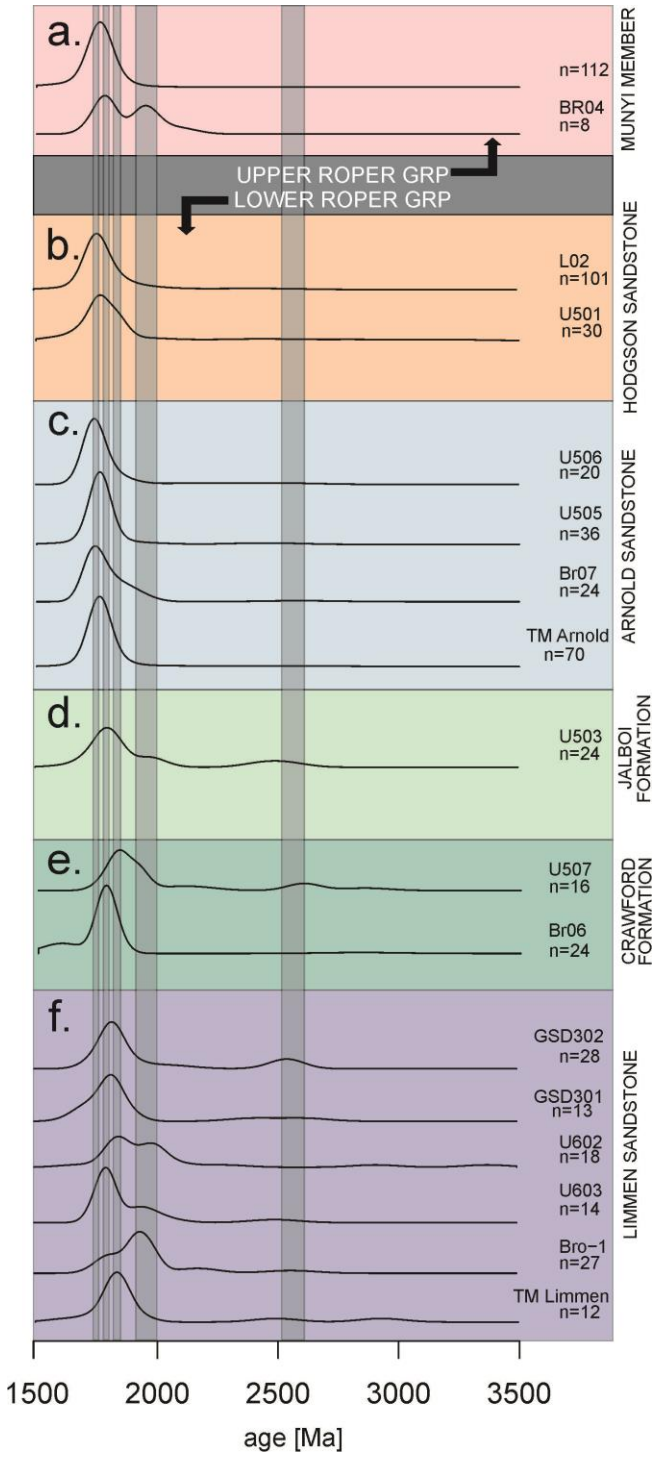

Figure 6. Kernel Density Estimate (KDE) plot for various samples within each of the targeted Formations in the lower Roper (Munyi Member is the exception as it forms the base of the upper Roper). (a) Munyi Member (b) Arnold Sandstone (c) Jalboi Formation (d) Crawford Formation (e) Hodgson Sandstone (f) Limmen Sandstone. Major peaks have been highlighted with only grains within 10% concordance included in the plot. Samples identified with 'TM' have been taken from Munson (2018). While Bro-1, Bro-6 and Bro-7 have were analyses by Yang et al. (2018).

REE Analysis in Detrital Zircons

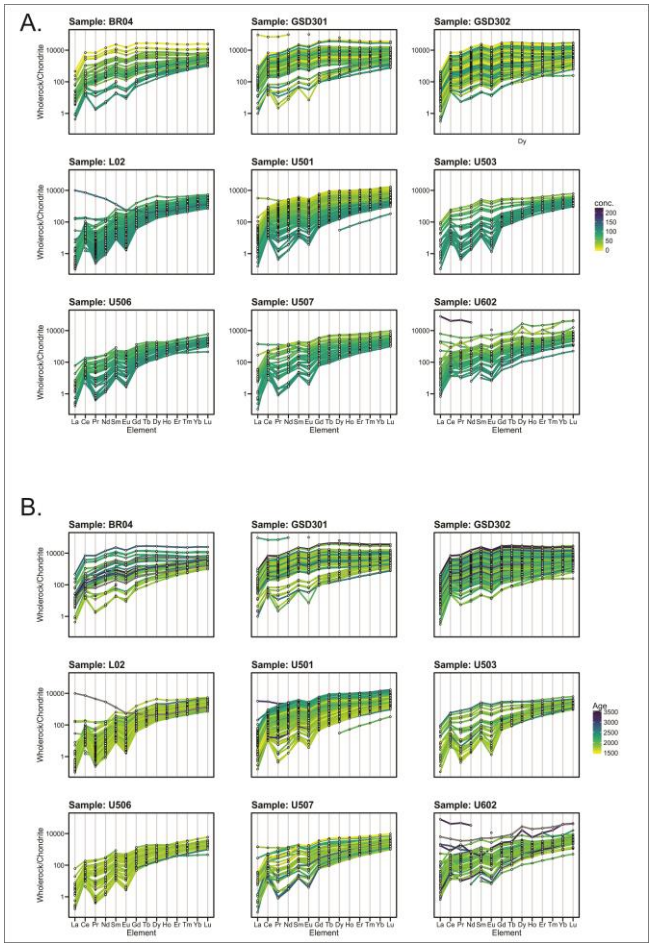

Figure 7. REE concentration plot. Samples were normalised to chondrite values and plotted per sample. (A) Trends are coloured based on concordance to identify correlations. (B) REE Trends are coloured based on analysed 207Pb/206Pb age.

Along with containing hafnium and zirconium, zircon is also a major reservoir for rare earth elements (Belousova *et al*., 2002). Their incompatibility often result in them being incorporated into the late crystallising zircon structure. Their high abundance and ratios can mean that when used with the correct proxies, trace elements can act as good provenance tools. The nine samples that were analysed for U–Pb also had their trace elements recorded, simultaneously. Rare earth element data were plotted on spider plots (Fig 7) and coloured based on concordance to identify any trends. All data, both

concordant and disconcordant data, were plotted in Figure 7 to maximise the possibility of identifying trends. Figure 7a shows that overall correlation between REE trends and concordance, which suggests that the discordant grains are no longer reflecting the original composition at the time of crystallisation. This trend can also be seen in Figure 8 where high Pb, U and Th is associated with discordant data.

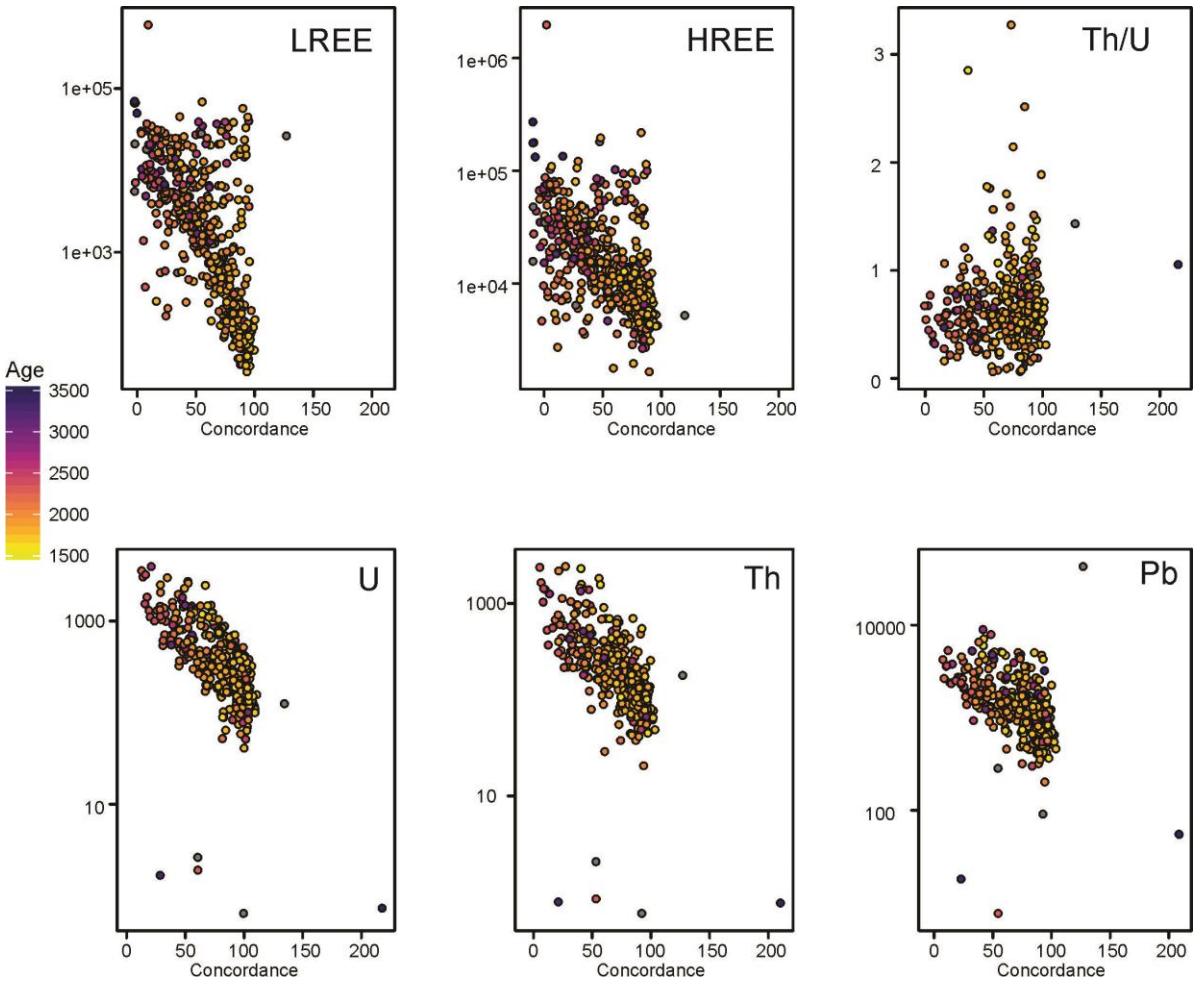

Figure 8. REE trends for LREE, HREE, Th/U ratio, U ppm, Th ppm and Pb ppm plotted against concordance using all data from samples U501 and L02 (Hodgson Sandstone), U503 (Jalboi Formation), U507 (Crawford Sandstone), U506 (Arnold Sandstone), GSD301, GSD302, U602 and U603 (Limmen Formation). Plotted using software R (Armistead, 2018).

The $(Yb/Sm)_n$ ratio can be used as a measure of the HREE enrichment of zircons. The average $(Yb/Sm)_n$ ratio for zircons is 44 (Belousova *et al.,* 2002). In Figure 9, we see a

significant spread in the ratio between all samples, with two dominant groups present at 1750 Ma. One group appears to be enriched in heavy REE compared to light REE and show a distinctive positive Ce anomaly as well as a negative Eu anomaly (Fig 7a). These are likely to represent one source and consistent with crystallisation from a granitoid, pegmatite or dolerite (Hoskin and Ireland, 2000; Belousoba *et al.*, 2002; Wang *et al.,* 2016).

The second group have the same negative Eu anomaly and positive Ce anomaly (Fig 7a), however have a much smaller Yb/Sm ratio (<44) and therefore do not have HREE enrichment.

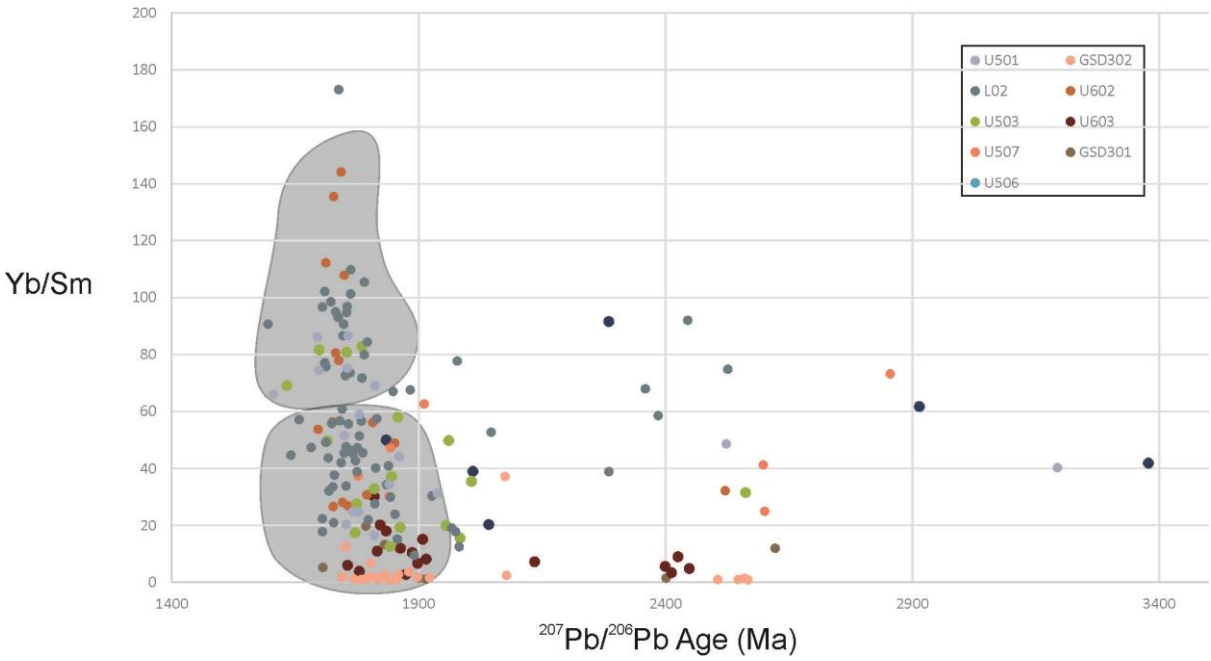

Figure 9. Yb/Sm vs 207Pb/206Pb age for samples U501 and L02 (Hodgson Sandstone), U503 (Jalboi Formation), U507 (Crawford Sandstone), U506 (Arnold Sandstone), GSD301, GSD302, U602 and U603 (Limmen Formation) using grains within 10% concordance.

Detrital Zircon Lu–Hf Isotopic Analysis

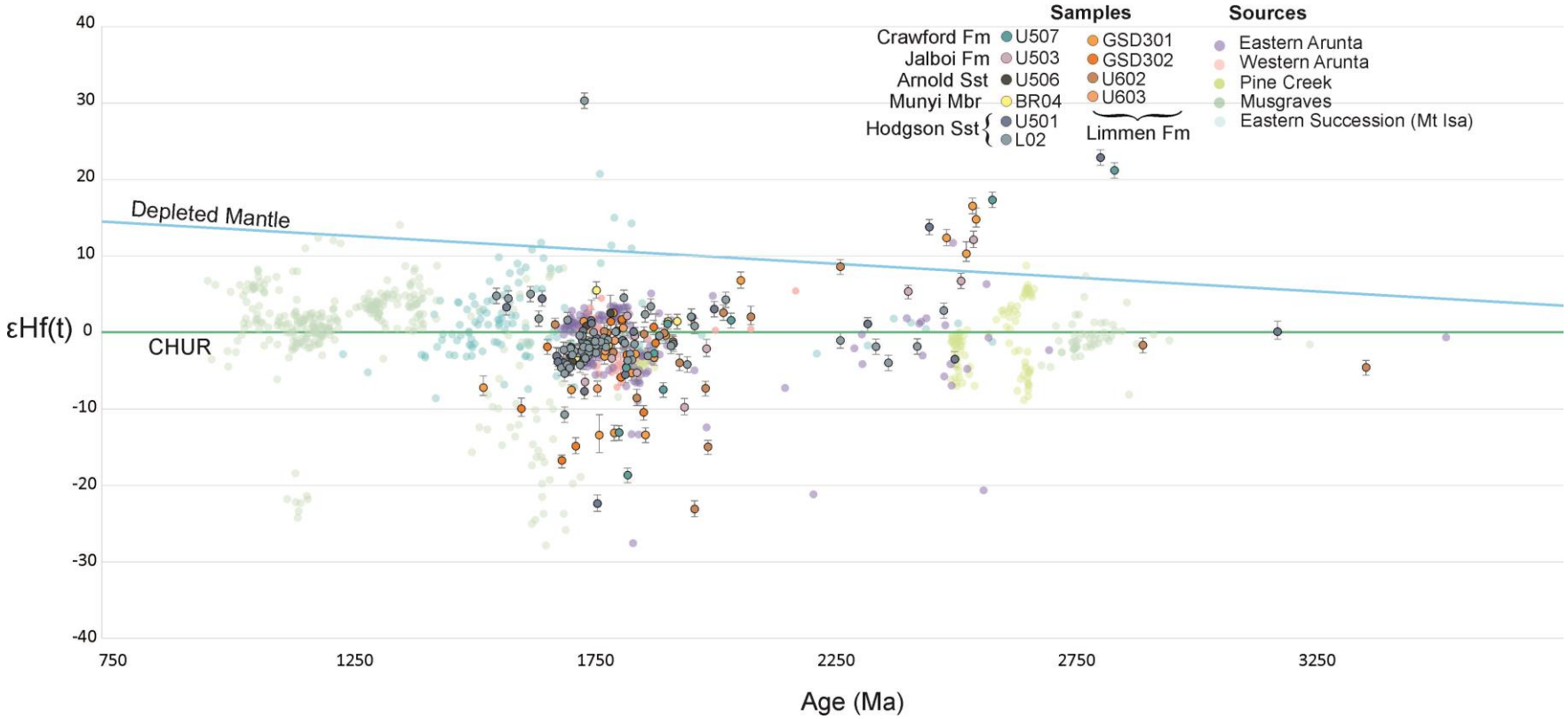

Figure 10. Epsilon Hf (t) values for samples U501 and L02 (Hodgson Sandstone), U503 (Jalboi Formation), U507 (Crawford Sandstone), U506 (Arnold Sandstone), GSD301, GSD302, U602 and U603 (Limmen Formation) using grains within 10% concordance and plotted against the corresponding analysed 207Pb/206Pb age.

Lu–Hf isotopes were undertaken on nine detrital samples and uncertainties on the Lu–Hf isotope data are quoted at the 2σ level (Appendix B). Lu–Hf data are presented as εHf(t) versus Pb^{207}–Pb^{206} age data (Fig 10).

LIMMEN SANDSTONE

Fifty six Hafnium analyses were collected from the Limmen sandstone (GSD301, GSD302, U602 and U603). These give a range of $\varepsilon_{Hf(t)}$ values -23.19 – +16.24. The two oldest grains, ca. 2914 Ma and 3378 Ma (U602), have $\varepsilon_{Hf(t)}$ vales that range between -1.87 and -4.77. Conversely, zircons with $^{207}Pb/^{206}Pb$ ages between 2042Ma to 2567Ma yield dominantly juvenile $\varepsilon_{Hf(t)}$ values (+1.82 to +16.24), suggesting a change in provenance. The five youngest grains, in the age range of ca. 1706–1543Ma have $\varepsilon_{Hf(t)}$ values have a significant spread in data from 0.82 to -16.85, with the more evolved zircons dominating the population. In general the data suggests that zircons with an older $^{207}Pb/^{206}Pb$ (>2000Ma) appear to have more positive $\varepsilon_{Hf(t)}$ value. This is supported by the four oldest grains (2567–2078 Ma) from the Limmen Samples in GSD3 preserving $\varepsilon_{Hf(t)}$ between +6.56 to +16.23. The younger grains show something completely different where grains in the age range 1726–1543 Ma in the GSD3 Limmen Fm yield preserve $\varepsilon_{Hf(t)}$ values of -2.07 to -16.85. Conversely, there doesn't appear to be a clear trend in data that falls between 1726-2078Ma. This suggests the possibility of multiple sources of the same age sourcing the basin at the time the Limmen was deposited.

HODGSON SANDSTONE

Sixty two analyses were conducted on samples from the Hodgson Sandstone (L02) .The youngest grains (n=3l, ca. 1658–1570) have an $\varepsilon Hf(t)$ range of +1.60 to +4.78, suggesting that these zircons were derived from juvenile sources, with negligible old, continental crust input. The four oldest grains (2359–2500 Ma) had $\varepsilon Hf(t)$ values from -4.16 to +2.63. There is a large spread in the $\varepsilon Hf(t)$ data within the 1800–1700 Ma zircons with values of -10.90 to +4.31 (with one outlier at +29.95).

CRAWFORD SANDSTONE

Ten analyses were conducted on the zircons from Crawford sandstone , (U507) A similar trend is observed, when compared to the Hodgson and Limmen sandstones, whereby there is a large spread in $\varepsilon Hf(t)$ data (-18.77– -2.94) between 1900–1800 Ma. The two youngest grains, ca. 1766Ma and 1786Ma, have $\varepsilon Hf(t)$ values of -1.38 and -1.83, respectively and therefore considerably evolved. While the two oldest grains, 2601Ma and 2855Ma had $\varepsilon Hf(t)$ values of +17.03 and +20.87, respectively. This suggests that these grains were sourced from an older dominantly juvenile source.

JALBOI FORMATION

Fourteen zircons were analysed in the Jalboi Formation (U503) and of those eleven with the age range 1699–2007Ma yielded $\varepsilon Hf(t)$ values between-9.93 to -1.96. Zircons with $^{207}Pb/^{206}Pb$ ages greater than ca. 2400 Ma preserve progressively more juvenile $\varepsilon Hf(t)$ signatures (+5.13 to +11.86).

ARNOLD SANDSTONE

The sample size for hafnium analyses in the Arnold Sandstone sample (U506) was small, with only 6 analyses. $\varepsilon Hf(t)$ values ranged from -4.00 to +2.31 (1807–1728 Ma). These values are representative of a moderately juvenile source with some crustal input.

MUNYI MEMBER

Six analyses from the Munyi Member sample (BR04). These data have an $\varepsilon Hf(t)$ range between -3.55 and +5.26. The youngest grain (ca. 1736 Ma) had $\varepsilon Hf(t)$ = -3.44 while the oldest grain (1976 Ma) had εHf (t) = +1.78.

Rb–Sr Radiogenic Isotopes in Shales

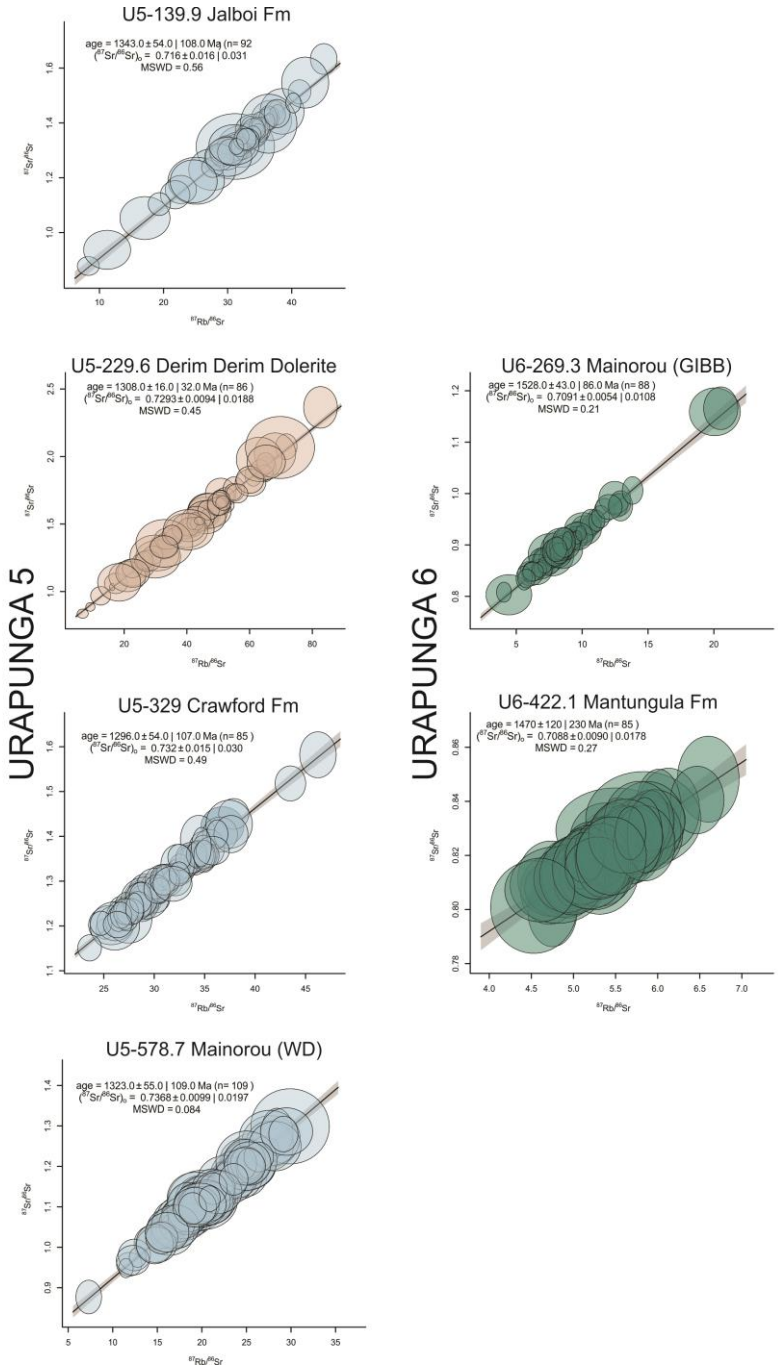

Figure 11. Rb–Sr isochron ages for the Derim Derim dolerite and 5 shales units throughout the Lower Roper group. Four samples were analysed from Urapunga 5, which represent the Jalboi Fm, Derim Derim Dolerite, Crawford Fm and Mainorou Wooden Duck (WD) Member. Two samples were analysed from Urapunga 6 which target the lower Formations with the Lower Roper, these include the Gibb Member within the Mainorou and the Mantungula Fm.

While sand units dominate the lower Roper Group, shale units are interbedded in most the Formations. Shale beds from the Jalboi Fm, Crawford Fm and the Mainorou Wooden Duck (all from Urapunga 5), along with samples from the Mainorou Formation, Gibb Member and the Mantungula Formation (both from Urapunga 6) were analysed using the laser Rb–Sr dating technique, which is currently in development (Fig 11). The Derim Derim dolerite was also sampled and dated using the same technique (U5-229.6). Errors are reported at the two sigma level.

JALBOI FORMATION

Ninety two analyses were conducted on a single shale lamina within the Jalboi Formation (U5-139.9). All analyses were included in the isochron, which returned a Rb–Sr age of 1343 ± 108 Ma (2σ error) (MSWD = 0.56, n=92) (Fig 9a). The lower intercept recorded a $(^{87}Sr/^{86}Sr)_o$ value of 0.716 ± 0.031.

DERIM DERIM DOLERITE

Eighty six analyses were conducted across a block sample of the Derim Derim Dolerite which intruded the Jalboi Formation in Urapunga 5. All analyses were included in the isochron, which recorded a Rb–Sr age of 1308 ± 32 Ma (MSWD=0.45, n=86) (Fig 9b). The $(^{87}Sr/^{86}Sr)_o$ yielded a value of 0.7293 ± 0.0188.

CRAWFORD FORMATION

Eighty five analyses were undertaken across a single mm-scale lamina within the Crawford Formation (U5-329). Again, all analyses were included in the isochron, which

produced a Rb–Sr age of 1296 ± 107 Ma (MSWD = 0.49, n=85) (Fig 9c). The lower intercept of the isochron returned a $(^{87}Sr/^{86}Sr)_o$ value of 0.732 ± 0.015.

MAINOROU FORMATION: WOODEN DUCK MEMBER

A total of 109 analyses were undertaken on the Wooden Duck Member (U5-578.7) of the Mainorou Formation. All analyses were included in the isochron that yielded a Rb–Sr age of 1323 ± 109 Ma (MSWD = 0.084, n=109) (Fig 9d). The lower intercept produced a $(^{87}Sr/^{86}Sr)_o$ value of 0.7368 ± 0.0197.

MAINOROU FORMATION: GIBB MEMBER

Eighty eight analyses were conducted on the Gibb Member (U6-269.3) of the Mainorou Formation. All analyses were included in the isochron plot, which yielded an age of 1528 ± 43 Ma (MSWD=0.21, n=88) (Fig 9e). An initial $^{87}Sr/^{86}Sr$ value was recorded at 0.7091 ± 0.0208, which is within error of seawater during the Mesoproterozoic (Shields and Veizer, 2002)..

MANTUNGULA FORMATION

Eighty five analyses were undertaken on the Mantungula Formation (U6-422.1). The isochron recorded an age of 1470 ± 120 Ma (MSWD = 0.27, n=85) (Fig 9f). A lower intercept yielded a $(^{87}Sr/^{86}Sr)_o$ value of 0.7088 ± 0.0178. Similar to U5-269.3, this value is within error of seawater value during the Mesoproterozoic (Shields and Veizer, 2002).

Rb–Sr Radiogenic Isotopes in Glauconites

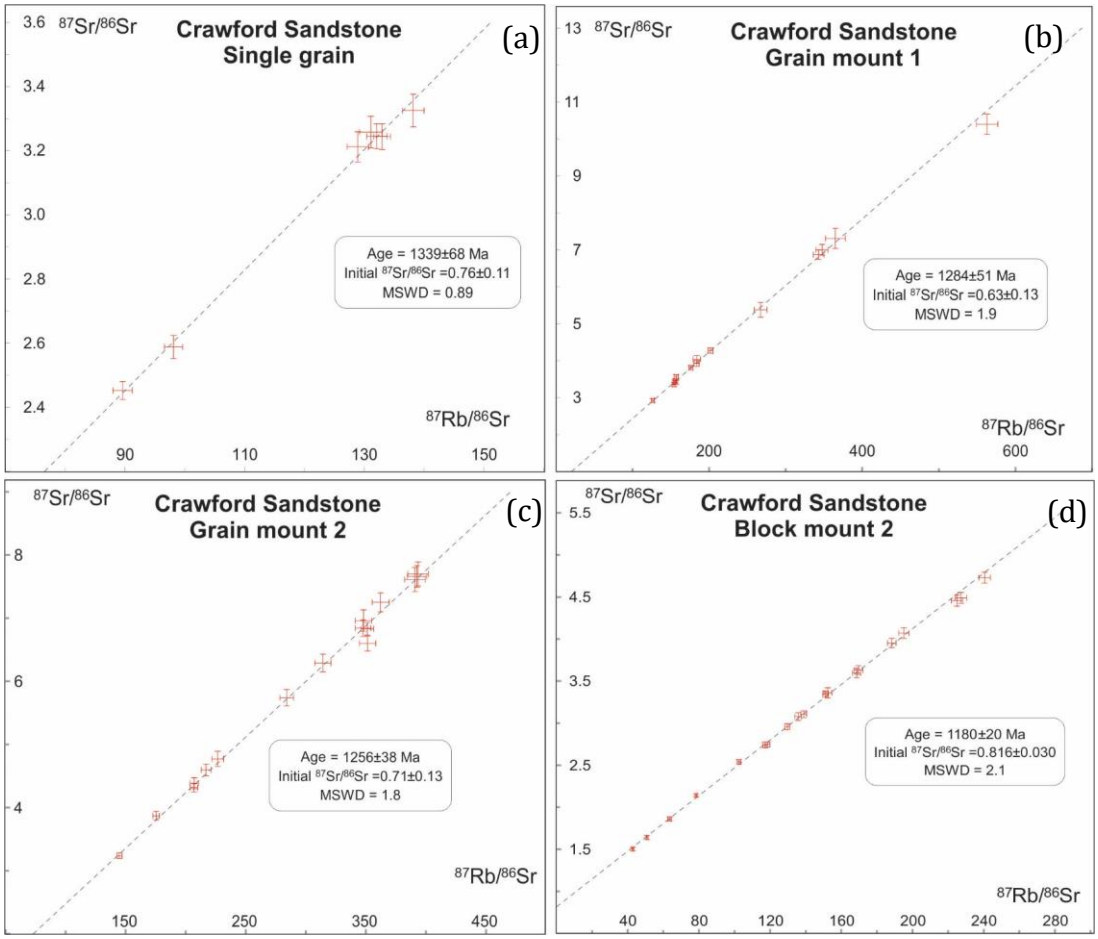

Figure 12. Rb–Sr isochrons for four Glauconite samples within the Crawford Formation, in various forms. (a) Analysis was performed across an individual grain to identify alteration or the effect of zoning within the grain. (b) Individual grains from sample U507 were mounted after the process of crushing and then an analysis was performed for each grain. (c) The same process as B, except grains from sample U508 were mounted and targeted. (d) Grains were targeted within a block of sample U508.

Glauconite pellets are abundant throughout the Crawford Sandstone and have been dated in this study using the developing in-situ laser Rb–Sr technique in an attempt to isolate an absolute age. Both mineral separate grain mounts (Fig 12a, b and c) and in-situ blocks (Fig 12d) were used to target glauconite. Figure 10a, 10b and 10c produced a Rb–Sr age that fell within error of each other (1339 ± 68 Ma, 1284 ± 51 Ma and 1256 ± 38 Ma,

respectively). The initial $^{87}Sr/^{86}Sr$ appears to vary across samples, ranging from 0.63±0.03 in analysis B to 0.816±0.030 in analysis D. It is evident in Fig 12a, which targeted an individual grain, that there are two distinct isotope signals. This could suggest zoning within the grain.

Sm–Nd Isotopic Analysis

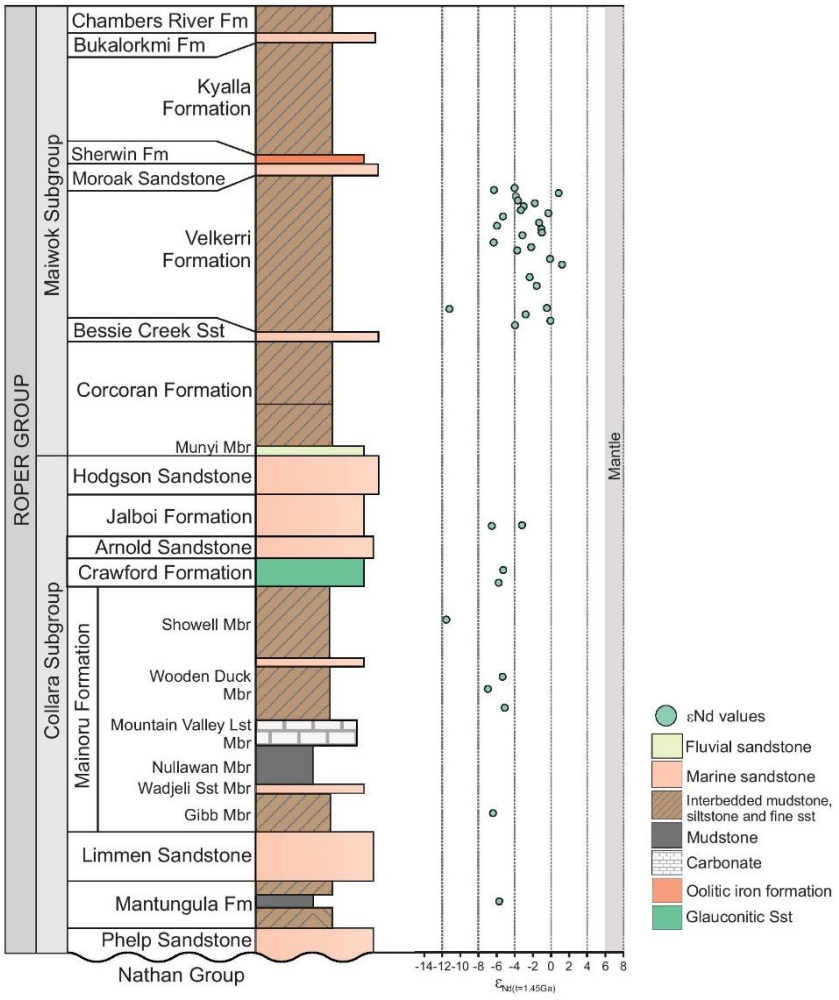

Figure 13. Composite εNd(t) record showing variation throughout the Roper Group. Velkerri Formation values were taken from Cox et al. (2016) while values throughout the Collara subgroup were a product of this study. Mantle values in the Mesoproterozoic (grey zone) were based on Goldstein et al. (1984). All εNd(t) values are calculated at 1.45Ga. See Appendix A for full results.

Whole rock geochemistry was undertaken on various shale units throughout the lower Roper Group to help constrain the source. Sm/Nd analyses were undertaken on 10 shale samples throughout the lower Roper Subgroup covering the Mantungula Formation, the Mainorou Formation, the Crawford Formation and the Jalboi Formation (Fig 13). Samples were taken from both Urapunga 5 and Urapunga 6 to produce a composite record of the Collara Subgroup. be , samples throughout The Collara Subgroup is substantially evolved with $\varepsilon_{Nd(t)}$ relative to the upper Roper Group Velkerri Formation (Cox et al. 2016), with values ranging from -3.14 to -11.4. The average $^{147}Sm/^{144}Nd$ for the Collara Subgroup is 0.10586 while the average $^{143}Nd/^{144}Nd$ ratio is 0.51043. The evolved nature of these samples suggests the incorporation of older continental crust.

DISCUSSION

What are the depositional constraints on the lower Roper Group?

U–PB SANDSTONE CONSTRAINTS

The Roper group is constrained by a previously published U–Pb baddeleyite age from the Derim Derim Dolerite at 1314 ± 1 Ma (Cox *et al*. 2018). This provides a minimum constraint for the deposition of the Jalboi Formation within the Urapunga Region. A maximum age constraint for Crawford, Arnold, Jalboi, Hodgson and Munyi are provided by SHRIMP U–Pb zircon ages of 1492 ± 4 Ma and 1493 ± 4 Ma from the rare tuffs in the Showell Member of the Mainorou Formation (Jackson *et al*., 1999; Munson *et al*., 2018).

New and existing (Munson 2018) detrital zircon U–Pb ages constrain the maximum depositional age of the lower Roper Group to: 1591 ± 90 Ma for the Hodgson Sandstone and 1580 ± 66 Ma for the Arnold Sandstone

Prior to this study no age constraint was given to the Jalboi Formation, other than the Derim Derim dolerite above and tuff ages below. Therefore a maximum depositional age has been identified to be 1633 ± 89 Ma. Additional absolute depositional constraints will be discussed further.

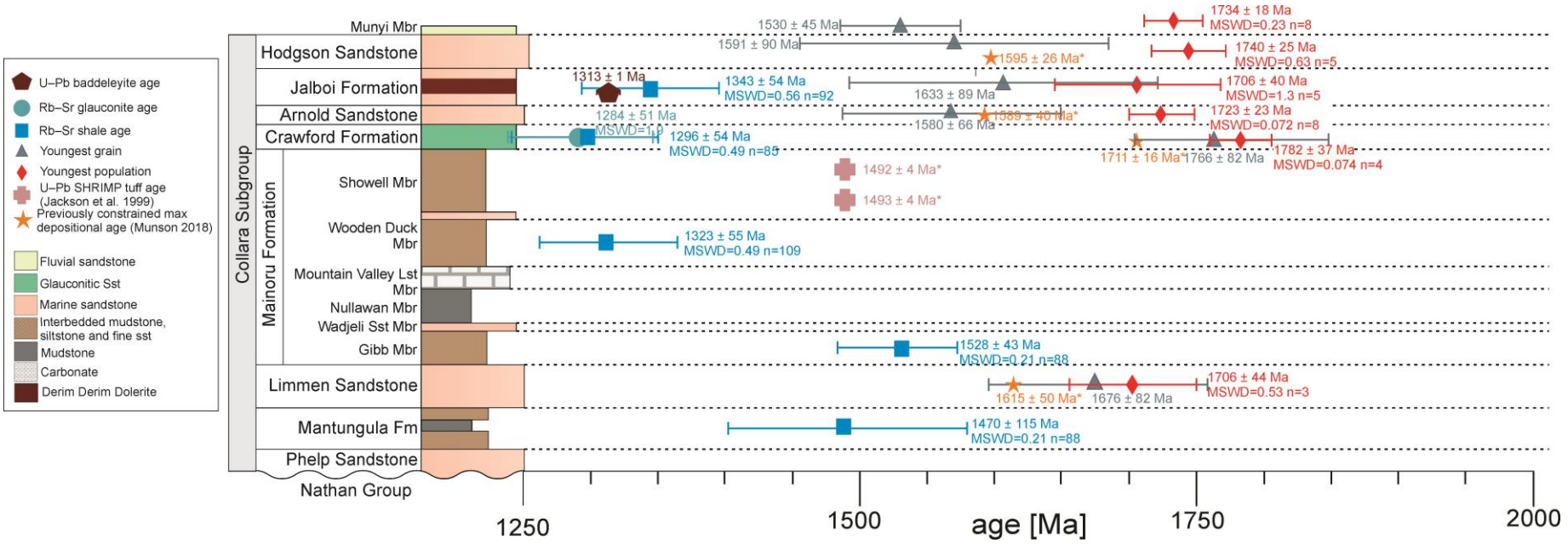

Figure 14. Compilation of U–Pb data from the lower Roper Group including baddeleyite age of the Derim Derim dolerite (Cox et al., 2018), Rb–Sr age of glauconite within the Crawford Formation, youngest concordant grain, youngest detrital zircon population (n=>3) along with previously published data on the Hodgson Sandstone, Arnold Sandstone, Crawford Formation and the Limmen Sandstone by Munson (2018) and U–Pb SHRIMP tuff ages from the Showell member of the Mainorou (Jackson et al., 1999). The maximum depositional age has been constrained by the youngest, concordant grain (red diamond) while the absolute depositional age for the Jalboi, Crawford, Wooden Duck (Mainorou), Gibb Member (Mainorou) and Mantungula Formation has be identified using Rb–Sr isotopic dating of shales within these Formations and members (blue box).

The youngest concordant grain preserved an age of 1766 ± 82 Ma for the Crawford Sandstone (U507). Which is within error of the maximum depositional age recorded by Munson *et al*., (2018), at 1713 ± 14 Ma. Fortunately, the Crawford unit was glauconite rich, interbedded with multiple shale units. Subsequently, Rb–Sr dating was used to help constrain the absolute depositional age. The maximum depositional age for the Limmen Sandstone, the oldest unit within the Collara Subgroup, is 1676 ± 82 Ma. This is slightly older than what Munson *et al*., (2018) reported.

HOW CAN WE FURTHER CONSTRAIN THE ABSOLUTE AGE OF THE LOWER ROPER?

WHAT ARE THE RB–SR GLAUCONITE AND SHALE AGES REPRESENTING?

To further constrain the age of the Jalboi a shale unit was also dated using Rb–Sr dating, an age of 1343 ± 54 Ma was calculated. As this technique is still being developed, it is difficult to say if this can be identified as the depositional age of the Jalboi, or whether it is dating a different event. Interestingly, the $^{87}Sr/^{86}Sr$ value is 0.716 and thus greater than the reported $^{87}Sr/^{86}Sr$ ratio of seawater during the Mesoproterozoic (Shields and Veizer, 2002). This could suggest the influence of fluids other than seawater and supports the theory of another event leading to the resetting of the shale unit within the Jalboi Formation.

The Crawford Formation (U5-329) shale unit recorded a Rb–Sr age of 1296 ± 54 Ma, which is within error of the age reported for both the Derim Derim dolerite (1308 ± 16Ma) and the shale unit within the Jalboi (1343 ± 54Ma). Glauconites were dated using the same, insitu technique as the shales and derived ages similar to the Jalboi shale. Three

of the four Rb–Sr glauconite ages fell within uncertainty of each other, however one sample recorded a slightly younger age of 1180 ± 20 Ma. This also happens to be the sample where analyses were undertaken on a glauconite rich block, rather than targeting individually mounted grains. This could suggest the dating of something other than glauconite. Analyses recorded $^{87}Sr/^{86}Sr$ = 0.63 ± 0.13 to 0.816 ± 0.030, which is quite variable. The minimum age constraint for Crawford Formation was the Derim Derim dolerite at 1313.8 ± 1 Ma. Therefore the ages isolated from the glauconites and shales appear to be too young, again supporting the theory of a resetting event.

Two shale samples were isolated from the Mainorou, the Wooden Duck Member (U5-578.7) and the Gibb Member (U6-269.3). The Wooden Duck sample returned an age of 1323.0±55Ma, while the Gibb Member recorded an age of 1528±43Ma. This is quite a significant difference considering both members belong to the same Formation. Remarkably, the Wooden Duck falls within error of the Derim Derim Dolerite, along with the other shales analyses from Urapunga 5. The older age recorded for the Gibb Member suggests a value that may represent an age closer to deposition, particularly as they fall within error of the Tuff ages in the Showell Member of the Mainorou (1492 ± 4Ma and 1493 ± 4 Ma) as reported by Jackson *et al*., (1999). Additionally, the $^{87}Sr/^{86}Sr$ ratio yielded for the Gibb Member is 0.7091 ± 0.0054 whereas the ratio is 0.7368 ± 0.0099 for the Wooden Duck. The Gibb Member corresponds to an intercept that is representative of the seawater during the Mesoproterozoic (Shields and Veizer, 2002). In contrast, the ratio

recorded for the Wooden Duck suggests a post depositional shift on the Rb–Sr system, which is not consistent in Urapunga 6 samples.

What we see here is two, definitive groups in the shales and glauconite samples which appear to reflect the presence or absence of the Derim Derim dolerite in the two Urapunga cores. Cox *et al*. (2018) proposed an emplacement temperature of 1250^{o}C for both sills and dykes during the Derim Derim event and provided evidence for magmatic thermal perturbation in the thermal maturity data. The effect this emplacement has had on the surrounding shales is further supported in this study, with evidence for the Rb–Sr isotopic system being reset with the presence of the Derim Derim dolerite.

Provenance and Tectonic Geography of the Lower Roper group

A compilation of U–Pb age data from this study and other publications (Munson *et al*. 2018; Yang *et al*. 2018; Subarkah, 2018) are coupled with hafnium and neodymium isotope data to help constrain the relationships between the surrounding source regions and deposition of the lower Roper Group.

In order to characterise and clarify the depositional history the lower Roper Group it is important to understand the surrounding orogeny's and exposed basement that were potentially sourcing the basin during its deposition.

THE ARUNTA REGION, AILERON PROVINCE AND TANAMI REGION (SOUTHERN SOURCE)

To the South of the McArthur Basin is the Arunta Region which comprises a 200,00km^2 exposure of deformed, Proterozoic rocks that record a series of geological events over a 1500 million year period (Kositcin *et al*. 2011). The region is divided into three provinces with unique ages and histories: the 1800-1700Ma Aileron Province, the 1690-1600Ma Warumpi Province and the Neoproterozoic to Cambrian Irindina Province (Scrimgeour, 2003). Both U–Pb and $\varepsilon_{Hf}(t)$ suggest the Aileron Province as being a likely source region during the deposition of the lower Roper group due to the moderately evolved hafnium signatures and dominant ~1750Ma age peak.

The Tanami Region is present to the North of the Arunta and comprises the Billabong complex, which forms the only known Neoarchean basement in the Northern Territory outside of the Pine Creek Orogen (Whelan *et al*. 2016). Recent redating of the complex yielded 3 distinct populations; 2532 ± 3 Ma, 2481 ± 4 Ma and 2479 ± 7 Ma. These Neoarchean dates are consistent with what we observe for zircons from the Limmen Sandstone, Crawford Formation and Jalboi Formation and propose a potential source for the deposition of these Formations.

PINE CREEK OROGEN AND HALLS CREEK OROGEN (NORTHERN SOURCES)

The Pine Creek Orogen is a Paleoproterozoic inlier covering 66,000km^2 of the northern margin of the exposed North Australian Craton (Plumb, 1979; Worden *et al*. 2006). The extent of the orogeny to the North is unknown with the Halls Creek and King Leopold

Orogens present to the southwest. As previously mentioned, Pine Creek comprises Neoarchean basement which is exposed in the Rum Jungle Complex (Worden *et al*. 2006). SHRIMP U–Pb zircon ages yielded ages of 1545–2520Ma and 2470 ± 47 Ma for the Rum Jungle (Central Domain) and Nanambu Complex (East) basement rocks (Worden *et al*. 2006). The ages of these terrains appear to be consistent with the older, Neoarchean detrital zircon cluster. However, $\varepsilon_{Hf}(t)$ suggests otherwise, with Pine Creek preserving a moderately juvenile signature whereas zircons of the same age identified in this study record a signature that plots well above the depleted mantle (Fig. 10).

MOUNT ISA INLIER

Positioned the southeast of the McArthur Basin is the Mount Isa Inlier which constitutes one of the largest areas (~61, 000km^2) of Proterozoic curst preserved on the Australian continent (Betts *et al.,* 2006; Belkinsop, 2008). It preserves an extensive record of mid-Proterozoic deformation, metamorphism and plutonism– the 1.6–1.5 Ga Isan Orogeny (Blake and Stewart, 1992; Giles *et al.,* 2002; Edmiston *et al.,* 2008). Yang *et al.,* (2018) identified a major peak of ca. 1560 Ma age detritus in the Bessie Creek sandstone, which is consistent with the age of the Isan Orogeny. It was suggested that this region was exhumed during the initial deposition of the upper Roper Group.

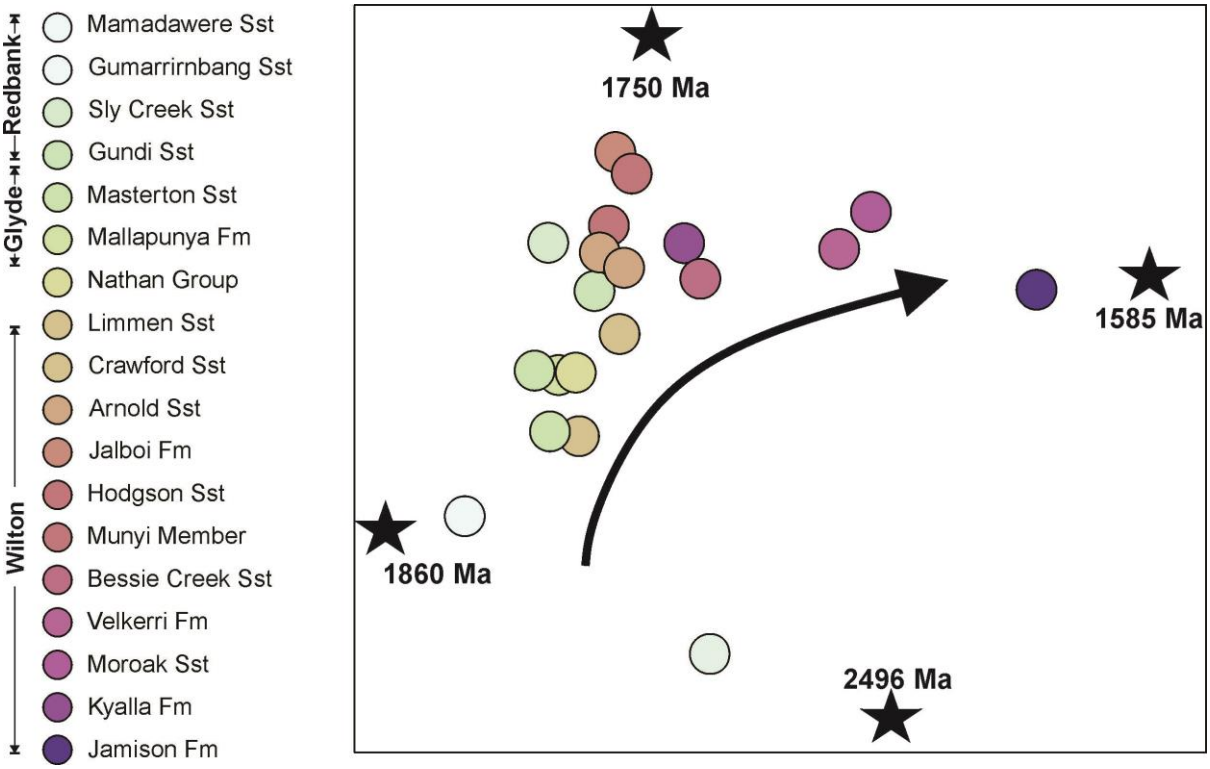

Figure 15. Multidimensional Scaling (MDS) Plot of sedimentary samples from the Wilton Package (this study; Munson 2018, Yang et al. 2018), Glyde Package (Blades et al. in prep) and Redbank Package (Blades et al. in prep). Samples that are closely similar are plotted near each other. Dark stars represent major peaks in the data as estimated by KDE plots. Wilton Package show mixed detrital ages however a progression from dominantly 1860 Ma aged sources to younger, 1585 Ma sources is evident with a transition from the older, lower Roper Group into the younger, upper Roper Group.

In Figure 14, eleven samples from this research and an additional 23 samples from Munson (2018), Yang *et al.* (2018) and Blades *et al.* (in prep) are plotted together. Samples from the lower Roper Group (Hodgson Sandstone to Limmen Sandstone) appear to plot between ca. 1860 Ma and ca. 1750 Ma. These ages are consistent with the Arunta Region and specifically reflect the age of silicate magmas that were thought to intrude between 1.86 Ga and 1.79 Ga (Kositcin *et al.*, 2015; Reno *et al.*, 2017) into the Jervois and Bonya domains of the Aileron Provenance.

The Munyi Member disconformably overlies the Hodgson Sandstone and forms the oldest member of the Maiwok Subgroup (Fig 2). Two samples from Lawrence and Broughton cores provided age peaks at 1550 Ma and 1776Ma, which appears to be consistent with Mt Isa sources and Arunta sources (Yang *et al*. 2018). The only Hafnium isotope data from the 1800–1750 Ma zircons within the Munyi Member have an evolved signature (ε_{Hf}(t) = -1.93 to -3.44), suggesting a reworked crustal source. The ca.1750 Ma population have ε_{Hf}(t) values between signature of +1.22–+1.78. These values suggest the zircons were derived from juvenile sources, with negligible old, continental crust input, although recent crustal additions cannot be excluded. Detrital zircons yielded from the Munyi Member are consistent with the Arunta Region, as seen in Fig 8.

Detrital zircon grains from the Hodgson Sandstone reflect, like the Munyi Member, the Arunta provenance as being the main source region to the basin at this time, given both hafnium isotope record and the major age peaks for the Formation (Fig 10). One major peak at exists at ca. 1850 Ma and another at ca. 2500 Ma. Both peaks record a relatively large spread in hafnium isotope signatures, with the ca. 1800 Ma detrital zircons ranging from -5.69 to +4.31 and the ca. 2500 Ma cluster preserving a Hf signature in the -4.16 to +13.51 range. As there is a much lower proportion of ca. 1560 Ma zircon grains in the Hodgson Sandstone, particularly relative to the upper Roper Group, as reported by Yang *et al*. (2018), it is suggested that the input from the Eastern Fold Belt of the Mount Isa Province is far less significant in the lower Roper Group.

The detrital age spectra of the Jalboi Formation lacks the presence of the younger ca. 1590 Ma population identified in the upper Roper Group and to some extent, the Hodgson Sandstone. This proposes a provenance change associated with the transition from the lower Roper Group (Collara) into the upper Roper Group (Maiwok). Two age clusters are identified in the Jalboi, ca. 1800Ma and ca. 2500Ma. A trend from a dominantly evolved source for the younger zircons into a more juvenile source in the older zircons is present.

A similar trend is identified for the Arnold Sandstone, where the younger detrital zircons (1749–1724 Ma) preserved a moderately evolved Hf signal (-4.00 to -2.10). However, this is not what Munson *et al*. (2018) identified. In fact, he observed a trend whereby the younger zircons represented a juvenile source and older grains were progressively more evolved. Further hafnium analysis of the Urapunga Arnold Sandstone may help support or disprove this.

Provenance for the Crawford Sandstone is constrained by both hafnium isotopes and neodymium isotopes. One major U–Pb age peak was identified at ca. 1804 Ma with two minor peaks either side at ca. 1766 Ma and ca.1900 Ma. An older, Archean cluster was also recognized in the Crawford, which was consistent with Munson *et al*. (2018). Two, distinctive clusters are present in the hafnium isotope record for the Crawford Sandstone, these coincide with what was seen in the Jalboi and the Arnold Formations and therefore suggest the basin was sourcing dominantly the Arunta during the deposition of the Crawford.

The εNd(t) data provides evidence for an evolved source, with a dominant -6 to -8 signature in the lower Roper Group into a slightly more juvenile source for the Velkerri. Cox *et al*. (2016) proposed a dominant flux from the Arunta during the deposition of shales from the Velkerri Formation in the upper Roper Group while Yang *et al.* (2018) also provided evidence for a dominantly Arunta sourced detritus of the Velkerri and Moroak Formations.

The Hf isotopic data for the Limmen sandstone is extensive, with four samples from the GSD-3 and Urapunga 5 wells. The U–Pb data suggests that zircons were derived from sources of late Palaeoproterozoic age and Archean age. Again, we see late Paleoproterozoic zircons preserving a dominantly evolved signature while the Archean zircons become progressively more juvenile, this appears to be consistent throughout the whole Lower Roper. Rare Earth Element data suggests two, distinct age peaks at 1700-1800 Ma which are characterised by their slope (Yb/Sm). This may support the idea that multiple sources of the same age were sourcing the lower Roper and reflect two, compositionally different melts.

What is the Tectonic Geography during the deposition of the lower Roper Group?

Through the incorporation of U–Pb age data with associated $\varepsilon_{Hf}(t)$ values and εNd from the shale units, we can attempt to constrain the tectonic geography and its evolution during the deposition of the lower Roper Group. Integrated data across all formations suggest a dominant Arunta Region source, with prominent Aileron and Tanami influences

which are located to south and southwest of the McArthur Basin. We propose older zircon populations to be derived from the Billabong Complex within the Tanami while younger zircons, in the 1700–1800Ma age range to be predominantly sourced from the Aileron Provenance.

We suggest an uplift of the Arunta region at 1.45Ga as a result of intracratonic rifting. Morrissey *et al*. (2018) identified evidence for this in the Gawler within the South Australian Craton (SAC) and due the proximity of the North Australian Craton at this time we propose similar events to result in the uplift of the Arunta.

Supporting Morrissey *et al*. (2018) theory, we suggest rifting between Laurentia and the Australian Cratons to occur post 1.45 Ga. This would explain the widespread magmatism between the two regions at 1.45 Ga and the possibility of intracontinental extension leading to the uplift of the Arunta region, as suggested in this study.

Yang *et al*. (2018) suggested exhumation of the Arunta at ca. 1.35 Ga as a result of the subduction and closure of the Mirning Ocean. However, we propose the region was exhumed at an earlier date (1.45 Ga) which is supported heavily by $\varepsilon_{Hf}(t)$, U–Pb ages and εNd data provided in this study. Yang *et al.* (2018) also identified an abundance of ca. 1560 Ma detritus in the Bessie Creek Sandstone and proposed a Mount Isa source. We see similar age detritus in the Hodgson Sandstone (top of the lower Roper) and Munyi Member (base of the upper Roper). This shift was suggested to be the result of the North Australian Craton rifting from Laurentia and consequently creating a series of rift basins that would explain the exhumation of the Mount Isa Province.

We therefore propose a provenance change from a dominantly Arunta source during the deposition of the lower Roper into an eastern, Mount Isan source as we transition into the upper Roper.

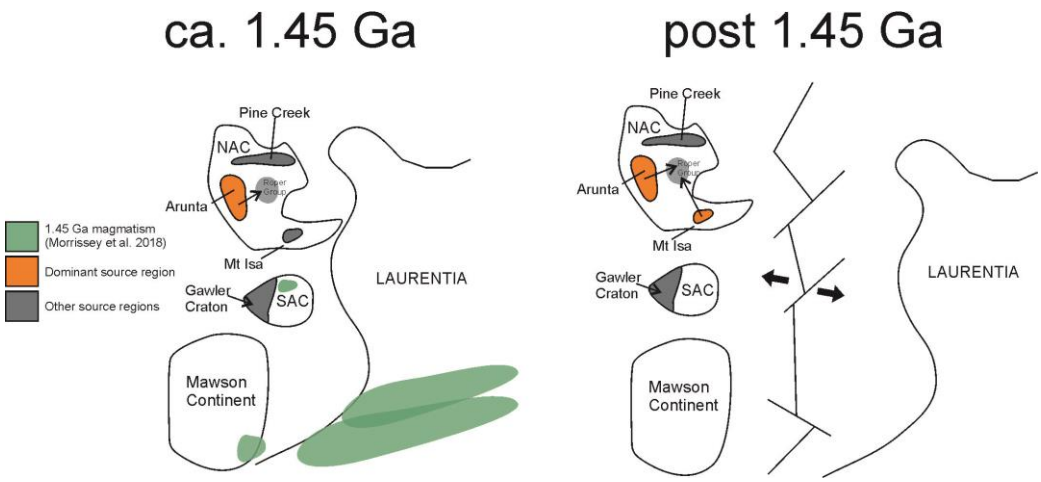

Figure 16. Tectonic geography of the regions around the Roper Group modified after Yang et al. (2018) and Morrissey et al. (2018) (a) We see evidence for an Arunta source and abundant magmatism and metamorphism across the Mawson continent and Laurentia, supporting Morrissey et al. (2018) theory. (b) Transitioning into the Hodgson Sandstone and Munyi Member (upper Roper Group), we have Mt Isan age detritus ca. 1560 Ma, suggesting exhumation of eastern Australia. We propose this to be the result of rifting between Laurentia and the Mawson Continent and Australian Cratons.

CONCLUSIONS

Coupled detrital zircon U–Pb and Lu–Hf isotopic systems along with εNd(t) values and Rb–Sr age dates presented in this study provide new constraints on the age, provenance and tectonic geography of the lower Roper. The main conclusions and suggestions from this study are:

- New U–Pb (zircon) data provide constraints on the maximum depositional ages for sands within the lower Roper Group. The Arnold Sandstone and overlying Jalboi Formation and Hodgson Sandstone were deposited between ca. 1633 Ma and 1580 Ma. The youngest unit dated within this study, the Munyi Member (upper Roper), gave an age of 1530 ± 45 Ma, which records the transition into the upper Roper Group. Using a new developmental technique, Rb–Sr (LA-ICP-MS-QQQ), interbedded shales from the lower Roper Group were analysed (Mantungula Formation and lower Mainorou Formation) to provide further constraints on the deposition of these groups. These gave isochron ages of 1470 ± 115 Ma and 1528 ± 43 Ma, consistent with new and previously published U–Pb data.
- Rb–Sr data collected from Urapunga 5, in glauconitic sands and shales, reflect a resetting of the isotopic system at 1343–1180 Ma. We suggest that this resetting event is related to the intrusion of the Dermin Derim dolerite at ca. 1313 Ma. This interpretation is supported by data collected within Urapunga 6, where shale ages have been inferred to represent an age closer to that of deposition.

- The εNd(t) data from the lower Roper Group provides evidence for an evolved source, with a dominant εNd(t) values between -6 and -8. These signatures suggest a dominantly crustal source, with little mantle derived material. These data are consistent with interpretations that the lower Roper group is depositionally connected to the Arunta region at this time.
- Subtle provenance changes occur between the upper and lower Roper Groups, from dominant ca. 1860 and 1750 Ma peaks to an influx of ca. 1585 Ma detritus. We interpret the age spectra of the lower Roper Group to be related to the northern Arunta region, consistent with intracratonic rifting during the Mesoproterozoic. The observed shift in provenance within the upper Roper group towards ca 1585 Ma, is indicative of Isan sources. This has been suggested to be the consequence of the exhumation and erosion of the Mt Isa inlier, as a result of the rifting of Laurentia from the Australian cratons (SAC and NAC) post 1.45 Ga.

ACKNOWLEDGEMENTS

I would firstly like to thank my supervisors, Dr Alan Collins and Dr Morgan Blades for not only sharing their abundance of knowledge but also for supporting and guiding me along the way. You let me learn for myself, but always ensured I was on the right path. To Dr Sarah Gilbert and Dr Dave Kelsey from Adelaide Microscopy, thank you for the polishing, imaging and LA-ICP-MS training. I would also like to acknowledge David Bruce and his assistance in the lab and processing the data and Dr Justin Payne for his guidance in using the multi collector. Of course, thank you to the ARC Linkage Project (LP160101353) and specifically Santos, NTGS, Origin and Imperial Oil and Gas for funding this project. I hope it can be of use.

To Sheree Armistead, Dr Grant Cox, Dr Juraj Farkas for their general help and guidance in various aspects of my project.

To my partner and family, thank you for supporting me the last 8 months. I'm lucky to have the support outside of university.

Finally, to the honours cohort. Specifically; April Shannon, Gabrielle Redden and Laura Easton. What a great team we made this year!

REFERENCES

ALLEN, P.A., ERIKSSON, P.G., ALKMIM, F.F., BETTS, P.G., CATUNEANU, O., MAZUMDER, R., MENG, Q. & YOUNG, G.M., 2015. Classification of basins, with special reference to Proterozoic examples. Geol. Soc. London Memoirs **43** (1), 5–28.

BANSAL, U., BANERJEE, S., RUIDIAS, D.K., & PANDE, K., 2018. Origin and geochemical characterization of the glauconites in the Upper Cretaceous Lameta Formation, Narmada Basin, central India. *Journal of Paleogeography* **7**(2), 99-116.

STEWART, A.J. AND BLAKE, D.H. 1992. Detailed Studies of the Mount Isa Inlier, *Australian Geological Survey Organization Bulletin* **234**, 1-12

CLOSE, D.F., 2014. The McArthur Basin: NTGS' approach to a frontier petroleum basin with known base metal prospectivity. Annual Geoscience Exploration Seminar (AGES) Proceedings, Alice Springs, Northern Territory 15–16 March 2016. Northern Territory Geological Survey, Darwin. pp. 85–89.

COX, G.C., JARRETT, A., EDWARDS, D., CROCKFORD, P.W., HALVERSON, G.P., COLLINS, A.S., POIRIER, A. & LI, Z. 2016. Basin redox amd primary productivity within the Mesoproterozoic Roper Seaway. *Chemical Geology* **440**, 101-114.

COX, G.M., BLADES, M.L., COLLINS, A.S., FURKAS, J., GLORIE, S., FODEN, J.D., YANG, B. & PAYNE, J.L., The Derim Derim Event: Impact on hydrocarbon development. Annual Geoscience Exploration Seminar (AGES) Proceedings, Alice Springs, Northern Territory 20–21 March 2018. Northern Territory Geological Survey, Darwin.

EDMISTON, M.A., LEPONG, P. & BLENKINSOP, T.G. 2008. Structure of the Isan Orogeny under cover to the east of the Mount Isa Inlier revealed by multiscale edge analysis and forward and inverse modelling of aeromagnetic data. *Precambrian Research* **163** (1-2), 69-80.

GILES, D., BETTS, P. & LISTER, G. 2002. Fair-field continental backarc setting for the 1.80-1.67 Ga basins of northeastern Australia. *Geology* **30**, 823-826.

GOLDSTEIN, S.L., O'NIONS, R.K. & HAMILTON, P.J. 1984. A Sm–Nd isotopic study of atmospheric dusts and particulates from major river systems. *Earth Planet. Sci. Lett.* **70** (2), 221–236.

GRIFFIN, W.L., WANG, X., JACKSON, S.E., PEARSON, N.J., O'REILLY, S.Y., XU, X. & ZHOU, X. 2002. Zircon chemistry and magma mixing, SE China: in-situ analysis of Hf isotopes, Tonglu and Pingtan igneous complexes. *Lithos,* **61**(3), 237-269.

JACKSON, S.E., PEARSON, N.J., GRIFFIN, W.L. & BELOUSOVA, E.A. 2004. The application of laser ablation-inductively coupled plasma-mass spectrometry to in situ U–Pb zircon geochronology. *Chemical Geology*, **211**(1), 47-69.

KASTING J.F. AND ONO, S., 2006. Paleoclimates: the first two billion years. *Phils. Trans. R. Soc. Lond. Ser. B Biol. Sci.* **361**(1470), 917-929.

KOSITCIN, N., MAGEE, C.W., WHELAN, J.A. AND CHAMPION, D.C. 2011 New SHRIMP geochronology from the Arunta Region: 2009-2010. *Geoscience Australia, Record*, 2011/14, 75p.

LYONS, T.W., REINHARD, C.T. & PLANAVSKY, N.J., 2014. The rise of oxygen in Earths early ocean and atmosphere. Nature **506**(7488), 307-315.

MERDITH, A.S., COLLINS, A.S., WILLIAMS, S.E., PISAREVSKY, S., FODEN, J.D., ARCHIBALD, D.B., BLADES, M.L., ALESSIO, B.L., ARMISTEAD, S., PLAVSA, D., CLARK, C. & MULLER, D., 2017. A full-plate global reconsytruction of the Neoproterozoic. *Gondwana Research* **50**, 84-134.

MUNSON, T.J., 2016. Sedimentary characterisation of the Wilton package, greater McArthur Basin. Northern Territory. Northern Territory Geological Survey, Record 2016-003.

MUNSON, T.J., 2017. Unconventional petroleum resources of the Roper Group, McArthur Basin. Northern Territory Geological Survey, Record 2017-002.

MUNSON, T.J., 2018. NTGS laser ablation ICP-MS U–Pb and Lu-Hf geochronology project: Roper Group (McArthur Basin), overlying ungrouped units (Beetaloo Sub-basin), Renner Group (Tomkinson Province), and Tijunna Group (Birrindudu Basin). Northrn Territory Geological Survey, Record 2018-007.

PAYNE, J.L., PEARSON, N.J., GRANT, K.J. & HALVERSON, G.P. 2013. Reassessment of relative oxide Formation rates and molecular interferences on in situ lutetium–hafnium analysis with laser ablation MC-ICP-MS. *Journal of Analytical Atomic Spectrometry,* **28**(7), 1068-1079.

PLUMB, K.A. 1979. Structure and tectonic style of the Precambrian shields and platforms of northern Australia. *Tectonophysics* **58** (3-4), 291-325.

PLANAVSKY, N.J., REINHARD, C.T., WANG, X., THOMSON, D., MCGOLDRICK, P., RAINBIRD, R.H., JOHNSON, T., FISCHER, W.W. & LYONS, T.W. 2014. Low Mid-Proterozoic atmospheric oxygen levels and the delayed rise of animals. *Science* **346**(6209), 635-638.

PLANAVSKY, N.J., SLACK, J.F., CANNON, W.F., O'CONNELL, B., ISSON, T.T., AESAL, D., JACKSON, J.C., HARDISTY, D.S., LYONS, T.W. AND BEKKER, A. 2018. Evidence for episodic oxygenation in a weakly redox-buffered deep mid-Proterozoic ocean. *Chemical Geology* **483**, 581-594.

REINHARD, C.T., PLANAVSKY, N.J., ROBBINS, L.J., PARTIN, C.A., LALONDE, S.V., BEKKER, A., KONHAUSER, K.O. & LYONS, T.W. 2013. Proterozoic ocean redox and biogeochemical stasis. *Proc. Natl. Acad. Sci.* **110** (14), 5357-5362.

RENO, B.L., WEISHEIT, A., BEYER, E.E., MCGLOIN, M.V. AND KOSITCIN, N. 2017. Proterozoic tectonothermal evolution of the northeastern sector of the Aileron Province. Annual Geoscience Exploration Seminar (AGES) Proceedings, Alice Springs, Northern Territory 28–29 March 2017. Northern Territory Geological Survey, Darwin.

SAHA, D. 2017. Proterozoic tectonics and trans-Indian mobile belts: a status report. Proc. Indian Natl. Sci. Acad. 82 (3), 445–460.

SANDIFORD, M., HAND, M. & MCLAREN, S. 2001. Tectonic feedback, intraplate orogeny and the geochemical structure of the crust: a central Australian perspective. *Geol. Soc. Lond. Spec. Publ*. 184 (1), 195–218.

SCRIMGEOUR, I.R. AND RAITH, J.G. 2001. Tectonic and thermal events in the northeastern Arunta Province. Northern Territory Geological Survey. Report 12.

SHIELDS, G., AND VEIZER, J., 2002. Precambrian marine carbonate isotope database: Version 1.1. *Geochem. Geophy. Geosy*. 3, 1031.

SLÁMA, J., KOŠLER, J., CONDON, D.J., CROWLEY, J.L., GERDES, A., HANCHAR, J.M., HORSTWOOD, M.S.A., MORRIS, G.A., NASDALA, L., NORBERG, N., SCHALTEGGER, U., SCHOENE, B., TUBRETT, M. N. &

WHITEHOUSE, M. J. 2008. PLEŠOVICE ZIRCON—A NEW NATURAL REFERENCE MATERIAL FOR U–PB AND HF ISOTOPIC MICROANALYSIS. *CHEMICAL GEOLOGY*, **249**(1–2), 1-35.

TAYLOR, S. R. & MCLENNAN, S. M. 1985. The Continental Crust: Its Composition and Evolution, Blackwell Scientific Publications, Oxford, 1985.

VERMEESCH, P. 2013. Multi-sample comparison of detrital age distributions. *Chemical Geology*, **341**, 140-146.

WHELAN, J.A., BEYER, E.E., DONNELLAN, N., BLEEKERM W., CHAMBERLIN, K.R., SODERLUND, U. & ERNST R.E. 1.4 billion years of Northern Territory geology: Insights from collaborative U–Pb zircon and baddeleyite dating. Annual Geoscience Exploration Seminar (AGES) Proceedings, Alice Springs, Northern Territory 15–16 March 2016. Northern Territory Geological Survey, Darwin.

WOODHEAD, J., HERGT, J., SHELLEY, M., EGGINS, S. & KEMP, R. 2004. Zircon Hf-isotope analysis with an excimer laser, depth profiling, ablation of complex geometries, and concomitant age estimation. *Chemical Geology,* **209**(1–2), 121-135.

WORDEN, K. E., CLAOUÉ-LONG, J. C. AND SCRIMGEOUR, I. 2006. Summary of results: Joint NTGS-GA geochronology project: Pine Creek Orogen, Tanami Region, Arunta Region and Amadeus Basin, July-December 2004*. Northern Territory Geological Survey*, Darwin, N.T

YANG, B., SMITH, T.M., COLLINS, A.S., MUNSON, T.J., SCHOMAKER, B., NICHOLLS, D., COX, G.M., FARKAS, J. & GLORIE, S. 2018. Spatial and temporal variation in detrital zircon age provenance of the hydrocarbon-bearing upper Roper Group, Beetaloo Sub-basin, Northern Territory, Australia. *Precambrian Research* **304,** 140-155.

YANG, B., COLLINS, A.S., BLADES, M.L., CAPOGRECO, N., PAYNE, J.L., MUNSON, T.J. & COX, G.M. in review. Middle-late Mesoproterozoic tectonic geography of the North Australia Craton: U–Pb and Hf isotopes of detrital zircons in the Beetaloo Sub-basin, Northern Territory, Australia.

ZHANG, S., WANG, X., WANG, H., BJERRYM, C.J., HAMMARLUNG, E.U., MAFALDA COSTA, M., CONNELLY, J.N., ZHANG, B., SU, J. & CANFIELD D.E. 2016. Sufficient oxygen for animal respiration 1400 million years ago. P*roc. Natl. Acad. Sci.* **113**(7), 1731-1736.

ZHAO, J.X. AND BENNETT, V.C. 1995. SHRIMP U-Pb zircon geochronology of granites in the Arunta Inlier, central Australia: implications for Proterozoic crustal evolution. *Precambrian Research* **71**, 17-43.

ZHAO, J.X. AND MCCULLOCH, M.T. 1995. Geochemical and Nd isotopic systematics of granites from the Arunta Inlier, central Australia: implications for Proterozoic crustal evolution. In: Collins, W.J. and Shaw, R.D. (eds) Time Limits on Tectonic Events and Crustal Evolution Using Geochronology: Some Australian Examples. *Precambrian Research* **71**, 265-299.

PPENDIX A: SUPPLEMENTARY TABLES

Table 4. Supplementary Table Sm-Nd isotopic compositions of shale units throughout the Lower Roper.

Sample Name	Strat Depth	Formation	Est. Age (Myr)	[Nd]	[Sm]	Sm/Nd	147Sm/144Nd	143Nd/144Nd	error	eNd(0)	eNd(t)	eNd(t) error	Tdm	143Nd/144Nd(T)	CHUR(T)	eNd(T)	Lambda	e(Lambda*T)-1	147Sm/144Nd(T)
U5-149.1	149.1	Jalboi Fm	1450	26.2322795	4.414375033	0.168	0.101742146	0.511573369	0.000004	-20.77	-3.15	0.08	2.12	0.510604	0.510765	-3.15	6.54E-12	0.009528106	0.1066
U5-150.5	150.5	Jalboi Fm	1450	103.805438	17.71105054	0.171	0.103155388	0.511418641	0.000021	-23.79	-6.44	0.41	2.36	0.510436	0.510765	-6.44	6.54E-12	0.009528106	0.1080
U5-375.2	375.2	Crawford Sandstone	1450	68.7258361	10.28066805	0.150	0.090441769	0.511361219	0.000002	-24.91	-5.19	0.04	2.19	0.510499	0.510765	-5.19	6.54E-12	0.009528106	0.0953
U5-392.5	392.5	Crawford Sandstone	1450	41.840156	6.959002291	0.166	0.100559101	0.511431911	0.000002	-23.53	-5.70	0.04	2.29	0.510474	0.510765	-5.70	6.54E-12	0.009528106	0.1054
U5-412.45	412.45	Mainorou Fm/Showell Creek	1450	45.4478824	9.745541114	0.214	0.129646263	0.511418311	0.000002	-23.79	-11.39	0.04	3.09	0.510183	0.510765	-11.39	6.54E-12	0.009528106	0.1345
U5-448.5	448.5	Mainorou Fm/Wooden Duck	1450	45.8739225	7.423631467	0.162	0.097840402	0.511427816	0.000002	-23.61	-5.27	0.04	2.24	0.510496	0.510765	-5.27	6.54E-12	0.009528106	0.1027
U5-547.8	547.8	Mainorou Fm/Wooden Duck	1450	57.9254145	9.232973696	0.159	0.096369624	0.511331934	0.000002	-25.48	-6.87	0.04	2.34	0.510414	0.510765	-6.87	6.54E-12	0.009528106	0.1012
U5-571.2	571.2	Mainorou Fm/Wooden Duck	1450	40.2181195	6.539300954	0.163	0.098305375	0.511444272	0.000028	-23.29	-5.03	0.55	2.23	0.510508	0.510765	-5.03	6.54E-12	0.009528106	0.1032
U6-251.4	251.4	Mainorou Fm/Gibb	1450	59.9031874	12.79631077	0.214	0.129152419	0.511673135	0.000002	-18.82	-6.31	0.04	2.62	0.510443	0.510765	-6.31	6.54E-12	0.009528106	0.1340
U6-422.1	422.1	Mantugula Fm	1450	81.6486118	15.04505129	0.184	0.111407022	0.511538325	0.000001	-21.45	-5.64	0.02	2.37	0.510477	0.510765	-5.64	6.54E-12	0.009528106	0.1163

Table 5. Supplementary table Sm-Nd isotopic compositions of various shale units throughout the Lower Roper Group with associated Blank and Standard compositions.

sample	U5-150.5	U5-375.2	U5-392.5	U5-412.45	U5-448.5	U5-547.8	U5-571.2	U6-251.4	U6-422.1	U5-149.1	Sco-1	Blank
input age of rock T (Ma)	*1450*	*1450*	*1450*	*1450*	*1450*	*1450*	*1450*	*1450*	*1450*	*1450*	*0*	*0*
Unmixed 143/144Nd	**0.511419**	**0.511361**	**0.511432**	**0.511418**	**0.511428**	**0.511332**	**0.511444**	**0.511673**	**0.511538**	**0.511573**	**0.512081**	**#VALUE!**
Nd ugg^{-1}	**103.8**	**68.7**	**41.8**	**45.4**	**45.9**	**57.9**	**40.2**	**59.9**	**81.6**	**26.2**	**26**	**#VALUE!**
Sm ugg^{-1}	**17.7**	**10.3**	**7**	**9.7**	**7.4**	**9.2**	**6.5**	**12.8**	**15**	**4.4**	**5**	**#VALUE!**
147Sm/144N	**0.1032**	**0.0904**	**0.1006**	**0.1296**	**0.0978**	**0.0964**	**0.0983**	**0.1292**	**0.1114**	**0.1017**	**0.1166**	**#VALUE!**
eNd (T=0)	**-23.79**	**-24.91**	**-23.53**	**-23.79**	**-23.61**	**-25.48**	**-23.29**	**-18.82**	**-21.45**	**-20.77**	**-10.87**	**#VALUE!**
143Nd/144N	**0.510436**	**0.510499**	**0.510474**	**0.510183**	**0.510496**	**0.510414**	**0.510508**	**0.510443**	**0.510477**	**0.510604**	**0.512081**	**#VALUE!**
eNd (T)	**-6.44**	**-5.19**	**-5.7**	**-11.39**	**-5.27**	**-6.87**	**-5.03**	**-6.31**	**-5.64**	**-3.15**	**-10.87**	**#VALUE!**
TDM (Ma)	**2359**	**2189**	**2288**	**3089**	**2241**	**2335**	**2228**	**2623**	**2372**	**2123**	**1661**	**#VALUE!**
TCHUR (Ma)	**1982**	**1828**	**1908**	**2760**	**1862**	**1980**	**1846**	**2172**	**1961**	**1707**	**1061**	**#VALUE!**
DM at age o	**0.511106**	**0.511106**	**0.511106**	**0.511106**	**0.511106**	**0.511106**	**0.511106**	**0.511106**	**0.511106**	**0.511106**	**0.51315**	**0.51315**
CHUR at age	**0.510765**	**0.510765**	**0.510765**	**0.510765**	**0.510765**	**0.510765**	**0.510765**	**0.510765**	**0.510765**	**0.510765**	**0.512638**	**0.512638**
JNdi-1 Phoenix TIMS reference material measured 14/4/2018 to 21/4/2018, 143/144Nd = .512105 ± .000005 (2sd), 1												
Nd Model assumptions												
Lambda	6.54E-12	a^{-1}										
143Nd/144N	0.512638	Goldstein *et al* (1984)										
147Sm/144N	0.1966	Goldstein *et al* (1984)										
143Nd/144N	0.51315	Goldstein *et al* (1984)										
147Sm/144N	0.2145	Goldstein *et al* (1984)										
Earth Age	4.62E+09											
Sample measurements												
Sm Nd spik	H rm2	H rm2	H rm2	H rm2	H rm2	H rm2	H rm2	H rm2	H rm2	H rm2	H rm2	H rm2
sample wt	0.04723	0.05091	0.05812	0.04935	0.05085	0.04974	0.05456	0.05072	0.06928	0.05118	0.07893	0
Sm Nd spik	0.56385	0.50998	0.49174	0.50782	0.4982	0.5178	0.51355	0.50268	0.51303	0.49298	0.5883	0.06218
measured 143/144Nd	0.51145	0.511401	0.511487	0.51148	0.511486	0.511381	0.511508	0.511718	0.511563	0.511673	0.512158	3.965727
2 se	0.000021	0.000002	0.000002	0.000002	0.000002	0.000002	0.000028	0.000002	0.000001	0.000004	0.000002	0.117655
measured 150/144 Nd	0.375678	0.412836	0.480998	0.51019	0.494699	0.453844	0.51938	0.436618	0.346282	0.6797	0.582787	0
measured 147/149 Sm	3.883126	5.053532	6.01747	4.750985	6.385831	6.096503	6.892378	4.395725	3.136378	8.843603	7.021292	1.921127
measured 152/149 Sm	1.873956	1.889607	1.879926	2.343018	1.895176	1.706093	1.875595	1.809	1.882316	2.186805	1.895909	1.895909

Table 6. Hf results for sample L02 (Hodgson Sandstone) part 1 conducted using a New Wave UP-193 ArF excimer laser attached to a Thermo-Scientific Neptune Multi-Collector ICP-MS at the University of Adelaide.

Sample N	f176/Hf177	2 S.E.	µ176/Hf177	U/Pb AGE	Hf Chur (t)	Hf DM (t)	Hf NC(t)	Hf_i	Epsilon	2s	T(DM)	T(NC)
EC_L02_01	0.281579	2.77E-05	0.0007337	1724	0.281687	0.281995	0.281923	0.281555	-4.69	0.970114	2.67	2.518036
EC_L02_02	0.2816176	2.85E-05	0.0007045	1740	0.281677	0.281983	0.281911	0.281594	-2.92	0.998626	2.58	2.424365
EC_L02_03	0.2816551	3.22E-05	0.0011284	1793	0.281642	0.281944	0.281873	0.281617	-0.91	1.126818	2.5	2.345537
EC_L02_04	0.2816268	2.37E-05	0.0006888	1802	0.281637	0.281938	0.281866	0.281603	-1.18	0.829408	2.52	2.3691
EC_L02_04	0.2816064	3.12E-05	0.0013204	1705	0.281699	0.282009	0.281937	0.281564	-4.82	1.093014	2.67	2.510601
EC_L02_04	0.2819203	3.39E-05	0.0014465	1641	0.281741	0.282057	0.281983	0.281875	4.78	1.185122	2.03	1.875703
EC_L02_04	0.2815141	2.36E-05	0.0006371	1885	0.281583	0.281876	0.281805	0.281491	-3.25	0.825171	2.71	2.560785
EC_L02_05	0.2816212	2.50E-05	0.0007384	1748	0.281672	0.281978	0.281905	0.281597	-2.66	0.873287	2.57	2.41466
EC_L02_05	0.2817103	3.46E-05	0.0011747	1891	0.281579	0.281872	0.281801	0.281668	3.17	1.211705	2.33	2.178064
EC_L02_06	0.2814518	2.21E-05	0.0012133	1967	0.28153	0.281815	0.281746	0.281406	-4.37	0.775019	2.84	2.69423
EC_L02_07	0.2816146	3.28E-05	0.0010407	1975	0.281524	0.281809	0.28174	0.281576	1.82	1.147697	2.48	2.328193
EC_L02_09	0.2815771	2.86E-05	0.0006083	1751	0.28167	0.281975	0.281903	0.281557	-4	1.002564	2.65	2.49832
EC_L02_10	0.2816676	3.16E-05	0.0018475	1779	0.281652	0.281955	0.281883	0.281605	-1.64	1.1061	2.53	2.37826
EC_L02_11	0.2816322	2.57E-05	0.000593	1776	0.281653	0.281957	0.281885	0.281612	-1.46	0.899375	2.52	2.365128
EC_L02_12	0.2814249	3.57E-05	0.0011406	1712	0.281695	0.282004	0.281932	0.281388	-10.9	1.249579	3.04	2.881951
EC_L02_14	0.2816503	3.56E-05	0.0011372	1762	0.281663	0.281967	0.281895	0.281612	-1.78	1.245344	2.53	2.372951
EC_L02_16	0.2815881	3.27E-05	0.001091	1909	0.281567	0.281858	0.281788	0.281549	-0.66	1.143046	2.57	2.42434
EC_L02_17	0.2815788	2.77E-05	0.0008795	1744	0.281674	0.28198	0.281908	0.28155	-4.42	0.970826	2.67	2.517894
EC_L02_18	0.281294	2.31E-05	0.000812	2500	0.281181	0.281417	0.281354	0.281255	2.63	0.809825	2.84	2.709049
EC_L02_19	0.281912	3.25E-05	0.0007612	1595	0.28177	0.282091	0.282017	0.281889	4.21	1.137116	2.03	1.872934
EC_L02_20	0.2816282	2.91E-05	0.0006524	1732	0.281682	0.281989	0.281917	0.281607	-2.67	1.018453	2.56	2.402481
EC_L02_21	0.2825127	1.55E-05	2.29E-05	1753	0.281668	0.281974	0.281902	0.282512	29.95	0.543224	0.57	0.410418
EC_L02_22	0.2816044	3.40E-05	0.0009236	1761	0.281663	0.281968	0.281896	0.281574	-3.18	1.189163	2.61	2.456831
EC_L02_25	0.2817549	2.48E-05	0.000523	1835	0.281615	0.281913	0.281842	0.281737	4.31	0.868328	2.22	2.06285
EC_L02_27	0.2815116	2.40E-05	0.0004191	1933	0.281552	0.28184	0.28177	0.281496	-1.97	0.840685	2.67	2.522401
EC_L02_28	0.2816275	2.96E-05	0.0009464	1796	0.28164	0.281942	0.28187	0.281595	-1.6	1.035631	2.54	2.389781
EC_L02_31	0.2816012	3.25E-05	0.0008543	1777	0.281653	0.281956	0.281884	0.281572	-2.86	1.139195	2.6	2.450033

Table 7. Hf results for sample L02 (Hodgson Sandstone) part 2 conducted using a New Wave UP-193 ArF excimer laser attached to a Thermo-Scientific Neptune Multi-Collector ICP-MS at the University of Adelaide.

Sample N	f176/Hf177	2 S.E.	µ176/Hf177	U/Pb AGE	Hf Chur (t)	Hf DM (t)	Hf NC(t)	Hf_i	Epsilon	2s	T(DM)	T(NC)
EC_L02_32	0.2815575	3.11E-05	0.0010124	1848	0.281607	0.281903	0.281833	0.281522	-3.01	1.090097	2.67	2.516698
EC_L02_33	0.2816496	2.43E-05	0.0008215	1724	0.281687	0.281995	0.281923	0.281623	-2.29	0.849837	2.53	2.372789
EC_L02_35	0.2816248	2.65E-05	0.0007418	1777	0.281653	0.281956	0.281884	0.2816	-1.88	0.927358	2.54	2.391115
EC_L02_36	0.2816038	2.07E-05	0.000317	2047	0.281477	0.281756	0.281687	0.281591	4.05	0.723037	2.4	2.252463
EC_L02_37	0.2816785	2.94E-05	0.0008872	1879	0.281587	0.28188	0.28181	0.281647	2.14	1.030498	2.38	2.230641
EC_L02_39	0.2819413	2.96E-05	0.0008857	1570	0.281787	0.282109	0.282035	0.281915	4.56	1.036918	1.99	1.831142
EC_L02_41	0.2816096	2.35E-05	0.0007466	1762	0.281663	0.281967	0.281895	0.281585	-2.76	0.82153	2.59	2.432399
EC_L02_42	0.2816927	2.69E-05	0.00123	1772	0.281656	0.28196	0.281888	0.281651	-0.16	0.940206	2.44	2.283179
EC_L02_43	0.2813213	2.25E-05	0.0007845	2285	0.281322	0.281578	0.281512	0.281287	-1.25	0.787185	2.9	2.764524
EC_L02_44	0.2815908	2.25E-05	0.0003262	1798	0.281639	0.281941	0.281869	0.28158	-2.11	0.787279	2.58	2.422219
EC_L02_45	0.2816341	2.37E-05	0.000528	1758	0.281665	0.28197	0.281898	0.281616	-1.73	0.828957	2.52	2.366448
EC_L02_52	0.2815656	2.32E-05	0.0003688	1857	0.281601	0.281897	0.281826	0.281553	-1.72	0.810946	2.6	2.445906
EC_L02_53	0.2812952	3.77E-05	0.0017605	2359	0.281274	0.281523	0.281458	0.281216	-2.05	1.319101	3.01	2.872639
EC_L02_55	0.2816254	2.68E-05	0.0004351	1751	0.28167	0.281975	0.281903	0.281611	-2.08	0.93935	2.54	2.382319
EC_L02_56	0.2811888	2.41E-05	0.0006119	2445	0.281217	0.281458	0.281394	0.28116	-2.03	0.842837	3.08	2.941067
EC_L02_57	0.2816564	3.03E-05	0.0009132	1710	0.281696	0.282006	0.281933	0.281627	-2.46	1.059079	2.53	2.372301
EC_L02_58	0.2815227	2.46E-05	0.0006915	1852	0.281604	0.281901	0.28183	0.281498	-3.76	0.861062	2.72	2.564704
EC_L02_59	0.281596	3.08E-05	0.0008679	1717	0.281692	0.282	0.281928	0.281568	-4.4	1.077845	2.65	2.494935
EC_L02_103	0.2816318	2.56E-05	0.0007338	1787	0.281646	0.281949	0.281877	0.281607	-1.4	0.895335	2.52	2.369964
EC_L02_104	0.2816768	2.59E-05	0.000749	1749	0.281671	0.281977	0.281905	0.281652	-0.67	0.906841	2.45	2.295406
EC_L02_105	0.2815388	2.77E-05	0.0010737	1843	0.28161	0.281907	0.281836	0.281501	-3.86	0.970851	2.72	2.563878

Table 8. Hf results for sample L02 (Hodgson Sandstone) part 3 conducted using a New Wave UP-193 ArF excimer laser attached to a Thermo-Scientific Neptune Multi-Collector ICP-MS at the University of Adelaide.

Sample N	f176/Hf177	2 S.E.	µ176/Hf177	U/Pb AGE	Hf Chur (t)	Hf DM (t)	Hf NC(t)	Hf_i	Epsilon	2s	T(DM)	T(NC)
EC_L02_108	0.2815975	2.51E-05	0.0007387	1753	0.281668	0.281974	0.281902	0.281573	-3.39	0.877729	2.62	2.462668
EC_L02_109	0.281626	2.50E-05	0.0007949	1763	0.281662	0.281966	0.281894	0.281599	-2.22	0.875439	2.55	2.400179
EC_L02_110	0.2815733	3.29E-05	0.0006397	1722	0.281688	0.281997	0.281924	0.281552	-4.83	1.15132	2.68	2.524784
EC_L02_111	0.281619	2.13E-05	0.0006864	1728	0.281685	0.281992	0.28192	0.281597	-3.12	0.747144	2.58	2.426773
EC_L02_112	0.2816945	2.91E-05	0.0011159	1743	0.281675	0.281981	0.281909	0.281658	-0.61	1.018623	2.44	2.28672
EC_L02_113	0.2816408	2.74E-05	0.0007573	1775	0.281654	0.281958	0.281886	0.281615	-1.38	0.957423	2.51	2.358922
EC_L02_116	0.2811741	2.74E-05	0.0007566	2385	0.281257	0.281503	0.281439	0.28114	-4.16	0.959973	3.16	3.0189
EC_L02_63	0.2815945	2.89E-05	0.0008315	1755	0.281667	0.281972	0.2819	0.281567	-3.56	1.012441	2.63	2.47477
EC_L02_69	0.2816478	6.35E-05	0.0022506	1837	0.281614	0.281912	0.281841	0.281569	-1.58	2.222886	2.57	2.421585
EC_L02_72	0.2815543	2.16E-05	0.0004349	1982	0.28152	0.281804	0.281735	0.281538	0.64	0.757022	2.55	2.404862
EC_L02_84	0.2815708	2.83E-05	0.0009929	1712	0.281695	0.282004	0.281932	0.281539	-5.55	0.990433	2.72	2.560433
EC_L02_88	0.2818141	2.91E-05	0.0012517	1658	0.28173	0.282044	0.281971	0.281775	1.6	1.019761	2.24	2.083709
EC_L02_91	0.2816482	2.89E-05	0.0007515	1818	0.281626	0.281926	0.281854	0.281622	-0.14	1.012147	2.47	2.318957
EC_L02_99	0.2817601	2.20E-05	0.000903	1718	0.281691	0.282	0.281927	0.281731	1.41	0.770718	2.3	2.143764

Table 9. Hf results for sample U501 (Hodgson Sandstone) part 1 conducted using a New Wave UP-193 ArF excimer laser attached to a Thermo-Scientific Neptune Multi-Collector ICP-MS at the University of Adelaide.

Sample N	f176/Hf177	2 S.E.	u176/Hf177	U/Pb AGE	Hf Chur (t)	Hf DM (t)	Hf NC(t)	Hf_i	Epsilon	2s	T(DM)	T(NC)
EC_U501_1	0.281601	2.82E-05	0.0007424	2023	0.281493	0.281774	0.281705	0.281572	2.82	0.987406	2.45	2.307032
EC_U501_1	0.2813362	2.39E-05	0.0005769	2342	0.281285	0.281536	0.28147	0.28131	0.91	0.836841	2.82	2.682358
EC_U501_1	0.2816285	3.45E-05	0.0008352	1855	0.281602	0.281898	0.281827	0.281599	-0.11	1.207375	2.5	2.347212
EC_U501_1	0.2816768	4.31E-05	0.0015434	1778	0.281652	0.281955	0.281884	0.281625	-0.97	1.510177	2.49	2.337048
EC_U501_1	0.2810945	2.83E-05	0.0006689	2523	0.281166	0.2814	0.281337	0.281062	-3.69	0.989238	3.24	3.102848
EC_U501_1	0.2816403	2.90E-05	0.0007481	2826	0.280967	0.281172	0.281112	0.2816	22.54	1.014851	1.92	1.790076
EC_U501_1	0.2810546	3.20E-05	0.0010738	1780	0.281651	0.281954	0.281882	0.281018	-22.46	1.118741	3.77	3.623332
EC_U501_2	0.2815203	2.84E-05	0.0005303	1938	0.281548	0.281837	0.281767	0.281501	-1.69	0.993614	2.66	2.509769
EC_U501_2	0.2808131	3.88E-05	0.0015173	3194	0.280723	0.280893	0.280838	0.28072	-0.1	1.356387	3.55	3.438992
EC_U501_3	0.2814782	2.69E-05	0.0007204	1838	0.281613	0.281911	0.28184	0.281453	-5.69	0.941779	2.82	2.66972
EC_U501_3	0.2817157	2.56E-05	0.0013716	1750	0.28167	0.281976	0.281904	0.28167	0	0.896993	2.41	2.255621

Table 10. Hf results for sample U501 (Hodgson Sandstone) part 2 conducted using a New Wave UP-193 ArF excimer laser attached to a Thermo-Scientific Neptune Multi-Collector ICP-MS at the University of Adelaide.

Sample N	f176/Hf177	2 S.E.	u176/Hf177	U/Pb AGE	Hf Chur (t)	Hf DM (t)	Hf NC(t)	Hf_i	Epsilon	2s	T(DM)	T(NC)
EC_U501_4	0.281734	4.06E-05	0.0010867	1767	0.281659	0.281963	0.281892	0.281698	1.36	1.422435	2.34	2.186775
EC_U501_4	0.2818798	2.90E-05	0.0011448	1665	0.281725	0.282039	0.281966	0.281844	4.2	1.014176	2.09	1.930497
EC_U501_4	0.2816139	2.98E-05	0.0009813	1834	0.281616	0.281914	0.281843	0.28158	-1.28	1.044153	2.55	2.401067
ec_u501_6	0.2816583	3.04E-05	0.0007005	1749	0.281671	0.281977	0.281905	0.281635	-1.27	1.062426	2.49	2.331742
EC_U501_6	0.2816176	2.82E-05	0.0007811	2470	0.281201	0.28144	0.281376	0.281581	13.51	0.986862	2.17	2.032669
EC_U501_6	0.2818326	8.64E-05	0.0043666	1768	0.281659	0.281963	0.281891	0.281686	0.98	3.024681	2.37	2.210645
EC_U501_6	0.2814759	3.42E-05	0.0008724	1753	0.281668	0.281974	0.281902	0.281447	-7.86	1.198388	2.89	2.7324
EC_U501_6	0.2816264	3.00E-05	0.0008554	1755	0.281667	0.281972	0.2819	0.281598	-2.45	1.049698	2.56	2.407942
EC_U501_7	0.2816226	3.58E-05	0.0011636	1832	0.281617	0.281915	0.281844	0.281582	-1.24	1.254254	2.55	2.397068
EC_U501_8	0.2815906	2.90E-05	0.0007219	1757	0.281666	0.281971	0.281899	0.281567	-3.52	1.016196	2.63	2.474091
EC_U501_8	0.281622	3.03E-05	0.0006676	1735	0.28168	0.281987	0.281915	0.2816	-2.84	1.060141	2.57	2.41504
EC_U501_9	0.2815988	3.77E-05	0.0005957	1710	0.281696	0.282006	0.281933	0.281579	-4.14	1.319443	2.63	2.473879
EC_U501_9	0.2816385	3.23E-05	0.0007738	1695	0.281706	0.282017	0.281944	0.281614	-3.28	1.129867	2.57	2.40937
EC_U501_9	0.2816099	2.63E-05	0.0006016	1698	0.281704	0.282015	0.281942	0.28159	-4.03	0.920316	2.61	2.457233
EC_U501_9	0.2818982	3.73E-05	0.001275	1591	0.281773	0.282094	0.28202	0.28186	3.08	1.304797	2.1	1.938764

Table 11. Hf results for sample U507 (Crawford Formation) conducted using a New Wave UP-193 ArF excimer laser attached to a Thermo-Scientific Neptune Multi-Collector ICP-MS at the University of Adelaide.

Sample N	f176/Hf177	2 S.E.	ı176/Hf177	U/Pb AGE	Hf Chur (t)	Hf DM (t)	Hf NC(t)	Hf_i	Epsilon	2s	T(DM)	T(NC)
EC_U507_0	0.2816277	2.91E-05	0.0009593	1786	0.281647	0.281949	0.281878	0.281595	-1.84	1.017033	2.55	2.395801
EC_U507_0	0.2816248	2.95E-05	0.0006258	2601	0.281115	0.281341	0.281279	0.281594	17.03	1.032831	2.06	1.930551
EC_U507_0	0.2811032	2.65E-05	0.0006279	1843	0.28161	0.281907	0.281836	0.281081	-18.78	0.926458	3.6	3.45455
EC_U507_0	0.2812828	2.55E-05	0.0009678	1825	0.281622	0.281921	0.281849	0.281249	-13.22	0.892247	3.26	3.11041
EC_U507_0	0.2813674	2.54E-05	0.0005769	1917	0.281562	0.281852	0.281782	0.281346	-7.66	0.888913	3	2.850858
EC_U507_1	0.2816907	3.64E-05	0.002084	1766	0.28166	0.281964	0.281892	0.281621	-1.39	1.273788	2.51	2.352247
EC_U507_1	0.281512	2.15E-05	0.000572	1898	0.281574	0.281866	0.281796	0.281491	-2.95	0.753317	2.7	2.55306
EC_U507_1	0.2815046	2.52E-05	0.0007916	1840	0.281612	0.281909	0.281838	0.281477	-4.8	0.881461	2.77	2.617628
EC_U507_1	0.2815835	2.92E-05	0.000912	2855	0.280947	0.28115	0.281091	0.281534	20.87	1.023046	2.04	1.915519
EC_U507_1	0.2816076	2.08E-05	0.0006916	1926	0.281556	0.281846	0.281776	0.281582	0.93	0.726694	2.49	2.342098
EC_U507_1	0.2815264	2.70E-05	0.0004493	2058	0.28147	0.281747	0.281679	0.281509	1.37	0.946482	2.57	2.423202

Table 12. Hf results for sample U503 (Jalboi Formation) conducted using a New Wave UP-193 ArF excimer laser attached to a Thermo-Scientific Neptune Multi-Collector ICP-MS at the University of Adelaide.

Sample N	f176/Hf177	2 S.E.	ı176/Hf177	U/Pb AGE	Hf Chur (t)	Hf DM (t)	Hf NC(t)	Hf_i	Epsilon	2s	T(DM)	T(NC)
EC_U503_0	0.2814868	3.40E-05	0.001211	1862	0.281598	0.281893	0.281822	0.281444	-5.46	1.18835	2.83	2.675111
EC_U503_0	0.2816401	2.82E-05	0.0005197	1819	0.281626	0.281925	0.281854	0.281622	-0.12	0.985592	2.47	2.318607
EC_U503_0	0.281629	2.10E-05	0.0004495	1771	0.281657	0.281961	0.281889	0.281614	-1.52	0.733351	2.52	2.364282
EC_U503_1	0.2813669	2.93E-05	0.0005508	2536	0.281158	0.28139	0.281327	0.28134	6.49	1.024106	2.64	2.508341
EC_U503_1	0.2817025	2.72E-05	0.0010506	1842	0.281611	0.281908	0.281837	0.281666	1.96	0.951668	2.36	2.211465
EC_U503_1	0.2815944	3.11E-05	0.0003538	1858	0.2816	0.281896	0.281825	0.281582	-0.65	1.090191	2.53	2.382366
EC_U503_1	0.2816273	3.79E-05	0.0008017	1699	0.281703	0.282014	0.281941	0.281602	-3.61	1.327202	2.59	2.433012
EC_U503_2	0.2815472	2.50E-05	0.0004621	1810	0.281631	0.281932	0.28186	0.281531	-3.55	0.873889	2.67	2.518664
EC_U503_2	0.281659	3.15E-05	0.0012153	1715	0.281693	0.282002	0.281929	0.28162	-2.61	1.102698	2.54	2.384972
EC_U503_3	0.2813991	2.31E-05	0.0005376	2426	0.28123	0.281473	0.281408	0.281374	5.13	0.807601	2.64	2.498897
EC_U503_3	0.2815079	3.47E-05	0.0018287	2007	0.281503	0.281785	0.281716	0.281438	-2.32	1.212881	2.75	2.603565
EC_U503_4	0.2815392	3.22E-05	0.001334	2562	0.281141	0.281371	0.281308	0.281474	11.86	1.126128	2.34	2.209029
EC_U503_4	0.2815137	2.81E-05	0.000993	1754	0.281668	0.281973	0.281901	0.281481	-6.64	0.984563	2.81	2.659772
EC_U503_5	0.2813258	3.22E-05	0.0019307	1961	0.281533	0.28182	0.28175	0.281254	-9.93	1.125603	3.17	3.021661

Table 13. Hf results for sample U602 (Limmen Formation) conducted using a New Wave UP-193 ArF excimer laser attached to a Thermo-Scientific Neptune Multi-Collector ICP-MS at the University of Adelaide.

Sample N	f176/Hf177	2 S.E.	µ176/Hf177	U/Pb AGE	Hf Chur (t)	Hf DM (t)	Hf NC(t)	Hf_i	Epsilon	2s	T(DM)	T(NC)
EC_U602_0	0.2816049	3.43E-05	0.0014404	1919	0.281561	0.281851	0.281781	0.281552	-0.3	1.20026	2.56	2.410308
EC_U602_0	0.2805392	2.70E-05	0.0011207	3378	0.2806	0.280753	0.2807	0.280466	-4.77	0.946273	3.97	3.859707
EC_U602_0	0.2816141	2.71E-05	0.0010688	1877	0.281588	0.281882	0.281811	0.281576	-0.42	0.949522	2.54	2.383993
EC_U602_0	0.2816153	3.53E-05	0.0011306	1834	0.281616	0.281914	0.281843	0.281576	-1.42	1.236483	2.56	2.409226
EC_U602_1	0.281579	2.87E-05	0.0008166	2042	0.281481	0.281759	0.281691	0.281547	2.36	1.005323	2.5	2.350071
EC_U602_1	0.2815866	3.39E-05	0.0010545	1813	0.281629	0.281929	0.281858	0.28155	-2.81	1.184798	2.63	2.476346
EC_U602_1	0.2814807	3.22E-05	0.0015676	1951	0.28154	0.281827	0.281757	0.281423	-4.17	1.125495	2.82	2.669076
EC_U602_1	0.2809381	3.12E-05	0.0018916	1982	0.28152	0.281804	0.281735	0.280867	-23.19	1.092968	3.97	3.822642
EC_U602_2	0.2808958	2.70E-05	0.0007135	2914	0.280908	0.281105	0.281047	0.280856	-1.87	0.946488	3.43	3.313224
EC_U602_2	0.2815455	4.01E-05	0.0012702	2099	0.281444	0.281717	0.281649	0.281495	1.82	1.405174	2.57	2.429389
EC_U602_2	0.281687	3.11E-05	0.0013857	1794	0.281642	0.281943	0.281872	0.28164	-0.07	1.087217	2.45	2.295126
EC_U602_2	0.2814057	3.21E-05	0.0015095	1862	0.281598	0.281893	0.281822	0.281352	-8.71	1.124985	3.02	2.870183
EC_U602_3	0.281344	2.69E-05	0.0013081	2005	0.281505	0.281787	0.281718	0.281294	-7.48	0.941099	3.06	2.910963
EC_U602_3	0.2816201	2.60E-05	0.0014563	2285	0.281322	0.281578	0.281512	0.281557	8.34	0.909923	2.33	2.190042
EC_U602_3	0.2810965	2.42E-05	0.0005123	2010	0.281502	0.281783	0.281714	0.281077	-15.08	0.84568	3.51	3.366648
EC_U602_3	0.2817534	2.35E-05	0.0006981	1692	0.281708	0.282019	0.281946	0.281731	0.82	0.823073	2.32	2.158252
EC_U602_4	0.2815558	2.46E-05	0.0012465	1937	0.281549	0.281837	0.281768	0.28151	-1.39	0.860377	2.64	2.490768

Table 14. Hf results for sample U603 (Limmen Formation) conducted using a New Wave UP-193 ArF excimer laser attached to a Thermo-Scientific Neptune Multi-Collector ICP-MS at the University of Adelaide.

Sample N	f176/Hf177	2 S.E.	µ176/Hf177	U/Pb AGE	Hf Chur (t)	Hf DM (t)	Hf NC(t)	Hf_i	Epsilon	2s	T(DM)	T(NC)
EC_U603_0	0.2815991	2.66E-05	0.000935	1796	0.28164	0.281942	0.28187	0.281567	-2.6	0.932489	2.6	2.449938
EC_U603_0	0.2816191	2.24E-05	0.0007789	1816	0.281628	0.281927	0.281856	0.281592	-1.25	0.784869	2.54	2.384637
EC_U603_0	0.2816573	2.55E-05	0.0008886	1834	0.281616	0.281914	0.281843	0.281626	0.38	0.893675	2.45	2.300809
EC_U603_2	0.2814681	2.82E-05	0.0008555	1780	0.281651	0.281954	0.281882	0.281439	-7.51	0.987719	2.89	2.733004

Table 15. Hf results for sample U506 (Arnold Sandstone) conducted using a New Wave UP-193 ArF excimer laser attached to a Thermo-Scientific Neptune Multi-Collector ICP-MS at the University of Adelaide.

Sample N	f176/Hf177	2 S.E.	µ176/Hf177	U/Pb AGE	Hf Chur (t)	Hf DM (t)	Hf NC(t)	Hf_i	Epsilon	2s	T(DM)	T(NC)
U506-01	0.2816215	3.46E-05	0.0007812	1724	0.281687	0.281995	0.281923	0.281596	-3.23	1.209688	2.59	2.430246
U506-03	0.2816196	2.15E-05	0.0005638	1749	0.281671	0.281977	0.281905	0.281601	-2.49	0.752224	2.56	2.405161
U506-04	0.2816552	2.27E-05	0.0008503	1725	0.281686	0.281995	0.281922	0.281627	-2.1	0.793153	2.52	2.362232
U506-05	0.2816049	3.24E-05	0.001004	1728	0.281685	0.281992	0.28192	0.281572	-4	1.134242	2.63	2.47943
U506-06	0.2817086	4.13E-05	0.0007467	1757	0.281666	0.281971	0.281899	0.281684	0.64	1.444216	2.38	2.222302
U506-07	0.2817291	6.70E-05	0.0008984	1807	0.281633	0.281934	0.281862	0.281698	2.31	2.346305	2.32	2.161772

Table 16. Hf results for sample BR04 (Munyi Member) conducted using a New Wave UP-193 ArF excimer laser attached to a Thermo-Scientific Neptune Multi-Collector ICP-MS at the University of Adelaide.

Sample N	f176/Hf177	2 S.E.	u176/Hf177	U/Pb AGE	Hf Chur (t)	Hf DM (t)	Hf NC(t)	Hf_i	Epsilon	2s	T(DM)	T(NC)
BR04-01	0.2816101	3.09E-05	0.000965	1976	0.281524	0.281808	0.281739	0.281574	1.78	1.081347	2.48	2.33128
BR04-04	0.2818382	3.25E-05	0.0011251	1778	0.281652	0.281955	0.281884	0.2818	5.26	1.137645	2.11	1.95854
BR04-16	0.2816033	2.65E-05	0.000682	1946	0.281543	0.281831	0.281761	0.281578	1.24	0.927078	2.49	2.339454
BR04-21	0.2816302	2.66E-05	0.0011048	1927	0.281556	0.281845	0.281775	0.28159	1.22	0.931613	2.48	2.325437
BR04-24	0.2816037	3.11E-05	0.0006434	1736	0.281679	0.281986	0.281914	0.281582	-3.44	1.087898	2.61	2.452235
BR04-33	0.2816037	3.11E-05	0.0006434	1803	0.281636	0.281937	0.281865	0.281582	-1.93	1.087898	2.57	2.414972

Table 17. Hf results for sample GSD302 (Limmen Formation) conducted using a New Wave UP-193 ArF excimer laser attached to a Thermo-Scientific Neptune Multi-Collector ICP-MS at the University of Adelaide.

Sample N	f176/Hf177	2 S.E.	u176/Hf177	U/Pb AGE	Hf Chur (t)	Hf DM (t)	Hf NC(t)	Hf_i	Epsilon	2s	T(DM)	T(NC)
GSD3-02-1	0.2816921	4.20E-05	0.0029936	2567	0.281137	0.281367	0.281304	0.281545	14.51	1.468317	2.19	2.053423
GSD3-02-1	0.2816568	2.95E-05	0.0011921	2560	0.281142	0.281372	0.28131	0.281598	16.24	1.031114	2.08	1.943446
GSD3-02-1	0.2816513	5.22E-05	0.0029931	1922	0.281559	0.281849	0.281778	0.281542	-0.59	1.825829	2.58	2.430783
GSD3-02-1	0.2816754	3.26E-05	0.0025732	1768	0.281659	0.281963	0.281891	0.281589	-2.47	1.141253	2.57	2.419393
GSD3-02-1	0.2815951	4.72E-05	0.0022789	1859	0.2816	0.281895	0.281824	0.281515	-3.02	1.651429	2.68	2.52583
GSD3-02-1	0.2812519	2.72E-05	0.0013268	1880	0.281586	0.28188	0.281809	0.281205	-13.55	0.951698	3.32	3.173101
GSD3-02-1	0.2817017	4.78E-05	0.0022058	1820	0.281625	0.281924	0.281853	0.281626	0.02	1.67447	2.46	2.310824
GSD3-02-1	0.2816251	3.17E-05	0.0022549	2506	0.281177	0.281413	0.281349	0.281517	12.09	1.110115	2.28	2.148315
GSD3-02-1	0.2816956	2.88E-05	0.0013098	1745	0.281674	0.28198	0.281908	0.281652	-0.76	1.008267	2.45	2.297142
GSD3-02-1	0.281724	3.09E-05	0.0008291	1813	0.281629	0.281929	0.281858	0.281695	2.34	1.081237	2.32	2.164516
GSD3-02-3	0.2814823	1.93E-05	0.0003789	1726	0.281686	0.281994	0.281921	0.28147	-7.66	0.674655	2.85	2.698992
GSD3-02-3	0.2817355	3.02E-05	0.0009616	1752	0.281669	0.281975	0.281902	0.281704	1.23	1.056475	2.34	2.182619
GSD3-02-3	0.2816228	4.49E-05	0.0022196	1795	0.281641	0.281943	0.281871	0.281547	-3.33	1.572184	2.65	2.493333
GSD3-02-4	0.2815319	0.000113	0.0078595	1784	0.281648	0.281951	0.281879	0.281266	-13.57	3.964	3.25	3.09893
GSD3-02-4	0.2817135	3.37E-05	0.001734	1831	0.281618	0.281916	0.281845	0.281653	1.26	1.178417	2.4	2.244784
GSD3-02-5	0.281512	2.42E-05	0.0009847	1898	0.281574	0.281866	0.281796	0.281477	-3.47	0.846189	2.73	2.584784
GSD3-02-5	0.2816684	4.38E-05	0.0024853	1543	0.281804	0.282129	0.282054	0.281596	-7.39	1.53406	2.7	2.536613
GSD3-02-5	0.2813291	2.94E-05	0.0021816	1815	0.281628	0.281928	0.281857	0.281254	-13.29	1.027705	3.26	3.106226
GSD3-02-6	0.281621	7.11E-05	0.0040843	1840	0.281612	0.281909	0.281838	0.281478	-4.74	2.487485	2.77	2.614357
GSD3-02-6	0.2816596	2.82E-05	0.000863	1800	0.281638	0.281939	0.281868	0.28163	-0.28	0.986016	2.47	2.312702
GSD3-02-6	0.2815669	4.43E-05	0.0027543	2547	0.28115	0.281382	0.281319	0.281433	10.05	1.549317	2.44	2.305057
GSD3-02-7	0.2815382	3.66E-05	0.0024826	1851	0.281605	0.281901	0.28183	0.281451	-5.46	1.280688	2.82	2.666612
GSD3-02-8	0.2816928	3.22E-05	0.0012872	2078	0.281457	0.281733	0.281664	0.281642	6.56	1.125998	2.27	2.12606

Table 18. Hf results for sample GSD301 (Limmen Formation) conducted using a New Wave UP-193 ArF excimer laser attached to a Thermo-Scientific Neptune Multi-Collector ICP-MS at the University of Adelaide.

Sample N	f176/Hf177	2 S.E.	ı176/Hf177	U/Pb AGE	Hf Chur (t)	Hf DM (t)	Hf NC(t)	Hf_i	Epsilon	2s	T(DM)	T(NC)
GSD03_01	0.2816714	2.81E-05	0.0018072	1800	0.281638	0.281939	0.281868	0.28161	-1	0.984449	2.51	2.356548
GSD03_01	0.2815807	3.88E-05	0.001661	1841	0.281611	0.281909	0.281838	0.281523	-3.15	1.357971	2.67	2.519151
GSD03_01	0.2812637	1.98E-05	0.0012214	1706	0.281699	0.282009	0.281936	0.281224	-16.85	0.692383	3.39	3.2329
GSD03_01	0.2816899	2.73E-05	0.0006757	1808	0.281633	0.281933	0.281862	0.281667	1.21	0.956432	2.38	2.229251
GSD03_01	0.2813017	2.52E-05	0.0003306	1876	0.281589	0.281883	0.281812	0.28129	-10.61	0.881293	3.14	2.994641
GSD03_01	0.2816804	2.71E-05	0.0006502	1676	0.281718	0.282031	0.281958	0.28166	-2.07	0.948109	2.48	2.321277
GSD03_01	0.2812769	3.12E-05	0.0005902	1735	0.28168	0.281987	0.281915	0.281257	-15	1.090982	3.3	3.145535
GSD03_01	0.2816809	2.44E-05	0.0006097	1831	0.281618	0.281916	0.281845	0.28166	1.49	0.854601	2.38	2.230899
GSD03_01	0.2815155	3.94E-05	0.0015548	1622	0.281753	0.282071	0.281997	0.281468	-10.13	1.377421	2.92	2.764489
GSD03_01	0.2818129	0.000108	0.0079062	1901	0.281572	0.281864	0.281794	0.281528	-1.59	3.795655	2.62	2.473884
GSD03_01	0.2816106	2.55E-05	0.0005982	1897	0.281575	0.281867	0.281797	0.281589	0.5	0.893737	2.5	2.344367
GSD03_01	0.2816195	9.30E-05	0.0049184	1829	0.281619	0.281918	0.281846	0.281449	-6.05	3.254372	2.84	2.684038

Table 19. All U–Pb data for sample GSD302 (Limmen Sandstone)

Analysis	$^{207}Pb/^{235}U$		$^{206}Pb/^{238}U$		rho	Conc (%)	$^{207}Pb/^{206}Pb$			$^{206}Pb/^{238}U$	
GSD302											
GSD302_32	4.946	0.15	0.3327	0.0096	0.323	105.9361		1752	78	1856	44
GSD302_87	6.96	0.25	0.3878	0.012	0.48814	101.9249		2078	76	2118	52
GSD302_74	5.26	0.19	0.3363	0.01	0.76513	100.8644		1851	76	1867	50
GSD302_33	6.86	0.22	0.388	0.011	0.61872	101.7831		2075	72	2112	52
GSD302_69	11.48	0.33	0.4947	0.013	0.58067	101.6883		2547	64	2590	56
GSD302_171	5.03	0.19	0.3316	0.011	0.70165	101.7099		1813	79	1844	53
GSD302_43	4.76	0.16	0.3176	0.0083	0.3986	99.60762		1784	73	1777	41
GSD302_53	5.44	0.22	0.3396	0.0099	0.60255	99.20969		1898	81	1883	47
GSD302_118	11.22	0.32	0.474	0.013	0.36604	97.8125		2560	65	2504	53
GSD302_22	4.82	0.15	0.3159	0.0082	0.0248	98.11425		1803	80	1769	40
GSD302_35	4.81	0.19	0.3176	0.0086	0.40644	98.99721		1795	86	1777	42
GSD302_128	4.62	0.17	0.3118	0.0096	0.15469	99.15158		1768	91	1753	46
GSD302_64	5	0.14	0.3226	0.0079	0.38109	98.09783		1840	68	1805	40
GSD302_54	10.89	0.35	0.4724	0.014	0.65902	97.99449		2543	66	2492	60
GSD302_6	5.78	0.18	0.3447	0.0093	0.60043	96.75456		1972	70	1908	44
GSD302_105	11.1	0.35	0.4649	0.013	0.72043	95.79275		2567	67	2459	56
GSD302_66	4.67	0.18	0.3044	0.0097	0.5986	95.11111		1800	83	1712	48
GSD302_94	4.92	0.15	0.3125	0.0093	0.73922	94.44744		1855	75	1752	46
GSD302_136	4.71	0.17	0.305	0.011	0.38512	94.17582		1820	91	1714	56
GSD302_163	4.34	0.16	0.2951	0.01	0.68351	95.35817		1745	78	1664	51
GSD302_31	4.2	0.2	0.2854	0.011	0.75822	93.68482		1726	81	1617	53
GSD302_134	5.01	0.18	0.3188	0.009	0.39701	94.84043		1880	81	1783	44
GSD302_75	4.73	0.16	0.3029	0.01	0.40946	92.93862		1841	82	1711	52
GSD302_49	4.65	0.14	0.3008	0.0086	0.66098	92.73621		1831	72	1698	44
GSD302_143	9.93	0.37	0.431	0.015	0.8697	92.09896		2506	66	2308	70
GSD302_126	5.15	0.19	0.3157	0.011	0.71584	91.88345		1922	73	1766	52
GSD302_131	4.71	0.18	0.3013	0.0091	0.34006	91.23185		1859	84	1696	45

Table 20. All U–Pb data for sample GSD302 (Limmen Sandstone)

Analysis	$^{207}Pb/^{235}U$		$^{206}Pb/^{238}U$		rho	Conc (%)	$^{207}Pb/^{206}Pb$		$^{206}Pb/^{238}U$	
GSD302_77	4.38	0.17	0.2802	0.0093	0.53785	87.94914	1809	75	1591	47
GSD302_23	4.71	0.24	0.291	0.012	0.68838	88.33601	1869	95	1651	62
GSD302_55	4.41	0.14	0.2882	0.0082	0.7615	89.86226	1815	73	1631	41
GSD302_151	4.345	0.12	0.282	0.0082	0.57084	88.44666	1809	71	1600	41
GSD302_57	5.2	0.21	0.3124	0.012	0.82723	88.56275	1976	73	1750	57
GSD302_27	4.42	0.13	0.2841	0.008	0.72085	87.08108	1850	73	1611	40
GSD302_56	8.68	0.37	0.389	0.015	0.82614	85.35109	2478	68	2115	69
GSD302_60	5.19	0.22	0.3005	0.011	0.63241	83.97022	2015	83	1692	52
GSD302_146	9.12	0.42	0.389	0.017	0.88705	82.40343	2563	64	2112	81
GSD302_115	5.59	0.24	0.314	0.013	0.86715	84.61538	2093	68	1771	63
GSD302_133	9.04	0.3	0.378	0.013	0.56027	80.31128	2570	73	2064	60
GSD302_61	5.24	0.16	0.2996	0.0086	0.53784	82.73839	2045	74	1692	44
GSD302_129	3.98	0.15	0.2624	0.008	0.46069	83.38889	1800	77	1501	41
GSD302_3	4.21	0.17	0.2727	0.01	0.88337	84.07367	1846	70	1552	52
GSD302_156	5.09	0.18	0.2915	0.011	0.61465	81.133	2030	83	1647	54
GSD302_139	4.27	0.14	0.2625	0.0083	0.76042	79.08325	1898	70	1501	42
GSD302_92	10.09	0.3	0.3745	0.01	0.62666	74.02457	2768	65	2049	48
GSD302_44	4.41	0.19	0.2623	0.0083	0.51462	77.16049	1944	87	1500	43
GSD302_124	5.83	0.24	0.299	0.012	0.94567	75.43702	2231	66	1683	60
GSD302_90	4.29	0.16	0.2648	0.011	0.7201	77.84647	1941	75	1511	54
GSD302_165	4.35	0.22	0.266	0.014	0.89482	77.41935	1953	72	1512	71
GSD302_71	5.006	0.14	0.2791	0.0072	0.28866	75.52381	2100	73	1586	36
GSD302_11	5.87	0.22	0.2864	0.0099	0.85052	69.66051	2327	67	1621	50
GSD302_25	3.523	0.12	0.2314	0.0069	0.51297	73.23867	1831	74	1341	36
GSD302_65	3.53	0.16	0.2266	0.0097	0.79105	71.64667	1834	76	1314	51
GSD302_116	3.69	0.18	0.235	0.012	0.75669	72.45989	1870	79	1355	61
GSD302_169	4.13	0.14	0.246	0.0086	0.72121	71.01304	1994	73	1416	44
GSD302_12	3.724	0.12	0.2303	0.0065	0.54217	70.37428	1897	73	1335	34
GSD302_20	3.45	0.15	0.2251	0.0094	0.84346	71.77375	1821	77	1307	50

Table 21. All U–Pb data for sample GSD302 (Limmen Sandstone)

Analysis	$^{207}Pb/^{235}U$		$^{206}Pb/^{238}U$		rho	Conc (%)	$^{207}Pb/^{206}Pb$		$^{206}Pb/^{238}U$	
GSD302_130	3.985	0.12	0.2348	0.0067	0.42581	68.84498	1974	73	1359	35
GSD302_160	3.452	0.12	0.2142	0.0066	0.41672	67.13212	1862	85	1250	35
GSD302_110	8.68	0.34	0.311	0.012	0.42274	61.4977	2831	75	1741	59
GSD302_79	3.41	0.15	0.2173	0.011	0.82962	67.7488	1879	72	1273	56
GSD302_153	3.77	0.22	0.218	0.013	0.90381	63.62268	1993	74	1268	70
GSD302_48	6.48	0.23	0.2676	0.0093	0.80402	58.12714	2627	66	1527	47
GSD302_166	8.32	0.23	0.2822	0.0086	0.85218	54.67896	2928	63	1601	43
GSD302_121	4.81	0.17	0.242	0.0081	0.75452	60.52061	2305	70	1395	42
GSD302_24	3.421	0.11	0.2053	0.0056	0.61436	61.44025	1958	74	1203	30
GSD302_83	3.17	0.11	0.1962	0.007	0.76442	61.31775	1882	75	1154	38
GSD302_86	3.38	0.14	0.2097	0.0085	0.73872	62.56384	1958	78	1225	45
GSD302_46	3.57	0.23	0.211	0.014	0.89188	61.1829	2012	78	1231	73
GSD302_114	3.1	0.12	0.1946	0.0074	0.65621	61.33333	1875	84	1150	39
GSD302_99	5.69	0.44	0.247	0.018	0.94438	56.3099	2504	68	1410	93
GSD302_155	3.65	0.31	0.21	0.018	0.97752	59.54836	2037	67	1213	99
GSD302_72	3.18	0.19	0.193	0.011	0.77641	57.7472	1962	80	1133	60
GSD302_113	3.87	0.36	0.217	0.021	0.96158	59.66587	2095	71	1250	110
GSD302_101	2.82	0.17	0.1773	0.01	0.90965	55.95302	1873	76	1048	56
GSD302_170	2.83	0.17	0.178	0.011	0.94117	56.12354	1878	72	1054	60
GSD302_52	2.84	0.2	0.174	0.011	0.8849	52.77207	1948	76	1028	61
GSD302_40	4.957	0.14	0.2064	0.0061	0.33683	46.87864	2579	74	1209	33
GSD302_123	2.92	0.2	0.177	0.012	0.95872	52.88754	1974	70	1044	66
GSD302_45	3.41	0.23	0.183	0.013	0.94347	49.54002	2174	69	1077	74
GSD302_67	2.372	0.11	0.1533	0.0071	0.89008	50.9111	1811	70	922	40
GSD302_138	2.789	0.095	0.1625	0.0051	0.73339	48.25871	2010	67	970	28
GSD302_119	3.33	0.27	0.175	0.016	0.95412	47.29422	2199	69	1040	90
GSD302_125	3.33	0.13	0.1731	0.0062	0.8238	46.01611	2234	71	1028	34
GSD302_13	4.05	0.14	0.1817	0.0053	0.81777	43.45719	2476	65	1076	29
GSD302_18	4.03	0.2	0.186	0.013	0.87263	44.5122	2460	76	1095	70

Table 22. All U–Pb data for sample GSD302 (Limmen Sandstone)

Analysis	$^{207}Pb/^{235}U$		$^{206}Pb/^{238}U$		rho	Conc (%)	$^{207}Pb/^{206}Pb$		$^{206}Pb/^{238}U$	
GSD302_106	1.97	0.15	0.1031	0.0087	0.96016	29.02784	2191	71	636	52
GSD302_108	1.763	0.067	0.1001	0.0039	0.79798	29.67617	2069	72	614	23
GSD302_98	1.894	0.091	0.1026	0.0046	0.87247	29.0397	2166	72	629	27
GSD302_93	1.567	0.046	0.095	0.0027	0.7545	30.23256	1935	67	585	16
GSD302_149	2.18	0.12	0.1025	0.0045	0.76393	26.52027	2368	77	628	26
GSD302_7	2.48	0.22	0.104	0.0083	0.96983	25.15699	2548	67	641	49
GSD302_62	1.623	0.07	0.0948	0.0043	0.86176	28.80435	2024	73	583	25
GSD302_148	1.432	0.058	0.0907	0.0034	0.76296	29.62374	1887	75	559	20
GSD302_96	2.168	0.11	0.0993	0.0059	0.62891	24.7561	2460	78	609	34
GSD302_63	1.81	0.072	0.0922	0.0034	0.77397	25.45779	2239	73	570	20
GSD302_167	1.715	0.077	0.0911	0.0041	0.88902	25.90028	2166	62	561	24
GSD302_137	1.572	0.089	0.0925	0.0061	0.87342	27.54607	2062	80	568	36
GSD302_154	1.693	0.055	0.0866	0.0026	0.74436	24.07741	2222	67	535	15
GSD302_158	1.91	0.11	0.0884	0.0052	0.93605	22.64229	2407	67	545	30
GSD302_145	1.699	0.063	0.0847	0.0026	0.7787	23.14488	2264	69	524	15
GSD302_122	1.805	0.072	0.0865	0.0031	0.73481	22.61753	2361	71	534	19
GSD302_127	1.58	0.19	0.086	0.01	0.9582	25.58361	2099	83	537	62
GSD302_84	1.565	0.051	0.0821	0.0023	0.77022	23.49353	2164	65	508.4	14
GSD302_164	1.355	0.052	0.0799	0.0032	0.80474	25.0887	1973	70	495	19
GSD302_2	1.24	0.039	0.0779	0.0026	0.77431	25.55438	1894	68	484	15
GSD302_88	1.236	0.058	0.0746	0.0033	0.77289	24.03946	1926	74	463	20
GSD302_21	2.021	0.07	0.0816	0.0029	0.74925	19.1812	2638	66	506	17
GSD302_4	1.277	0.043	0.0766	0.0027	0.87462	24.01416	1978	70	475	16
GSD302_34	2.186	0.061	0.08	0.0028	0.64169	17.58242	2821	67	496	17
GSD302_30	1.296	0.051	0.0742	0.0025	0.81257	22.72055	2029	71	461	15
GSD302_70	1.158	0.037	0.071	0.0022	0.48558	23.1761	1908	72	442.2	13
GSD302_107	1.702	0.068	0.0739	0.0023	0.57631	18.24324	2516	71	459	14
GSD302_97	1.342	0.047	0.0717	0.0022	0.71907	20.48691	2177	71	446	13
GSD302_37	1.762	0.066	0.073	0.0027	0.76947	17.38132	2612	68	454	16

Table 23. All U–Pb data for sample GSD302 (Limmen Sandstone)

Analysis	$^{207}Pb/^{235}U$		$^{206}Pb/^{238}U$		rho	Conc (%)	$^{207}Pb/^{206}Pb$		$^{206}Pb/^{238}U$	
GSD302_102	4.35	0.22	0.183	0.012	0.87883	41.72134	2591	72	1081	66
GSD302_36	2.715	0.1	0.1581	0.0068	0.66735	46.5288	2031	80	945	38
GSD302_132	2.62	0.18	0.157	0.011	0.96062	47.36575	1974	71	935	61
GSD302_26	2.77	0.18	0.154	0.011	0.94132	44.15709	2088	74	922	59
GSD302_38	2.25	0.11	0.1419	0.0065	0.88847	45.40138	1881	71	854	36
GSD302_159	2.599	0.089	0.1481	0.0056	0.78049	43.36585	2050	73	889	31
GSD302_78	2.48	0.13	0.1418	0.0077	0.89061	41.71959	2047	78	854	44
GSD302_29	3.01	0.14	0.1476	0.0055	0.87271	39.09211	2269	68	887	31
GSD302_51	2.3	0.15	0.1366	0.0082	0.93217	41.86165	1966	71	823	46
GSD302_168	2.38	0.15	0.1357	0.0084	0.96042	40	2045	66	818	47
GSD302_100	2.878	0.11	0.1391	0.0054	0.52603	36.13264	2322	80	839	30
GSD302_162	2.341	0.091	0.1318	0.0044	0.75826	38.33574	2079	74	797	25
GSD302_152	2.187	0.071	0.1256	0.0049	0.83379	37.44472	2035	71	762	28
GSD302_42	2.01	0.13	0.119	0.0084	0.95788	35.5665	2030	68	722	48
GSD302_104	4.66	0.15	0.1335	0.0052	0.48716	25.21712	3224	74	813	30
GSD302_10	1.952	0.1	0.1132	0.0055	0.88909	34.10776	2023	74	690	31
GSD302_85	1.84	0.055	0.111	0.0034	0.68308	34.75141	1951	70	678	20
GSD302_144	2.947	0.11	0.1193	0.0049	0.85611	27.75448	2623	63	728	29
GSD302_16	1.92	0.18	0.114	0.011	0.96554	34.26295	2008	74	688	65
GSD302_157	2.411	0.077	0.1137	0.0042	0.67197	29.12295	2383	67	694	24
GSD302_41	1.969	0.082	0.1086	0.0049	0.8578	31.12986	2133	67	664	28
GSD302_161	1.674	0.051	0.1004	0.0027	0.67392	31.85434	1936	68	616.7	16
GSD302_103	3.933	0.12	0.1174	0.0038	0.7327	22.80534	3144	62	717	22
GSD302_140	1.786	0.083	0.1046	0.0049	0.80017	31.85885	2012	75	641	28
GSD302_135	1.751	0.1	0.1024	0.0057	0.74582	31.44433	1994	85	627	33
GSD302_19	2.021	0.059	0.1053	0.003	0.57851	29.5299	2191	69	647	18
GSD302_117	1.82	0.2	0.112	0.014	0.97141	33.73313	2001	71	675	77
GSD302_76	2.1	0.15	0.108	0.0073	0.96464	29.90108	2224	66	665	43
GSD302_150	8.61	0.45	0.0968	0.006	0.55333	12.89554	4614	90	595	36

Table 24. All U–Pb data for sample GSD302 (Limmen Sandstone)

Analysis	$^{207}Pb/^{235}U$		$^{206}Pb/^{238}U$		rho	Conc (%)	$^{207}Pb/^{206}Pb$		$^{206}Pb/^{238}U$	
GSD302_17	1.245	0.041	0.069	0.0023	0.62793	20.60374	2087	69	430	14
GSD302_111	1.191	0.043	0.069	0.0022	0.51737	21.22107	2031	78	431	14
GSD302_39	1.35	0.11	0.0701	0.0052	0.89638	19.50783	2235	83	436	31
GSD302_112	1.676	0.086	0.0671	0.0036	0.9259	15.95301	2639	65	421	22
GSD302_14	1.505	0.076	0.0621	0.0034	0.91864	14.78095	2625	63	388	21
GSD302_95	1.123	0.032	0.0602	0.0017	0.59734	17.39492	2165	66	376.6	10
GSD302_81	1.535	0.046	0.059	0.0018	0.46216	13.57721	2720	66	369.3	11
GSD302_109	1.181	0.041	0.0593	0.0024	0.81592	16.1938	2291	68	371	14
GSD302_68	1.076	0.03	0.058	0.0017	0.69032	16.82554	2161	65	363.6	10
GSD302_80	1.651	0.049	0.0572	0.0017	0.35441	12.3637	2898	69	358.3	10
GSD302_5	0.922	0.026	0.05507	0.0014	0.47095	17.3183	1995	67	345.5	8.6
GSD302_172	1.104	0.051	0.0557	0.0022	0.91541	15.41519	2264	66	349	14
GSD302_47	0.889	0.039	0.0541	0.0027	0.9212	17.35791	1953	71	339	17
GSD302_91	0.837	0.039	0.0496	0.0025	0.90329	15.6078	1999	67	312	16
GSD302_8	1.33	0.11	0.0508	0.0044	0.97777	11.55104	2753	64	318	27
GSD302_141	0.874	0.032	0.0469	0.0019	0.82009	13.74651	2146	68	295	12
GSD302_147	0.845	0.065	0.0475	0.0038	0.94761	14.29942	2084	70	298	23
GSD302_50	0.872	0.033	0.0434	0.002	0.77265	11.8872	2305	74	274	12
GSD302_59	1.239	0.054	0.0418	0.0026	0.86776	8.861186	2968	80	263	16
GSD302_15	0.665	0.03	0.0383	0.0017	0.90076	11.76128	2061	71	242.4	11
GSD302_120	1	0.13	0.0388	0.0047	0.98215	9.087523	2685	72	244	29
GSD302_58	0.757	0.038	0.0378	0.0023	0.8876	10.36876	2305	79	239	14
GSD302_142	0.627	0.025	0.0302	0.0012	0.79867	8.204691	2345	68	192.4	7.4
GSD302_28	1.006	0.047	0.025	0.0017	0.87919	4.686118	3393	77	159	11
GSD302_89	0.496	0.021	0.0278	0.0012	0.85729	8.530691	2069	70	176.5	7.2
GSD302_1	0.46	0.032	0.0213	0.0019	0.86098	5.533118	2476	100	137	12
GSD302_73	0.745	0.043	0.01559	0.001	0.91005	2.685884	3712	65	99.7	6.5
GSD302_82	0.688	0.039	0.01578	0.00057	0.35738	2.886744	3523	75	101.7	3.2
GSD302_9	0.552	0.031	0.01435	0.00056	0.32165	2.664731	3445	110	91.8	3.6

Table 25. All U–Pb data for sample BR04 (Munyi Member)

Analysis	$^{207}Pb/^{235}U$		$^{206}Pb/^{238}U$		rho	Conc (%)	$^{207}Pb/^{206}Pb$		$^{206}Pb/^{238}U$	
GSD301										
GSD301_31	4.49	0.16	0.3099	0.0086	0.14438	103.8186	1676	82	1740	42
GSD301_38	4.64	0.15	0.3198	0.0094	0.44378	102.9971	1735	80	1787	46
GSD301_44	5.125	0.15	0.3291	0.0088	0.41822	100.1092	1831	74	1833	43
GSD301_66	5.02	0.19	0.3255	0.012	0.38455	99.23455	1829	92	1815	57
GSD301_28	5.29	0.15	0.3302	0.009	0.29129	97.97441	1876	73	1838	44
GSD301_45	12.22	0.4	0.4888	0.014	0.54478	97.78795	2622	65	2564	61
GSD301_52	5.36	0.17	0.3299	0.0099	0.4914	96.58075	1901	72	1836	48
GSD301_21	4.22	0.21	0.289	0.013	0.96202	95.83822	1706	69	1635	66
GSD301_12	4.885	0.14	0.3126	0.0083	0.65735	95.16567	1841	71	1752	41
GSD301_25	4.61	0.21	0.3047	0.012	0.59903	94.69027	1808	90	1712	57
GSD301_26	4.52	0.15	0.2986	0.0081	0.61032	93.9208	1793	75	1684	40
GSD301_8	4.51	0.17	0.2953	0.0088	0.27445	93.70433	1779	82	1667	44
GSD301_63	8.77	0.26	0.4019	0.012	0.59336	90.83715	2401	68	2181	54
GSD301_59	5.05	0.24	0.305	0.013	0.62801	89.4517	1915	88	1713	64
GSD301_58	4.19	0.17	0.2796	0.01	0.72365	89.35811	1776	78	1587	52
GSD301_43	8.94	0.33	0.3828	0.011	0.60694	82.56228	2529	76	2088	50
GSD301_37	8.45	0.59	0.371	0.025	0.78996	81.22236	2487	87	2020	120
GSD301_24	3.99	0.14	0.2565	0.0079	0.71084	80.42646	1829	75	1471	41
GSD301_16	3.96	0.25	0.245	0.014	0.82475	73.83569	1911	81	1411	71
GSD301_2	4.16	0.3	0.25	0.018	0.93629	71.57895	1995	75	1428	97
GSD301_6	3.25	0.25	0.214	0.015	0.82674	68.73614	1804	94	1240	78
GSD301_47	3.022	0.09	0.2036	0.0053	0.52801	68.58128	1741	71	1194	28
GSD301_9	3.13	0.13	0.2039	0.0086	0.75644	67.02187	1783	78	1195	46
GSD301_3	3.7	0.18	0.222	0.011	0.55524	65.97152	1966	92	1297	61
GSD301_10	5.09	0.26	0.2594	0.011	0.89002	65.85258	2252	70	1483	57

Table 26. All U–Pb data for sample BR04 (Munyi Member) part 1

Analysis	$^{207}Pb/^{235}U$		$^{206}Pb/^{238}U$		rho	Conc (%)	$^{207}Pb/^{206}Pb$		$^{206}Pb/^{238}U$	
BR04										
BR04_24	4.63	0.15	0.3114	0.0087	0.4517	100.6336	1736	75	1747	43
BR04_17	4.8	0.15	0.3204	0.0084	0.30095	100.1118	1789	75	1791	41
BR04_33	4.64	0.18	0.3048	0.0092	0.27249	95.00832	1803	88	1713	46
BR04_4	4.52	0.23	0.2959	0.0079	0.010359	93.92576	1778	100	1670	39
BR04_16	5.25	0.16	0.3157	0.0083	0.48449	90.85303	1946	69	1768	41
BR04_21	4.94	0.16	0.2999	0.0088	0.62601	87.70109	1927	80	1690	44
BR04_1	4.971	0.14	0.2923	0.008	0.1496	83.60324	1976	75	1652	40
BR04_13	5.19	0.17	0.2944	0.0082	0.65188	79.78877	2083	72	1662	41
BR04_23	4.42	0.14	0.2667	0.0077	0.83005	78.74871	1934	67	1523	39
BR04_18	4.3	0.19	0.265	0.012	0.84241	77.73797	1954	74	1519	60
BR04_10	5.63	0.33	0.291	0.015	0.62993	75.77296	2167	100	1642	73
BR04_32	5.3	0.18	0.2855	0.0095	0.31629	75.45497	2143	84	1617	48
BR04_8	6.14	0.22	0.2999	0.0082	0.34684	71.8232	2353	76	1690	41
BR04_11	7.98	0.27	0.3164	0.011	0.54216	66.23037	2674	78	1771	52

Table 27. All U–Pb data for sample BR04 (Munyi Member) part 2

Analysis	$^{207}Pb/^{235}U$		$^{206}Pb/^{238}U$		rho	Conc (%)	$^{207}Pb/^{206}Pb$		$^{206}Pb/^{238}U$	
BR04_12	4.73	0.18	0.2504	0.0066	0.38846	65.75342	2190	78	1440	34
BR04_7	10.48	0.34	0.3447	0.0097	0.35764	65.20848	2926	70	1908	47
BR04_3	5.2	0.2	0.2484	0.0073	0.86143	60.65365	2356	68	1429	38
BR04_19	11.46	0.44	0.3388	0.0092	0.45355	59.85355	3141	68	1880	44
BR04_2	2.77	0.17	0.179	0.011	0.88796	58.04692	1833	81	1064	61
BR04_20	6.78	0.22	0.266	0.0079	0.71937	56.44742	2691	67	1519	40
BR04_6	5.29	0.23	0.2398	0.0093	0.48933	56.39251	2456	80	1385	48
BR04_22	2.744	0.11	0.1737	0.0069	0.55139	55.61526	1861	89	1035	37
BR04_14	12.92	0.54	0.3137	0.0095	0.85413	51.38363	3433	61	1764	48
BR04_27	4.347	0.14	0.1973	0.006	0.6644	47.65818	2434	68	1160	33
BR04_31	2.25	0.18	0.146	0.014	0.912	45.64533	1906	83	870	76
BR04_5	14.24	1	0.275	0.016	0.92298	41.07425	3798	69	1560	83
BR04_15	2.604	0.089	0.1437	0.0052	0.75789	40.95644	2112	69	865	29
BR04_9	11.94	0.55	0.2529	0.0068	0.6664	39.87411	3654	74	1457	37
BR04_25	3.32	0.23	0.142	0.01	0.94851	33.95775	2509	68	852	58
BR04_28	1.47	0.056	0.0754	0.0023	0.39583	21.03774	2226	77	468.3	14
BR04_30	1.072	0.046	0.0563	0.0027	0.68447	15.98008	2209	70	353	16
BR04_29	0.948	0.034	0.0475	0.0015	0.74642	13.26087	2254	73	298.9	8.9
BR04_26	0.4	0.02	0.0146	0.0011	0.82281	3.359684	2783	91	93.5	6.9

Table 28. All U–Pb data for sample GSD301 (Limmen Formation) part 1

Analysis	$^{207}Pb/^{235}U$		$^{206}Pb/^{238}U$		rho	Conc (%)	$^{207}Pb/^{206}Pb$		$^{206}Pb/^{238}U$	
GSD301										
GSD301_31	4.49	0.16	0.3099	0.0086	0.14438	103.8186	1676	82	1740	42
GSD301_38	4.64	0.15	0.3198	0.0094	0.44378	102.9971	1735	80	1787	46
GSD301_44	5.125	0.15	0.3291	0.0088	0.41822	100.1092	1831	74	1833	43
GSD301_66	5.02	0.19	0.3255	0.012	0.38455	99.23455	1829	92	1815	57
GSD301_28	5.29	0.15	0.3302	0.009	0.29129	97.97441	1876	73	1838	44
GSD301_45	12.22	0.4	0.4888	0.014	0.54478	97.78795	2622	65	2564	61
GSD301_52	5.36	0.17	0.3299	0.0099	0.4914	96.58075	1901	72	1836	48
GSD301_21	4.22	0.21	0.289	0.013	0.96202	95.83822	1706	69	1635	66
GSD301_12	4.885	0.14	0.3126	0.0083	0.65735	95.16567	1841	71	1752	41
GSD301_25	4.61	0.21	0.3047	0.012	0.59903	94.69027	1808	90	1712	57
GSD301_26	4.52	0.15	0.2986	0.0081	0.61032	93.9208	1793	75	1684	40
GSD301_8	4.51	0.17	0.2953	0.0088	0.27445	93.70433	1779	82	1667	44
GSD301_63	8.77	0.26	0.4019	0.012	0.59336	90.83715	2401	68	2181	54
GSD301_59	5.05	0.24	0.305	0.013	0.62801	89.4517	1915	88	1713	64
GSD301_58	4.19	0.17	0.2796	0.01	0.72365	89.35811	1776	78	1587	52
GSD301_43	8.94	0.33	0.3828	0.011	0.60694	82.56228	2529	76	2088	50
GSD301_37	8.45	0.59	0.371	0.025	0.78996	81.22236	2487	87	2020	120
GSD301_24	3.99	0.14	0.2565	0.0079	0.71084	80.42646	1829	75	1471	41
GSD301_16	3.96	0.25	0.245	0.014	0.82475	73.83569	1911	81	1411	71
GSD301_2	4.16	0.3	0.25	0.018	0.93629	71.57895	1995	75	1428	97
GSD301_6	3.25	0.25	0.214	0.015	0.82674	68.73614	1804	94	1240	78
GSD301_47	3.022	0.09	0.2036	0.0053	0.52801	68.58128	1741	71	1194	28
GSD301_9	3.13	0.13	0.2039	0.0086	0.75644	67.02187	1783	78	1195	46
GSD301_3	3.7	0.18	0.222	0.011	0.55524	65.97152	1966	92	1297	61
GSD301_10	5.09	0.26	0.2594	0.011	0.89002	65.85258	2252	70	1483	57

Table 29. All U–Pb data for sample GSD301 (Limmen Formation) part 2

Analysis	$^{207}Pb/^{235}U$		$^{206}Pb/^{238}U$		rho	Conc (%)	$^{207}Pb/^{206}Pb$		$^{206}Pb/^{238}U$	
GSD301_35	4.49	0.22	0.2436	0.0099	0.60671	65.48507	2144	93	1404	52
GSD301_7	5.6	0.21	0.2683	0.0094	0.72054	65.10638	2350	72	1530	48
GSD301_40	8.04	0.27	0.3113	0.011	0.5645	64.6057	2701	68	1745	53
GSD301_70	3.533	0.12	0.2108	0.0081	0.54506	63.38826	1942	77	1231	43
GSD301_33	3.3	0.11	0.2037	0.0061	0.67572	62.54584	1909	74	1194	33
GSD301_15	3.17	0.18	0.1929	0.01	0.84017	60.57082	1892	78	1146	57
GSD301_14	2.87	0.19	0.184	0.012	0.9132	58.8907	1839	76	1083	63
GSD301_56	4.8	0.18	0.2281	0.0089	0.69686	55.8277	2368	70	1322	47
GSD301_5	2.43	0.27	0.163	0.018	0.97762	54.95702	1745	75	959	98
GSD301_20	2.51	0.27	0.164	0.017	0.97108	53.57737	1803	73	966	92
GSD301_13	2.439	0.088	0.1604	0.0049	0.72493	53.54551	1791	73	959	27
GSD301_23	3.03	0.17	0.1773	0.01	0.8925	53.06329	1975	73	1048	56
GSD301_49	4.787	0.14	0.214	0.0071	0.56819	51.22549	2448	70	1254	37
GSD301_50	2.259	0.065	0.1492	0.0039	0.50821	51.14155	1752	74	896	22
GSD301_11	2.466	0.089	0.154	0.0047	0.83831	50.38043	1840	69	927	28
GSD301_27	2.44	0.13	0.1464	0.0078	0.58351	45.44984	1934	100	879	44
GSD301_48	2.02	0.074	0.1319	0.004	0.74131	44.81211	1783	69	799	23
GSD301_4	1.83	0.13	0.1249	0.0081	0.92374	44.1928	1722	78	761	45
GSD301_61	1.85	0.076	0.1259	0.0059	0.61608	43.55023	1752	85	763	33
GSD301_67	1.764	0.079	0.1192	0.0047	0.81569	42.23889	1733	77	732	28
GSD301_64	1.583	0.087	0.1133	0.0062	0.91292	41.14861	1689	70	695	36
GSD301_68	1.784	0.1	0.1183	0.0066	0.92851	40.93235	1759	72	720	38
GSD301_30	1.672	0.088	0.1129	0.0059	0.8872	39.5977	1740	75	689	34
GSD301_22	1.72	0.19	0.103	0.01	0.98229	33.40426	1880	75	628	60
GSD301_39	1.34	0.04	0.0913	0.0026	0.63121	32.56217	1729	70	563	15
GSD301_60	1.419	0.084	0.0944	0.0056	0.83514	32.0974	1807	87	580	33
GSD301_18	1.386	0.067	0.0887	0.0043	0.6848	30.92437	1785	86	552	26
GSD301_57	2.819	0.098	0.1225	0.004	0.42034	29.90767	2491	74	745	23
GSD301_69	16.93	0.61	0.2177	0.0083	0.89467	28.79439	4421	55	1273	42

Table 30. All U–Pb data for sample GSD301 (Limmen Formation) part 3 and U602 (Limmen Sandstone) part 1

Analysis	$^{207}Pb/^{235}U$		$^{206}Pb/^{238}U$		rho	Conc (%)	$^{207}Pb/^{206}Pb$		$^{206}Pb/^{238}U$	
GSD301_41	2.95	0.16	0.1084	0.0043	0.91197	23.88329	2776	68	663	25
GSD301_19	1.178	0.064	0.0719	0.0038	0.9053	23.12468	1933	71	447	23
GSD301_46	1.302	0.075	0.0744	0.0037	0.91666	22.92899	2028	67	465	22
GSD301_29	1.544	0.063	0.0805	0.0038	0.93703	22.45725	2222	67	499	23
GSD301_62	0.919	0.03	0.061	0.002	0.71226	21.55932	1770	69	381.6	12
GSD301_55	0.934	0.04	0.0572	0.0024	0.35862	18.8719	1897	87	358	15
GSD301_65	0.801	0.024	0.0528	0.0017	0.58263	18.75636	1769	75	331.8	10
GSD301_53	0.741	0.021	0.05074	0.0014	0.39646	18.61144	1714	73	319	8.7
GSD301_17	0.858	0.044	0.053	0.0028	0.83836	17.65328	1892	75	334	17
GSD301_42	0.787	0.069	0.0475	0.0043	0.97515	14.90745	1999	70	298	26
GSD301_34	1.03	0.028	0.05171	0.0013	0.42517	14.43803	2251	66	325	7.9
GSD301_36	0.589	0.022	0.0373	0.0014	0.53896	12.79826	1844	83	236	8.7
GSD301_51	0.258	0.014	0.01231	0.00074	0.90675	3.367521	2340	69	78.8	4.7
GSD301_32	0.597	0.026	0.01406	0.00059	0.76994	2.58695	3479	60	90	3.7
U602										
U602_37	6.61	0.21	0.3806	0.009	0.33302	103.5821	2010	55	2082	43
U602_39	4.53	0.12	0.3135	0.0073	0.69816	103.8416	1692	43	1757	36
U602_35	8.82	0.17	0.4351	0.0088	0.38916	101.8818	2285	35	2328	39
U602_20	17.34	0.38	0.5967	0.014	0.64786	103.466	2914	36	3015	56
U602_11	6.59	0.14	0.3699	0.0085	0.60347	99.3144	2042	43	2028	40
U602_2	27.28	0.53	0.6973	0.015	0.50944	100.9177	3378	31	3409	57
U602_4	5.02	0.14	0.3209	0.0082	0.63811	97.76445	1834	47	1793	40
U602_25	4.63	0.16	0.3082	0.0091	0.65863	96.48829	1794	48	1731	45
U602_27	4.56	0.23	0.281	0.014	0.89057	85.44576	1862	54	1591	71
U602_3	4.47	0.12	0.2758	0.0069	0.53391	83.64411	1877	44	1570	35

Table 31. All U–Pb data for sample U602 (Limmen Sandstone) part 2

Analysis	$^{207}Pb/^{235}U$		$^{206}Pb/^{238}U$		rho	Conc (%)	$^{207}Pb/^{206}Pb$		$^{206}Pb/^{238}U$	
U602_36	4.48	0.089	0.2742	0.0057	0.2058	82.6455	1890	42	1562	29
U602_19	4.732	0.098	0.2793	0.0062	0.36078	80.07064	1982	38	1587	31
U602_23	5.285	0.098	0.2893	0.0061	0.66536	78.03716	2099	35	1638	31
U602_40	4.396	0.087	0.2685	0.0063	0.70661	79.09138	1937	35	1532	32
U602_31	4.74	0.18	0.2762	0.011	0.87142	78.25436	2005	40	1569	55
U602_41	3.908	0.085	0.252	0.0055	0.60879	78.99618	1833	41	1448	28
U602_18	4.401	0.093	0.2648	0.0056	0.65008	77.60123	1951	36	1514	29
U602_44	55.9	8.5	0.584	0.093	0.86479	60.59322	4720	170	2860	380
U602_13	3.663	0.1	0.2363	0.006	0.72091	75.62052	1813	45	1371	33
U602_10	10.14	0.55	0.351	0.013	0.78289	67.50261	2871	57	1938	62
U602_1	3.879	0.089	0.2337	0.006	0.81069	70.50547	1919	37	1353	31
U602_34	4.01	0.18	0.233	0.0085	0.13743	68.2002	1978	57	1349	44
U602_17	3.14	0.072	0.2037	0.0047	0.46153	66.90929	1786	44	1195	25
U602_42	5.9	2.4	0.246	0.056	0.65637	60.69869	2290	790	1390	280
U602_12	3.783	0.079	0.2177	0.0052	0.61472	62.8529	2019	34	1269	28
U602_6	3.43	0.19	0.208	0.011	0.90356	62.61586	1942	41	1216	61
U602_21	5.011	0.084	0.2277	0.005	0.60823	54.53795	2424	29	1322	26
U602_22	3.539	0.061	0.196	0.0041	0.44731	55.48077	2080	33	1154	22
U602_30	3.65	0.091	0.199	0.0057	0.81167	55.24575	2116	36	1169	31
U602_16	6.1	0.12	0.2264	0.0053	0.79973	47.5932	2763	32	1315	28
U602_24	3.203	0.066	0.1804	0.0042	0.77277	52.12092	2051	29	1069	23
U602_5	2.853	0.062	0.171	0.0041	0.66931	52.36869	1942	34	1017	23
U602_9	2.692	0.075	0.1636	0.0051	0.73487	51.42255	1898	44	976	28
U602_8	2.36	0.052	0.1515	0.0036	0.82619	49.2416	1846	35	909	20
U602_33	2.76	0.062	0.152	0.0035	0.38342	43.95181	2075	36	912	20
U602_38	2.109	0.074	0.135	0.0043	0.6399	45.45961	1795	50	816	25
U602_14	1.806	0.052	0.1093	0.003	0.86147	34.62934	1929	34	668	18
U602_43	5.4	2.1	0.163	0.057	0.67281	28.57143	3290	590	940	300

Table 32. All U–Pb data for sample L02 (Hodgson Sandstone) part 1

Analysis	$^{207}Pb/^{235}U$		$^{206}Pb/^{238}U$		rho	Conc (%)	$^{207}Pb/^{206}Pb$		$^{206}Pb/^{238}U$	
L02										
L02_33	5.08	0.17	0.3403	0.009	0.24804	109.4548	1724	64	1887	43
L02_80	4.98	0.15	0.3366	0.0092	0.61771	109.2982	1710	52	1869	44
L02_110	4.97	0.15	0.3368	0.0084	0.43989	108.5947	1722	57	1870	41
L02_50	4.98	0.12	0.3335	0.0076	0.29026	107.3495	1728	50	1855	37
L02_21	5.06	0.12	0.3383	0.0081	0.25566	107.0736	1753	54	1877	39
L02_57	4.805	0.098	0.3267	0.0068	0.47703	106.5497	1710	39	1822	33
L02_71	4.6	0.11	0.3188	0.0077	0.22964	106.0048	1682	50	1783	38
L02_112	4.98	0.15	0.331	0.0082	0.36398	105.6799	1743	57	1842	40
L02_75	4.93	0.14	0.3267	0.0072	0.4376	104.8331	1738	52	1822	35
L02_65	4.89	0.15	0.3263	0.0085	0.50689	104.7208	1737	52	1819	41
L02_24	4.28	0.13	0.3009	0.0069	0.10679	104.6943	1619	58	1695	34
L02_20	4.86	0.12	0.3242	0.0076	0.37059	104.4457	1732	44	1809	37
L02_22	5	0.12	0.33	0.0075	0.30091	104.3725	1761	52	1838	36
L02_111	4.84	0.15	0.3223	0.0074	0.39102	104.1667	1728	58	1800	36
L02_56	10.8	0.18	0.4846	0.01	0.56518	104.1309	2445	32	2546	45
L02_58	5.59	0.15	0.3485	0.0085	0.072384	104.0497	1852	58	1927	41
L02_14	5.07	0.16	0.3291	0.0078	0.3457	104.0295	1762	56	1833	38
L02_74	4.56	0.13	0.3138	0.0078	0.47558	103.3431	1705	49	1762	39
L02_64	5.22	0.14	0.3349	0.009	0.28426	103.3131	1811	51	1871	44
L02_84	4.63	0.13	0.3152	0.007	0.38707	103.1542	1712	47	1766	34
L02_89	4.81	0.13	0.324	0.0082	0.30357	103.0199	1755	53	1808	40
L02_19	3.962	0.1	0.2903	0.0068	0.14315	103.0094	1595	53	1643	34
L02_70	4.7	0.14	0.3177	0.0083	0.67892	102.9548	1726	52	1777	41
L02_104	4.87	0.18	0.3218	0.0075	0.67946	102.8016	1749	69	1798	37
L02_81	5.02	0.13	0.3289	0.0079	0.35236	102.6906	1784	50	1832	39
L02_34	4.814	0.11	0.3224	0.0069	0.45156	102.6796	1754	42	1801	34
L02_96	4.653	0.097	0.3111	0.0073	0.16297	102.346	1705	47	1745	36
L02_1	4.66	0.14	0.3146	0.0074	0.222	102.2622	1724	54	1763	36

Table 33. All U–Pb data for sample L02 (Hodgson Sandstone) part 2

Analysis	$^{207}Pb/^{235}U$		$^{206}Pb/^{238}U$		rho	Conc (%)	$^{207}Pb/^{206}Pb$		$^{206}Pb/^{238}U$	
L02_93	4.79	0.14	0.3192	0.0078	0.73139	102.1752	1747	54	1785	38
L02_62	4.92	0.15	0.326	0.0087	0.53583	102.0728	1785	52	1822	43
L02_55	4.69	0.13	0.3189	0.0082	0.62691	102.056	1751	45	1787	39
L02_41	4.839	0.097	0.3209	0.0078	0.17065	101.7594	1762	48	1793	38
L02_43	8.78	0.17	0.4342	0.0092	0.46942	101.7068	2285	34	2324	41
L02_45	4.73	0.14	0.3192	0.0078	0.22891	101.5358	1758	57	1785	38
L02_88	4.223	0.1	0.2975	0.0073	0.31017	101.2063	1658	53	1678	36
L02_11	4.89	0.12	0.3215	0.0083	0.38041	101.1261	1776	50	1796	41
L02_107	11.39	0.23	0.4854	0.011	0.62132	100.9105	2526	34	2549	46
L02_28	4.975	0.11	0.3241	0.0071	0.58535	100.7238	1796	36	1809	34
L02_82	5.13	0.13	0.3278	0.0082	0.42754	100.6612	1815	45	1827	40
L02_72	6.09	0.16	0.3596	0.0086	0.58029	100.2523	1982	41	1987	39
L02_83	5.19	0.14	0.3303	0.0076	0.2396	100	1839	52	1839	37
L02_15	4.88	0.13	0.3192	0.0071	0.5443	99.72067	1790	51	1785	35
L02_47	4.045	0.095	0.2889	0.0067	0.22466	99.69531	1641	49	1636	34
L02_92	4.88	0.13	0.3171	0.0077	0.39	99.38547	1790	52	1779	39
L02_42	4.801	0.12	0.3134	0.0073	0.37364	99.1535	1772	47	1757	36
L02_2	4.57	0.13	0.3068	0.0079	0.33456	99.08046	1740	52	1724	39
L02_5	4.5	0.15	0.308	0.01	0.63203	98.91304	1748	54	1729	49
L02_6	5.92	0.13	0.3509	0.0076	0.61837	98.52567	1967	37	1938	36
L02_7	6.01	0.15	0.3525	0.0095	0.71556	98.48101	1975	44	1945	45
L02_94	4.94	0.13	0.3183	0.007	0.30371	98.23497	1813	49	1781	34
L02_35	4.752	0.11	0.3095	0.0073	0.27552	97.80529	1777	47	1738	36
L02_103	4.75	0.12	0.3099	0.0069	0.20729	97.36989	1787	43	1740	34
L02_115	4.634	0.11	0.3059	0.0074	0.61529	96.90141	1775	40	1720	36
L02_67	4.66	0.16	0.304	0.0074	0.28195	96.77419	1767	64	1710	37
L02_59	4.336	0.11	0.2926	0.0074	0.42754	96.33081	1717	47	1654	37
L02_61	4.31	0.12	0.2935	0.0069	0.40682	95.89358	1729	51	1658	35
L02_32	5.01	0.13	0.3162	0.0073	0.55887	95.83333	1848	47	1771	36

Table 34. All U–Pb data for sample L02 (Hodgson Sandstone) part 3

Analysis	$^{207}Pb/^{235}U$		$^{206}Pb/^{238}U$		rho	Conc (%)	$^{207}Pb/^{206}Pb$		$^{206}Pb/^{238}U$	
L02_53	8.83	0.22	0.4191	0.01	0.77241	95.63374	2359	36	2256	47
L02_77	4.59	0.13	0.3039	0.0073	0.027035	95.47739	1791	57	1710	36
L02_86	4.391	0.097	0.2945	0.0073	0.72195	95.30086	1745	37	1663	36
L02_51	5.16	0.13	0.3226	0.0075	0.47136	95.2935	1891	43	1802	36
L02_108	4.459	0.11	0.2954	0.0067	0.42514	95.15117	1753	46	1668	33
L02_73	5.63	0.18	0.3368	0.009	0.67291	94.53994	1978	43	1870	43
L02_66	5.36	0.14	0.3256	0.0078	0.43919	94.49922	1927	47	1821	37
L02_12	4.198	0.092	0.2838	0.0065	0.2725	94.21729	1712	49	1613	32
L02_36	6.11	0.13	0.3467	0.0073	0.43969	93.69809	2047	39	1918	35
L02_68	4.3	0.12	0.2906	0.0069	0.20656	93.35605	1761	59	1644	34
L02_78	4.473	0.095	0.2942	0.0076	0.43069	93.31461	1780	42	1661	38
L02_105	4.821	0.1	0.3053	0.007	0.48385	93.16332	1843	42	1717	35
L02_44	4.55	0.12	0.295	0.0074	0.12747	92.65851	1798	54	1666	37
L02_116	8.65	0.16	0.4078	0.0088	0.59118	92.4109	2385	33	2204	40
L02_46	4.007	0.095	0.2761	0.0064	0.50586	92.14076	1705	42	1571	32
L02_25	4.65	0.16	0.2969	0.0076	0.24217	91.28065	1835	59	1675	38
L02_54	4.39	0.15	0.2904	0.0081	0.53812	91.1259	1803	58	1643	41
L02_52	4.801	0.1	0.3001	0.0071	0.65775	91.06085	1857	43	1691	35
L02_99	3.972	0.1	0.2736	0.0066	0.42935	90.86147	1718	47	1561	33
L02_17	4.14	0.15	0.2771	0.0089	0.86699	90.30963	1744	43	1575	45
L02_87	4.809	0.12	0.3011	0.0063	0.42307	90.06904	1883	44	1696	31
L02_85	4.371	0.11	0.2854	0.0066	0.60452	89.93885	1799	38	1618	33
L02_10	4.254	0.096	0.28	0.0066	0.51666	89.43227	1779	41	1591	33
L02_48	4.799	0.088	0.2983	0.0059	0.53016	89.28382	1885	34	1683	30
L02_76	4.53	0.12	0.2911	0.0066	0.66639	89.16576	1846	39	1646	33
L02_18	9.51	0.18	0.4124	0.0088	0.52375	89	2500	31	2225	40
L02_27	5.075	0.11	0.3027	0.0063	0.40801	88.15313	1933	40	1704	31
L02_31	4.169	0.099	0.2748	0.007	0.8142	88.01351	1777	40	1564	35
L02_109	4.05	0.12	0.2693	0.0084	0.64495	87.35111	1763	42	1540	42

Table 35. All U–Pb data for sample L02 (Hodgson Sandstone) part 4

Analysis	$^{207}Pb/^{235}U$		$^{206}Pb/^{238}U$		rho	Conc (%)	$^{207}Pb/^{206}Pb$		$^{206}Pb/^{238}U$	
L02_3	4.232	0.09	0.2739	0.0064	0.60043	87.22811	1793	38	1564	31
L02_40	3.731	0.084	0.2568	0.0052	0.30649	86.09001	1711	43	1473	26
L02_37	4.55	0.12	0.2835	0.0067	0.32044	85.57743	1879	51	1608	34
L02_91	4.148	0.1	0.2719	0.0067	0.6244	85.25853	1818	42	1550	34
L02_114	4.162	0.087	0.2683	0.006	0.56206	84.49227	1812	37	1531	31
L02_69	4.23	0.1	0.2684	0.0065	0.53751	83.39684	1837	41	1532	33
L02_63	3.83	0.12	0.2547	0.0059	0.47734	83.30484	1755	50	1462	30
L02_9	3.756	0.082	0.2539	0.0053	0.27582	83.2667	1751	40	1458	27
L02_39	3.08	0.15	0.2232	0.0063	0.3472	82.73885	1570	93	1299	33
L02_79	5.49	0.14	0.3054	0.0076	0.27516	82.58778	2079	45	1717	38
L02_60	3.814	0.087	0.2524	0.006	0.5616	81.69014	1775	39	1450	31
L02_97	3.934	0.1	0.2579	0.0057	0.21452	80.99671	1826	48	1479	29
L02_4	3.86	0.18	0.2538	0.011	0.73673	80.79911	1802	62	1456	55
L02_23	6.03	0.66	0.2958	0.0071	0.034892	80.28846	2080	120	1670	35
L02_49	4.252	0.092	0.2633	0.0064	0.60621	80.19169	1878	40	1506	33
L02_16	4.32	0.13	0.2682	0.009	0.60953	80.14667	1909	53	1530	46
L02_13	5.59	0.14	0.3022	0.0078	0.41417	79.89667	2129	48	1701	38
L02_113	4.32	0.14	0.2661	0.0069	0.64275	79.62284	1909	42	1520	35
L02_38	3.822	0.081	0.2485	0.0056	0.2736	79.26829	1804	41	1430	29
L02_106	3.76	0.15	0.2413	0.0067	0.64643	77.07641	1806	50	1392	35
L02_26	8.6	0.17	0.3518	0.0079	0.69925	74.3207	2613	31	1942	38
L02_95	3.544	0.086	0.2278	0.006	0.73692	73.21527	1807	40	1323	32
L02_102	4.026	0.086	0.2422	0.0051	0.74948	71.91358	1944	36	1398	26
L02_101	3.401	0.1	0.2209	0.0056	0.29503	71.80346	1791	57	1286	29
L02_90	3.029	0.096	0.2047	0.0062	0.54804	69.15566	1741	54	1204	32
L02_100	2.912	0.08	0.1989	0.0064	0.83371	69.03073	1692	37	1168	34
L02_30	3.249	0.056	0.2093	0.0041	0.44398	67.30769	1820	34	1225	22
L02_8	2.785	0.07	0.1932	0.0048	0.67887	67.21796	1693	38	1138	26
L02_29	5.32	0.12	0.2641	0.0061	0.78214	66.66667	2265	33	1510	31

Table 36. All U–Pb data for sample U506 (Arnold Sandstone)

Analysis	$^{207}Pb/^{235}U$		$^{206}Pb/^{238}U$		rho	Conc (%)	$^{207}Pb/^{206}Pb$		$^{206}Pb/^{238}U$	
U506										
U506_1	5.05	0.24	0.3337	0.0059	0.58454	107.6566	1724	97	1856	28
U506_19	4.98	0.25	0.3331	0.0061	0.45976	106.9861	1732	94	1853	30
U506_34	4.954	0.23	0.3316	0.0063	0.39757	105.9094	1743	94	1846	31
U506_5	4.84	0.23	0.3248	0.0062	0.4926	104.8611	1728	90	1812	30
U506_3	4.96	0.24	0.3237	0.0069	0.53329	103.3162	1749	89	1807	33
U506_39	4.648	0.22	0.3129	0.0057	0.37466	101.5634	1727	92	1754	28
U506_28	4.592	0.21	0.3096	0.0053	0.42685	101.5187	1712	92	1738	26
U506_27	4.62	0.25	0.3107	0.009	0.69509	100.6904	1738	98	1750	42
U506_7	5.12	0.25	0.3259	0.006	0.25283	100.6087	1807	93	1818	29
U506_11	4.49	0.24	0.302	0.0066	0.32016	100.4717	1696	100	1704	32
U506_44	10.88	0.6	0.474	0.013	0.79969	99.08766	2521	95	2498	55
U506_4	4.481	0.21	0.2986	0.0053	0.11604	97.62319	1725	100	1684	26
U506_30	4.613	0.22	0.3057	0.0054	0.28632	97.17354	1769	93	1719	27
U506_14	5.09	0.25	0.3186	0.0057	0.39378	96.27229	1851	96	1782	28
U506_6	4.45	0.22	0.2965	0.0067	0.57038	95.21912	1757	93	1673	33
U506_12	4.55	0.24	0.3001	0.0075	0.45228	94.20613	1795	100	1691	37
U506_33	4.28	0.23	0.2896	0.0064	0.54995	93.87171	1746	97	1639	32
U506_9	4.96	0.24	0.3067	0.006	0.42206	93.6078	1846	89	1728	30
U506_10	6.69	0.32	0.3476	0.0074	0.89512	88.9043	2163	87	1923	35
U506_23	4.134	0.2	0.2714	0.0068	0.68929	87.79796	1762	90	1547	35
U506_29	3.96	0.21	0.2624	0.009	0.82327	84.80226	1770	90	1501	46
U506_22	3.881	0.18	0.2576	0.0059	0.27991	84.3518	1751	95	1477	30
U506_37	3.65	0.22	0.2495	0.0094	0.79237	82.84229	1731	93	1434	48
U506_36	3.513	0.17	0.2349	0.0058	0.74455	78.60035	1729	89	1359	30
U506_18	3.466	0.16	0.2329	0.0043	0.72411	77.70737	1736	91	1349	23
U506_35	3.087	0.15	0.2134	0.005	0.66875	73.85892	1687	90	1246	26
U506_21	3.253	0.16	0.2158	0.0051	0.74396	73.45391	1714	90	1259	27
U506_24	3.25	0.2	0.2168	0.0097	0.55988	72.90583	1731	110	1262	51
U506_38	3.138	0.16	0.2125	0.005	0.7082	72.71663	1708	93	1242	27
U506_20	3.36	0.19	0.2128	0.0089	0.89127	67.99346	1834	91	1247	46
U506_25	2.724	0.13	0.1902	0.0053	0.64073	67.06515	1673	91	1122	28
U506_45	2.983	0.16	0.1951	0.0069	0.64471	63.84275	1806	100	1153	38
U506_43	3.324	0.17	0.2057	0.0058	0.86802	63.12205	1909	90	1205	31
U506_40	2.7	0.16	0.1836	0.0087	0.92166	62.15596	1744	87	1084	47
U506_26	2.559	0.14	0.1641	0.0066	0.32352	53.82499	1817	100	978	36

Table 37. All U–Pb data for sample U507 (Crawford Formation) part 1

Analysis	$^{207}Pb/^{235}U$		$^{206}Pb/^{238}U$		rho	Conc (%)	$^{207}Pb/^{206}Pb$		$^{206}Pb/^{238}U$	
U507										
U507_12	5.47	0.26	0.3502	0.0075	0.62451	104.8807	1844	91	1934	36
U507_14	5.06	0.28	0.3263	0.007	0.055918	102.4198	1777	110	1820	34
U507_17	6.66	0.23	0.381	0.01	0.30605	101.069	2058	70	2080	48
U507_6	12.48	0.61	0.5017	0.0097	0.20766	100.8468	2598	79	2620	42
U507_3	120	24	1.15	0.27	0.68608	99.5842	4810	160	4790	770
U507_13	5.033	0.24	0.3226	0.0066	0.5658	97.93478	1840	87	1802	32
U507_5	4.96	0.25	0.3147	0.0065	0.40462	97.40331	1810	95	1763	32
U507_16	5.55	0.31	0.3371	0.0086	0.24636	97.14434	1926	110	1871	42
U507_14	15.06	0.51	0.534	0.015	0.79797	96.56743	2855	56	2757	64
U507_13	5.34	0.2	0.3312	0.0082	0.56921	96.49398	1911	71	1844	40
U507_1	4.575	0.14	0.3007	0.0078	0.52953	95.07279	1786	63	1698	40
U507_6	4.79	0.15	0.3067	0.0074	0.31775	93.54314	1843	71	1724	37
U507_5	10.94	0.32	0.4477	0.012	0.36012	91.65705	2601	64	2384	52
U507_12	4.765	0.15	0.2973	0.008	0.62845	88.35616	1898	65	1677	40
U507_7	4.49	0.23	0.2838	0.0058	0.36872	88.21918	1825	91	1610	29
U507_9	4.88	0.19	0.3002	0.009	0.47323	88.21075	1917	73	1691	45
U507_11	3.91	0.18	0.2605	0.0093	0.54275	84.37146	1766	82	1490	47
U507_19	4.83	0.26	0.285	0.013	0.85153	82.70908	1949	81	1612	68
U507_9	5.85	0.33	0.316	0.011	0.28536	81.54982	2168	95	1768	54
U507_3	3.853	0.11	0.2534	0.0059	0.29986	81.45251	1790	65	1458	31
U507_4	3.602	0.12	0.2423	0.0064	0.47932	78.93845	1771	75	1398	33
U507_8	3.825	0.11	0.2474	0.0062	0.3366	78.33242	1823	66	1428	33

Table 38. All U–Pb data for sample U507 (Crawford Formation) part 2 and U603 (Limmen Sandstone) part 1

Analysis	$^{207}Pb/^{235}U$		$^{206}Pb/^{238}U$		rho	Conc (%)	$^{207}Pb/^{206}Pb$		$^{206}Pb/^{238}U$	
U507_2	3.583	0.13	0.239	0.0072	0.42952	78.11086	1768	78	1381	37
U507_10	2.91	0.14	0.2025	0.0091	0.82723	72.11422	1646	77	1187	48
U507_10	4.42	0.21	0.2458	0.0049	0.46335	68.04421	2081	88	1416	25
U507_16	2.422	0.09	0.1758	0.0048	0.75923	64.36498	1622	65	1044	26
U507_15	2.708	0.079	0.1857	0.0046	0.70161	63.17606	1738	61	1098	25
U507_2	3.311	0.17	0.2001	0.0059	0.43558	60.25641	1950	100	1175	32
U507_1	2.829	0.13	0.173	0.0042	0.52655	53.25413	1936	90	1031	23
U507_11	3.396	0.16	0.1789	0.005	0.65005	48.58059	2184	89	1061	27
U507_7	1.57	0.066	0.1199	0.0048	0.8387	47.86605	1523	69	729	28
U507_15	2.25	0.18	0.1125	0.0034	0.46887	30.49268	2253	120	687	19
U507_4	1.594	0.083	0.0941	0.0041	0.8183	28.89222	2004	88	579	24
U603										
U603_51	90.2	8.1	1.021	0.079	0.80686	98.49967	4599	93	4530	260
U603_36	4.53	0.16	0.3027	0.0086	0.43046	96.70829	1762	73	1704	43
U603_11	4.52	0.18	0.3008	0.0081	0.40087	96.46925	1756	78	1694	40
U603_28	5.81	0.19	0.3415	0.0094	0.44987	96.148	1973	67	1897	46
U603_1	4.61	0.15	0.298	0.0091	0.2319	94.04232	1796	77	1689	43
U603_39	5.17	0.17	0.3201	0.009	0.21372	93.7631	1908	76	1789	44
U603_7	4.57	0.15	0.2987	0.0079	0.39393	93.03867	1810	70	1684	39
U603_26	4.443	0.14	0.2926	0.0072	0.66284	92.92135	1780	67	1654	36
U603_43	4.27	0.2	0.2724	0.0096	0.3683	85.18112	1822	93	1552	49
U603_2	3.99	0.14	0.259	0.0074	0.35549	81.71806	1816	71	1484	38
U603_38	5.149	0.15	0.2947	0.0075	0.53227	81.64868	2038	61	1664	37
U603_50	12.5	3.2	0.437	0.073	-0.94283	81.46853	2860	660	2330	320
U603_3	4.013	0.14	0.2553	0.0069	0.58546	79.88004	1834	70	1465	36
U603_4	4.073	0.14	0.2544	0.0073	0.63716	77.63646	1887	71	1465	39
U603_25	4.018	0.14	0.2479	0.0068	0.46476	74.51697	1915	67	1427	35
U603_12	5.18	0.18	0.2782	0.0083	0.6824	74.05152	2135	64	1581	42
U603_20	7.35	0.23	0.319	0.0095	0.38065	70.54172	2529	63	1784	46

Table 39. All U–Pb data for sample U603 (Limmen Sandstone) part 2 and sample U501 (Hodgson Sandstone) part 1

Analysis	$^{207}Pb/^{235}U$		$^{206}Pb/^{238}U$		rho	Conc (%)	$^{207}Pb/^{206}Pb$		$^{206}Pb/^{238}U$	
U603_30	3.5	0.13	0.2208	0.0064	0.46404	69.02845	1863	77	1286	34
U603_31	6.1	0.24	0.2804	0.011	0.73855	66.36098	2399	66	1592	55
U603_64	37.1	8.7	0.53	0.12	0.88727	65.06849	4380	150	2850	560
U603_37	3.411	0.11	0.2107	0.0061	0.39872	64.91043	1898	70	1232	32
U603_14	5.99	0.18	0.2743	0.0069	0.77423	64.75954	2412	57	1562	35
U603_34	5.73	0.21	0.2653	0.0083	0.6961	62.51546	2425	66	1516	42
U603_49	26	11	0.459	0.092	0.96073	62.43523	3860	480	2410	400
U603_19	3.227	0.11	0.2006	0.0067	0.655	61.67539	1910	68	1178	36
U603_33	4.551	0.14	0.2063	0.0054	0.58141	49.38725	2448	62	1209	29
U603_15	1.699	0.054	0.1061	0.003	0.69105	34.68517	1874	65	650	17
U501										
U501_60	5.26	0.27	0.3511	0.0098	0.6238	110.8062	1749	100	1938	47
U501_92	4.63	0.21	0.3202	0.0079	0.43999	105.4181	1698	90	1790	39
U501_90	4.59	0.21	0.317	0.0066	0.2038	103.8012	1710	92	1775	33
U501_97	3.9	0.19	0.2893	0.0072	0.32878	103.1427	1591	90	1641	37
U501_32	5.41	0.26	0.3411	0.0073	0.10406	102.938	1838	93	1892	35
U501_81	4.63	0.22	0.3156	0.0089	0.60381	101.7867	1735	84	1766	44
U501_100	6.48	0.3	0.3741	0.0092	0.39929	101.1864	2023	86	2047	43
U501_8	4.68	0.2	0.3172	0.0065	0.41223	101.0814	1757	83	1776	32
U501_2	3.915	0.19	0.2848	0.0071	-0.01985	100.5604	1606	100	1615	36
U501_51	5.26	0.24	0.3359	0.0074	0.33628	100.2687	1861	84	1866	36
U501_102	9.09	0.4	0.4371	0.0097	0.49393	99.9146	2342	79	2340	44
U501_65	4.582	0.2	0.3107	0.0069	0.40529	99.31624	1755	90	1743	34
U501_17	15.09	0.66	0.5437	0.013	0.52032	99.15074	2826	73	2802	53
U501_114	5.15	0.24	0.3301	0.0075	0.3553	99.08356	1855	90	1838	36
U501_19	4.68	0.22	0.3111	0.0068	0.45216	98.03371	1780	88	1745	34
U501_124	10.81	0.48	0.4677	0.01	0.49331	97.9786	2523	72	2472	44
U501_91	4.15	0.22	0.291	0.0078	0.24711	97.05015	1695	97	1645	39
U501_27	5.49	0.28	0.3336	0.0078	0.2945	95.71723	1938	93	1855	38

Table 40. All U–Pb data for sample U501 (Hodgson Sandstone) part 2

Analysis	$^{207}Pb/^{235}U$		$^{206}Pb/^{238}U$		rho	Conc (%)	$^{207}Pb/^{206}Pb$		$^{206}Pb/^{238}U$	
U501_28	21.06	1.1	0.605	0.017	0.76097	95.46024	3194	73	3049	70
U501_64	4.437	0.2	0.2964	0.0072	0.62561	95.37935	1753	82	1672	36
U501_118	4.54	0.22	0.3009	0.0081	0.14317	95.27559	1778	98	1694	40
U501_63	4.39	0.2	0.2936	0.0068	0.50977	93.83484	1768	90	1659	34
U501_5	4.77	0.23	0.3043	0.0086	0.62674	93.26087	1840	89	1716	44
U501_23	4.61	0.21	0.2981	0.0062	-0.06864	92.82165	1811	90	1681	31
U501_41	3.798	0.18	0.2692	0.0065	0.49222	92.25225	1665	90	1536	33
U501_38	4.484	0.2	0.2946	0.007	0.5189	91.9337	1810	80	1664	35
U501_40	4.183	0.19	0.2821	0.0067	0.46153	90.88851	1767	84	1606	32
U501_39	3.92	0.23	0.2669	0.009	0.81569	87.08571	1750	98	1524	46
U501_74	4.31	0.21	0.2808	0.0084	0.62425	86.95415	1832	90	1593	43
U501_42	4.3	0.21	0.2745	0.0086	0.68665	85.16903	1834	89	1562	43
U501_59	4.59	0.21	0.2844	0.0075	0.64098	85.06596	1895	81	1612	38
U501_26	4.39	0.2	0.2758	0.0069	0.43976	84.27268	1863	90	1570	35
U501_1	4.37	0.23	0.274	0.013	0.75404	82.64331	1884	89	1557	64
U501_12	3.707	0.17	0.2507	0.0061	0.33811	82.6361	1745	93	1442	31
U501_14	8.52	0.42	0.375	0.013	0.67763	82.28916	2490	84	2049	60
U501_11	4.05	0.19	0.261	0.0073	0.60489	82.21366	1816	86	1493	37
U501_77	3.1	0.19	0.2247	0.0097	0.67566	81.79535	1593	95	1303	51
U501_79	3.67	0.18	0.2474	0.0071	0.77064	80.22472	1780	80	1428	38
U501_57	3.292	0.17	0.23	0.0071	0.71884	78.09022	1707	86	1333	37
U501_70	3.84	0.21	0.2477	0.0083	0.87887	77.0146	1849	78	1424	43
U501_45	3.93	0.18	0.2467	0.0056	0.66381	75.90618	1876	80	1424	30
U501_18	2.953	0.14	0.2087	0.0062	0.63672	73.70326	1658	89	1222	33
U501_66	4.238	0.19	0.2522	0.0054	-0.36261	73.4787	1972	86	1449	28
U501_47	3.586	0.17	0.2297	0.0053	0.59384	72.3127	1842	81	1332	28
U501_117	3.515	0.16	0.2243	0.0056	0.3757	71.17904	1832	88	1304	29
U501_13	3.459	0.17	0.2227	0.0058	0.2246	70.38043	1840	86	1295	31
U501_115	3.129	0.14	0.2104	0.0051	0.68451	70.00569	1757	81	1230	27

Table 41. All U–Pb data for sample U501 (Hodgson Sandstone) part 3

Analysis	$^{207}Pb/^{235}U$		$^{206}Pb/^{238}U$		rho	Conc (%)	$^{207}Pb/^{206}Pb$		$^{206}Pb/^{238}U$	
U501_121	3.65	0.18	0.2218	0.0067	0.76336	68.55479	1889	84	1295	37
U501_111	10.76	0.49	0.3652	0.0094	0.75872	68.48382	2935	72	2010	43
U501_53	3.5	0.21	0.2206	0.0079	0.69369	68.26156	1881	96	1284	42
U501_22	3.312	0.14	0.2116	0.005	0.72137	67.37473	1836	80	1237	27
U501_58	3.541	0.16	0.2179	0.0046	-0.12013	67.01847	1895	93	1270	24
U501_24	3.84	0.22	0.2292	0.0071	0.2832	66.96878	1986	110	1330	37
U501_50	3.6	0.19	0.2194	0.01	0.83636	65.75554	1939	84	1275	54
U501_7	3.554	0.16	0.2169	0.0051	0.55023	65.44232	1933	82	1265	27
U501_123	3.302	0.15	0.2068	0.0047	0.5063	64.51785	1877	89	1211	25
U501_33	3.88	0.24	0.22	0.0077	0.31043	61.64581	2078	120	1281	41
U501_35	3.367	0.16	0.203	0.0053	0.71216	61.5186	1936	82	1191	28
U501_29	3.639	0.18	0.2125	0.007	0.732	61.2537	2026	81	1241	37
U501_10	2.775	0.12	0.1785	0.0043	0.58367	57.75109	1832	82	1058	23
U501_75	10.1	0.44	0.3117	0.0074	0.75646	57.06823	3063	71	1748	36
U501_108	3.19	0.19	0.1907	0.0058	0.71186	56.61802	1987	91	1125	31
U501_89	2.937	0.15	0.1802	0.006	0.80701	55.95176	1907	82	1067	33
U501_112	9.31	0.45	0.2993	0.0089	0.81886	55.80549	3023	77	1687	44
U501_49	4.821	0.22	0.2273	0.0062	0.8919	55.58365	2373	74	1319	33
U501_25	3.485	0.15	0.1951	0.0041	0.22435	54.95452	2089	81	1148	22
U501_76	2.7	0.16	0.171	0.0097	0.94537	54.31635	1865	81	1013	53
U501_30	3.09	0.16	0.183	0.0059	0.56203	54.12294	2001	87	1083	32
U501_3	3.967	0.18	0.2022	0.0051	0.74248	53.2555	2227	79	1186	27
U501_72	3.095	0.16	0.1785	0.0073	0.8632	53.14228	1989	82	1057	40
U501_101	3.484	0.16	0.1912	0.0054	0.8561	52.93565	2129	79	1127	29
U501_99	2.89	0.16	0.1745	0.0083	0.85733	52.86299	1956	87	1034	45
U501_103	3.303	0.15	0.1846	0.0048	0.75338	52.27382	2089	79	1092	26
U501_61	3.03	0.19	0.176	0.0098	0.73547	51.71046	2017	96	1043	53
U501_125	3.07	0.17	0.1752	0.0091	0.82375	51.00737	2035	87	1038	49
U501_43	3.7	0.19	0.1915	0.0067	0.72716	50.97153	2213	82	1128	36

Table 42. All U–Pb data for sample U501 (Hodgson Sandstone) part 4

Analysis	$^{207}Pb/^{235}U$		$^{206}Pb/^{238}U$		rho	Conc (%)	$^{207}Pb/^{206}Pb$		$^{206}Pb/^{238}U$	
U501_105	5.41	0.24	0.2243	0.0065	0.57847	50	2608	76	1304	34
U501_69	7.84	0.5	0.257	0.013	0.96264	49.7479	2975	74	1480	69
U501_20	5.34	0.37	0.22	0.013	0.92575	49.42263	2598	75	1284	69
U501_119	2.102	0.11	0.1396	0.0047	0.81651	48.13967	1747	86	841	26
U501_104	3.135	0.14	0.1703	0.0046	0.78761	47.81382	2127	78	1017	24
U501_55	2.587	0.11	0.1544	0.0039	0.56709	46.93049	1971	81	925	22
U501_98	1.8	0.083	0.1275	0.0035	0.8507	46.83925	1661	80	778	21
U501_106	2.748	0.14	0.1555	0.0037	0.55005	44.8891	2074	82	931	20
U501_48	2.485	0.12	0.1473	0.0053	0.72888	44.80323	1982	84	888	29
U501_34	2.28	0.14	0.142	0.0069	0.85926	44.6186	1914	82	854	39
U501_56	2.71	0.12	0.153	0.0037	0.46271	44.49296	2061	80	917	21
U501_73	2.537	0.12	0.1485	0.0055	0.87129	44.09293	2023	77	892	31
U501_68	2.345	0.12	0.1418	0.0051	0.83121	43.86235	1947	80	854	29
U501_71	2.13	0.099	0.1314	0.0035	0.65484	42.22812	1885	83	796	20
U501_95	2.056	0.11	0.1289	0.0046	0.77069	41.94415	1862	83	781	26
U501_85	2.43	0.12	0.1397	0.0058	0.87004	41.76965	2023	80	845	33
U501_16	2.605	0.12	0.1454	0.0034	0.63012	41.62702	2102	79	875	19
U501_67	2.167	0.099	0.1325	0.003	0.55277	41.23393	1945	84	802	17
U501_46	2.391	0.1	0.1378	0.0036	0.67258	41.12704	2023	77	832	20
U501_82	2.389	0.1	0.1376	0.0027	0.49632	40.78547	2037	78	830.8	15
U501_83	2.637	0.13	0.1428	0.0058	0.87868	40.12087	2151	78	863	33
U501_4	2.5	0.11	0.1382	0.0038	0.71894	39.48864	2112	77	834	22
U501_96	2.592	0.11	0.14	0.0038	0.72031	39.20111	2153	80	844	21
U501_122	2.137	0.097	0.1268	0.0037	0.76282	39.09507	1967	84	769	21
U501_36	7.03	0.96	0.2	0.011	0.8085	38.14332	3070	180	1171	58
U501_109	2.312	0.12	0.1289	0.004	0.69236	37.82082	2065	83	781	23
U501_107	2.889	0.13	0.143	0.0034	0.6046	37.62549	2291	79	862	19
U501_84	2.259	0.11	0.1264	0.0047	0.82842	36.96591	2083	83	770	27
U501_93	2.407	0.11	0.1235	0.0038	0.70853	33.45227	2242	79	750	22

Table 43. All U–Pb data for sample U501 (Hodgson Sandstone) part 5

Analysis	$^{207}Pb/^{235}U$		$^{206}Pb/^{238}U$		rho	Conc (%)	$^{207}Pb/^{206}Pb$		$^{206}Pb/^{238}U$	
U501_44	2.549	0.12	0.1254	0.0047	0.83375	32.98656	2307	78	761	27
U501_94	2.08	0.094	0.1132	0.003	0.63452	32.39569	2133	75	691	18
U501_110	1.866	0.085	0.107	0.0029	0.68549	31.85798	2056	82	655	17
U501_113	2.34	0.14	0.1167	0.0047	0.8873	31.1296	2284	82	711	27
U501_9	1.97	0.11	0.1083	0.0059	0.81522	30.86247	2145	88	662	34
U501_54	1.956	0.086	0.1049	0.0027	0.71842	29.98605	2151	77	645	16
U501_120	1.307	0.057	0.0846	0.0022	0.62071	28.79121	1820	82	524	13
U501_21	1.78	0.082	0.099	0.0029	0.80695	28.66572	2121	81	608	17
U501_6	2.279	0.1	0.1093	0.0037	0.83371	28.58365	2337	78	668	21
U501_52	1.793	0.088	0.0981	0.0032	0.81798	28.41659	2122	80	603	19
U501_87	1.67	0.13	0.0906	0.007	0.96292	25.93284	2144	83	556	41
U501_78	1.97	0.092	0.0921	0.0027	0.46235	23.80353	2382	77	567	16
U501_80	2.322	0.12	0.091	0.0033	0.79057	20.95629	2677	72	561	19
U501_116	1.61	0.071	0.0765	0.0024	0.63926	19.98317	2377	78	475	14
U501_37	1.422	0.075	0.0705	0.0028	0.84023	19.06209	2303	80	439	17
U501_88	1.36	0.088	0.0655	0.0022	0.41457	17.30851	2363	89	409	13
U501_31	1.365	0.062	0.0626	0.0019	0.83148	16.08714	2433	79	391.4	11
U501_62	1.377	0.067	0.0617	0.0017	0.70682	15.63158	2470	82	386.1	10
U501_15	0.932	0.058	0.049	0.0029	0.88912	13.88638	2218	80	308	18
U501_86	0.874	0.055	0.0456	0.0036	0.95966	12.78396	2245	98	287	22

Table 44. All U–Pb data for sample U503 (Jalboi Formation) part 1

Analysis	$^{207}Pb/^{235}U$		$^{206}Pb/^{238}U$		rho	Conc (%)	$^{207}Pb/^{206}Pb$		$^{206}Pb/^{238}U$	
U503										
U503_46	6.1	0.3	0.3706	0.011	0.4008	103.8875	1955	89	2031	52
U503_16	5.46	0.26	0.3432	0.0082	0.28643	102.3143	1858	97	1901	40
U503_43	10.45	0.51	0.469	0.014	0.27895	101.3872	2451	85	2485	60
U503_19	4.44	0.21	0.3054	0.0077	0.63935	101.0594	1699	88	1717	38
U503_34	3.999	0.18	0.2895	0.0075	0.43201	100.3062	1633	89	1638	37
U503_23	4.4	0.22	0.3054	0.0078	0.67183	100.1166	1715	92	1717	39
U503_25	4.76	0.27	0.3152	0.0091	0.14874	100.0564	1774	110	1775	45
U503_47	4.62	0.22	0.3106	0.0082	0.22251	99.31585	1754	95	1742	41
U503_44	11.13	0.5	0.4768	0.012	V	98.0484	2562	78	2512	51
U503_8	4.66	0.22	0.3116	0.0082	0.46306	97.87115	1785	87	1747	40
U503_38	6.05	0.29	0.3536	0.0088	0.35977	97.15994	2007	96	1950	42
U503_51	4.58	0.21	0.308	0.0071	0.33157	96.91877	1785	84	1730	35
U503_50	4.4	0.21	0.2976	0.0078	0.35846	96.54776	1738	89	1678	39
U503_5	4.85	0.25	0.3125	0.0085	0.52148	96.26168	1819	87	1751	42
U503_22	4.72	0.23	0.3065	0.0087	0.29747	95.13812	1810	98	1722	43
U503_10	10.46	0.48	0.449	0.012	0.54227	94.2429	2536	80	2390	56
U503_45	4.79	0.24	0.3069	0.0074	0.15163	93.71274	1845	98	1729	37
U503_26	5.64	0.27	0.3342	0.0079	0.33177	93.64919	1984	90	1858	38
U503_2	4.85	0.22	0.3053	0.0086	0.4066	92.4275	1862	86	1721	41
U503_6	4.21	0.21	0.2862	0.0075	0.4495	91.58667	1771	83	1622	38
U503_52	5.21	0.24	0.3209	0.0081	0.42457	91.43294	1961	83	1793	40
U503_15	4.63	0.21	0.2941	0.0084	0.59838	90.39088	1842	82	1665	40
U503_32	8.86	0.48	0.405	0.012	0.43647	90.27205	2426	88	2190	57
U503_18	4.29	0.21	0.28	0.008	0.36878	87.6516	1814	96	1590	40
U503_42	4.26	0.22	0.2746	0.0085	0.49201	85.59693	1826	94	1563	43
U503_14	4.18	0.22	0.2682	0.0074	0.28695	82.40043	1858	99	1531	37

Table 45. All U–Pb data for sample U503 (Jalboi Formation) part 2 and sample U505 (Arnold Sandstone) part 1

Analysis	$^{207}Pb/^{235}U$		$^{206}Pb/^{238}U$		rho	Conc (%)	$^{207}Pb/^{206}Pb$		$^{206}Pb/^{238}U$	
U503_48	5.86	0.28	0.317	0.0098	0.61799	82.08333	2160	89	1773	48
U503_35	3.64	0.24	0.244	0.012	0.83701	79.37853	1770	89	1405	63
U503_37	4.39	0.2	0.2672	0.0071	0.46836	78.41727	1946	86	1526	36
U503_21	4.019	0.18	0.2544	0.0062	0.46898	78.20032	1867	81	1460	32
U503_9	3.47	0.17	0.2318	0.0061	0.68879	75.36476	1782	84	1343	32
U503_29	3.7	0.19	0.2201	0.0074	0.66674	65.42959	1967	87	1287	40
U503_31	2.92	0.15	0.1839	0.0058	0.5427	59.02703	1850	90	1092	33
U503_20	2.76	0.15	0.1734	0.0076	0.79948	55.11516	1867	87	1029	42
U503_28	2.368	0.11	0.1453	0.0033	0.57425	45.10814	1942	83	876	19
U503_49	3.88	0.22	0.1675	0.007	0.89767	39.32096	2533	76	996	38
U505										
U505 - 4	4.682	0.12	0.3237	0.0051	0.44745	94.9115	1716	50	1808	25
U505 - 6	4.664	0.11	0.3188	0.0046	0.18543	96.30045	1718	49	1784	23
U505 - 41	4.915	0.1	0.3284	0.0046	0.035715	96.72668	1773	49	1833	23
U505 - 34	4.656	0.11	0.3168	0.005	0.13117	98.08343	1740	51	1774	24
U505 - 39	4.801	0.1	0.3208	0.0048	0.24409	98.43837	1765	47	1793	24
U505 - 13	4.855	0.11	0.3229	0.0046	0.31833	98.55876	1778	46	1804	22
U505 - 23	4.807	0.11	0.3202	0.0047	0.35956	98.77095	1768	49	1790	23
U505 - 31	4.801	0.1	0.3182	0.0044	0.20419	98.9048	1761	47	1780.5	21
U505 - 2	5.21	0.15	0.3346	0.0061	0.43036	98.92415	1839	56	1859	29
U505 - 20	4.652	0.1	0.3132	0.0043	0.1969	99.11756	1741	46	1756.5	21
U505 - 10	4.646	0.11	0.3163	0.0049	0.14487	99.15302	1756	52	1771	24
U505 - 35	4.711	0.11	0.3146	0.0048	0.047119	99.2059	1749	53	1763	24
U505 - 24	4.84	0.11	0.3216	0.0054	0.695	99.38787	1786	46	1797	26
U505 - 38	5.631	0.12	0.348	0.0056	0.52566	99.42827	1913	45	1924	27
U505 - 33	4.63	0.1	0.3114	0.0043	0.25143	100.1145	1749	48	1747	21

Table 46. All U–Pb data for sample U505 (Arnold Sandstone) part 2

Analysis	$^{207}Pb/^{235}U$		$^{206}Pb/^{238}U$		rho	Conc (%)	$^{207}Pb/^{206}Pb$		$^{206}Pb/^{238}U$	
U505 - 9	4.722	0.12	0.3143	0.0049	0.094559	100.1703	1765	54	1762	24
U505 - 36	4.713	0.12	0.3139	0.0049	0.23019	100.1704	1764	52	1761	24
U505 - 45	4.596	0.1	0.3093	0.0048	0.53196	100.1725	1742	46	1739	23
U505 - 37	4.77	0.11	0.3153	0.0048	0.23916	100.2831	1771	48	1766	23
U505 - 11	4.726	0.11	0.3148	0.0049	0.3421	100.3398	1772	51	1766	24
U505 - 27	4.826	0.11	0.3182	0.0048	0.085316	100.3933	1787	49	1780	23
U505 - 12	4.584	0.1	0.3093	0.0045	0.25426	100.403	1744	48	1737	22
U505 - 42	4.11	0.097	0.2927	0.0044	0.17965	100.6042	1665	52	1655	22
U505 - 44	5.568	0.12	0.3428	0.005	0.23847	100.6316	1912	46	1900	24
U505 - 48	4.946	0.1	0.3214	0.0045	0.36285	100.9465	1813	45	1796	22
U505 - 28	9.87	0.21	0.4464	0.0069	0.20969	102.6459	2444	46	2381	31
U505 - 26	4.465	0.093	0.3013	0.0043	0.22037	102.9429	1749	47	1699	21
U505 - 1	4.674	0.11	0.3087	0.0043	0.12214	103.0565	1787	48	1734	21
U505 - 17	4.472	0.12	0.3013	0.005	0.31085	103.6535	1759	52	1697	25
U505 - 47	4.431	0.12	0.3003	0.0059	0.61008	103.7146	1759	50	1696	28
U505 - 40	4.59	0.1	0.3055	0.0046	0.27832	103.7835	1783	47	1718	23
U505 - 7	4.526	0.099	0.3008	0.0046	0.46595	104.8968	1778	46	1695	23
U505 - 3	4.28	0.097	0.2895	0.0045	0.27548	106.0976	1740	51	1640	22
U505 - 8	4.256	0.11	0.2852	0.0044	0.21752	108.8435	1760	54	1617	22
U505 - 19	3.391	0.099	0.25	0.0055	0.16613	109.8748	1580	66	1438	28
U505 - 29	9.01	0.21	0.4086	0.0067	0.2996	110.9651	2449	45	2207	31
U505 - 30	4.407	0.1	0.2863	0.0047	0.45673	111.3986	1808	48	1623	24
U505 - 25	3.949	0.1	0.269	0.0043	0.025838	113.6808	1745	56	1535	22
U505 - 14	4.244	0.11	0.2765	0.0045	0.48291	115.0668	1810	49	1573	23

Table 47. All U–Pb data for sample U505 (Arnold Sandstone) part 3 and sample L04 (Munyi Member) part 1

Analysis	$^{207}Pb/^{235}U$		$^{206}Pb/^{238}U$		rho	Conc (%)	$^{207}Pb/^{206}Pb$		$^{206}Pb/^{238}U$	
U505 - 18	3.998	0.099	0.2677	0.0047	0.6202	115.1733	1761	47	1529	24
U505 - 15	4.006	0.11	0.2697	0.0049	0.098747	115.2047	1773	60	1539	25
U505 - 46	3.796	0.092	0.2507	0.0044	0.43487	123.5784	1782	50	1442	23
U505 - 5	3.36	0.12	0.2323	0.0051	0.38327	127.786	1720	69	1346	27
U505 - 32	3.457	0.083	0.2306	0.0039	0.60466	132.7599	1775	47	1337	20
U505 - 22	3.27	0.14	0.2198	0.0049	0.44662	136.8462	1753	68	1281	26
U505 - 21	2.926	0.078	0.1952	0.0042	0.74549	152.2193	1749	48	1149	22
L04										
L04 - 145	5.228	0.1	0.3398	0.0049	0.45207	103.401	1823	44	1885	24
L04 - 119	3.92	0.099	0.287	0.0043	0.22565	103.0418	1578	52	1626	22
L04 - 118	4.846	0.11	0.3224	0.0051	0.22892	102.1554	1763	50	1801	25
L04 - 105	4.805	0.12	0.3218	0.0048	0.060501	101.6375	1771	52	1800	24
L04 - 127	4.641	0.12	0.3152	0.005	0.20667	101.436	1741	55	1766	25
L04 - 110	4.697	0.11	0.3153	0.0047	0.33161	100.9138	1751	48	1767	23
L04 - 73	4.7	0.11	0.3158	0.0046	0.16723	100.8542	1756	51	1771	23
L04 - 62	4.708	0.13	0.3167	0.0047	0.24389	100.7959	1759	57	1773	23
L04 - 60	4.712	0.1	0.3151	0.0043	0.06123	100.2442	1761	49	1765.3	21
L04 - 123	4.5	0.23	0.3053	0.009	0.050682	100.2319	1725	110	1729	39
L04 - 51	5.08	0.11	0.3274	0.0048	0.10605	100.0548	1824	48	1825	23
L04 - 59	4.836	0.12	0.3194	0.0055	0.56497	99.88833	1791	48	1789	27
L04 - 135	4.806	0.12	0.3191	0.0047	0.13305	99.88808	1787	54	1785	23
L04 - 71	4.719	0.12	0.3166	0.0048	0.22558	99.7749	1777	51	1773	24
L04 - 101	4.639	0.1	0.3101	0.0044	0.32739	99.48571	1750	49	1741	22
L04 - 147	4.687	0.11	0.3134	0.0047	0.14205	99.32165	1769	49	1757	23
L04 - 146	4.712	0.11	0.313	0.0048	0.2787	99.20949	1771	52	1757	24
L04 - 86	4.775	0.11	0.3153	0.0045	0.25016	99.10314	1784	50	1768	23

Table 48. All U–Pb data for sample L04 (Munyi Member) part 2

Analysis	$^{207}Pb/^{235}U$		$^{206}Pb/^{238}U$		rho	Conc (%)	$^{207}Pb/^{206}Pb$		$^{206}Pb/^{238}U$	
L04 - 85	4.714	0.096	0.3132	0.0045	0.4306	98.98592	1775	45	1757	22
L04 - 157	4.736	0.1	0.3136	0.0045	0.19548	98.93078	1777	47	1758	22
L04 - 57	4.71	0.094	0.3133	0.0044	0.43642	98.87451	1777	42	1757	21
L04 - 121	4.833	0.12	0.3174	0.0049	0.41098	98.83204	1798	50	1777	24
L04 - 156	4.685	0.096	0.3125	0.0045	0.41997	98.81623	1774	45	1753	22
L04 - 66	4.754	0.12	0.3148	0.0046	0.312	98.76889	1787	50	1765	22
L04 - 153	4.756	0.11	0.3156	0.0046	0.12678	98.60569	1793	51	1768	22
L04 - 125	4.774	0.11	0.3163	0.0045	0.27895	98.55395	1798	50	1772	22
L04 - 70	4.939	0.12	0.3203	0.0048	0.23068	98.13699	1825	52	1791	24
L04 - 141	4.75	0.1	0.312	0.0045	0.29239	97.38453	1797	45	1750	22
L04 - 92	4.591	0.094	0.306	0.0045	0.40734	97.0124	1774	46	1721	22
L04 - 130	4.552	0.11	0.3054	0.0051	0.43193	96.79415	1778	53	1721	26
L04 - 76	4.671	0.12	0.3092	0.0047	0.11469	96.7688	1795	54	1737	23
L04 - 133	4.762	0.11	0.3104	0.0051	0.54843	96.34956	1808	47	1742	25
L04 - 120	4.36	0.11	0.2954	0.006	0.63757	95.91719	1739	47	1668	30
L04 - 89	4.618	0.11	0.3058	0.0049	0.453	95.71269	1796	47	1719	24
L04 - 97	4.316	0.089	0.2936	0.0041	0.35018	95.10029	1745	46	1659.5	20
L04 - 96	4.76	0.14	0.3079	0.0057	0.11759	94.17529	1837	60	1730	28
L04 - 134	4.233	0.099	0.2863	0.0048	0.63508	92.53136	1754	48	1623	24
L04 - 109	4.164	0.092	0.2826	0.004	0.39327	92.23692	1739	48	1604	20
L04 - 63	4.355	0.1	0.289	0.006	0.51319	91.70404	1784	51	1636	30
L04 - 115	4.531	0.12	0.2939	0.005	0.32478	90.91407	1827	55	1661	25
L04 - 81	3.144	0.069	0.2389	0.0042	0.86062	90.3268	1530	45	1382	22
L04 - 61	4.162	0.099	0.2781	0.0043	0.63688	89.177	1774	44	1582	22
L04 - 113	4.408	0.1	0.2867	0.0049	0.35389	89.13282	1822	49	1624	24
L04 - 93	4.023	0.12	0.2716	0.0043	0.13207	88.61556	1748	61	1549	22
L04 - 49	3.948	0.11	0.2658	0.0061	0.82146	86.89181	1747	46	1518	31
L04 - 159	3.76	0.12	0.2602	0.006	0.72734	86.82984	1716	51	1490	31
L04 - 56	4.22	0.13	0.275	0.0049	0.52866	86.47156	1811	53	1566	25

Table 49. All U–Pb data for sample L04 (Munyi Member) part 3

Analysis	$^{207}Pb/^{235}U$		$^{206}Pb/^{238}U$		rho	Conc (%)	$^{207}Pb/^{206}Pb$		$^{206}Pb/^{238}U$	
L04 - 69	3.93	0.15	0.2638	0.0085	0.89403	86.09687	1755	51	1511	43
L04 - 80	3.976	0.098	0.2598	0.0051	0.78762	82.71262	1799	45	1488	26
L04 - 160	3.67	0.13	0.2476	0.0062	0.64883	81.20729	1756	68	1426	32
L04 - 55	4.053	0.088	0.2569	0.0037	0.26222	79.37534	1857	47	1474	19
L04 - 137	4.187	0.093	0.2593	0.0038	0.3594	78.08723	1903	47	1486	20
L04 - 139	3.69	0.12	0.2422	0.0062	0.81584	77.62354	1801	56	1398	32
L04 - 83	3.487	0.09	0.2345	0.0046	0.57593	77.2779	1756	51	1357	24
L04 - 122	3.33	0.099	0.2276	0.0041	0.5351	76.94994	1718	54	1322	22
L04 - 116	3.554	0.11	0.2366	0.005	0.64968	76.73767	1784	52	1369	26
L04 - 88	3.53	0.079	0.2347	0.0038	0.53622	76.60654	1774	46	1359	20
L04 - 131	4.06	0.17	0.2504	0.0045	0.11794	76.00211	1896	74	1441	23
L04 - 124	3.421	0.092	0.2263	0.0039	0.35708	73.62822	1786	56	1315	21
L04 - 74	3.051	0.072	0.2101	0.0037	0.72569	71.16387	1727	46	1229	20
L04 - 129	3.074	0.083	0.2097	0.0039	0.46207	71.04806	1727	57	1227	21
L04 - 111	3.228	0.082	0.2149	0.0038	0.41492	70.34753	1784	53	1255	20
L04 - 98	3.113	0.07	0.2095	0.0031	0.39446	69.22078	1771	46	1225.9	17
L04 - 91	3.072	0.1	0.206	0.005	0.72035	69.08987	1747	59	1207	27
L04 - 107	3.111	0.077	0.2087	0.0037	0.72664	69.06109	1768	47	1221	20
L04 - 136	2.914	0.083	0.2014	0.0044	0.83713	69.04206	1712	46	1182	24
L04 - 154	2.8	0.12	0.1934	0.0066	0.92874	66.56926	1711	48	1139	35
L04 - 95	2.931	0.081	0.1981	0.0046	0.78864	66.49543	1752	47	1165	25
L04 - 84	2.899	0.092	0.1952	0.0038	0.66131	66.22478	1735	55	1149	20
L04 - 132	2.906	0.069	0.1966	0.0034	0.63286	66.00114	1753	47	1157	18
L04 - 140	2.332	0.066	0.1743	0.0038	0.59311	65.98726	1570	56	1036	21
L04 - 58	2.945	0.088	0.1973	0.0042	0.42314	65.96591	1760	59	1161	23
L04 - 108	2.242	0.062	0.1694	0.0035	0.47427	65.2652	1546	62	1009	19
L04 - 67	3.56	0.16	0.2156	0.0085	0.17458	65.08019	1933	71	1258	45
L04 - 75	2.915	0.092	0.1928	0.0044	0.38133	65.04854	1751	62	1139	24

Table 50. All U–Pb data for sample L04 (Munyi Member) part 4

Analysis	$^{207}Pb/^{235}U$		$^{206}Pb/^{238}U$		rho	Conc (%)	$^{207}Pb/^{206}Pb$		$^{206}Pb/^{238}U$	
L04 - 152	2.51	0.093	0.1801	0.0054	0.95448	65	1640	45	1066	29
L04 - 103	2.816	0.067	0.1898	0.004	0.6839	63.89047	1753	47	1120	22
L04 - 52	2.815	0.075	0.1897	0.0032	0.48988	63.56413	1762	50	1120	17
L04 - 79	5.44	0.2	0.2556	0.0075	0.78299	61.46751	2385	52	1466	38
L04 - 114	2.728	0.061	0.1823	0.003	0.73025	61.2025	1763	46	1079	16
L04 - 104	10.5	1.1	0.322	0.0086	0.40549	60.13378	2990	190	1798	42
L04 - 138	2.499	0.063	0.1721	0.0032	0.72132	59.70845	1715	48	1024	18
L04 - 87	2.672	0.083	0.177	0.0038	0.40616	59.65909	1760	64	1050	21
L04 - 144	2.916	0.067	0.1865	0.003	0.4061	59.43905	1854	47	1102	16
L04 - 99	2.753	0.091	0.1778	0.0039	0.65287	57.94393	1819	53	1054	21
L04 - 94	2.402	0.061	0.1646	0.0032	0.83716	57.16773	1723	45	985	19
L04 - 77	2.4	0.072	0.1634	0.0037	0.79249	56.26082	1733	50	975	20
L04 - 142	2.346	0.052	0.1576	0.003	0.82092	54.22657	1739	44	943	16
L04 - 82	2.659	0.076	0.1664	0.0042	0.54321	53.47709	1855	53	992	23
L04 - 65	2.058	0.044	0.1463	0.0023	0.68104	53.42441	1647	45	879.9	13
L04 - 54	1.955	0.05	0.1418	0.003	0.84573	53.10559	1610	47	855	17
L04 - 158	2.355	0.058	0.1564	0.003	0.75673	52.40492	1788	47	937	17
L04 - 155	2.154	0.062	0.1479	0.003	0.43116	51.71611	1719	53	889	17
L04 - 72	2.109	0.1	0.1455	0.0065	0.93324	51.46542	1706	50	878	37
L04 - 128	2.451	0.069	0.1575	0.0031	0.57602	51.19435	1842	51	943	17
L04 - 50	2.122	0.085	0.1458	0.0037	0.83982	50.54755	1735	52	877	21
L04 - 90	2.297	0.079	0.1524	0.0035	0.54472	50.49724	1810	59	914	20
L04 - 68	2.099	0.061	0.1441	0.0034	0.80671	50.46512	1720	51	868	19
L04 - 149	2.102	0.089	0.1443	0.0055	0.9674	50.29002	1724	44	867	31
L04 - 148	2.1	0.053	0.1433	0.0024	0.46739	49.82102	1732	52	862.9	14
L04 - 143	1.842	0.052	0.1337	0.0033	0.86589	49.54072	1633	47	809	19
L04 - 112	1.933	0.065	0.134	0.0024	0.12878	47.41954	1709	70	810.4	14

Table 51. All U–Pb data for sample L04 (Munyi Member) part 5

Analysis	$^{207}Pb/^{235}U$		$^{206}Pb/^{238}U$		rho	Conc (%)	$^{207}Pb/^{206}Pb$		$^{206}Pb/^{238}U$	
L04 - 102	1.857	0.07	0.1276	0.0032	0.85267	44.89559	1724	58	774	18
L04 - 106	1.879	0.055	0.1272	0.0024	0.46521	44.44444	1737	57	772	14
L04 - 117	1.872	0.051	0.1252	0.0024	0.57452	43.47826	1748	52	760	14
L04 - 53	1.568	0.036	0.1119	0.0019	0.77238	41.88725	1632	45	683.6	11
L04 - 64	1.78	0.051	0.1178	0.0032	0.91855	40.12311	1787	43	717	18
L04 - 126	1.363	0.057	0.0947	0.0031	0.83368	34.39528	1695	57	583	18
L04 - 150	1.194	0.034	0.0857	0.0016	0.58935	32.38852	1637	55	530.2	9.5
L04 - 78	1.442	0.057	0.0946	0.0028	0.74942	32.38731	1797	57	582	16
L04 - 151	1.097	0.049	0.0749	0.0029	0.93137	26.80115	1735	49	465	18
L04 - 100	0.754	0.028	0.0531	0.0016	0.52197	20.04209	1663	67	333.3	10

Table 52. REE data for concordant data in sample U501 (Hodgson Sandstone)

	Age	Error	Concordance	La	Ce	Pr	Nd	Sm	Eu	Gd	Tb	Dy	Ho	Er	Tm	Yb	Lu	Lu/La	Lu/Gd	Eu*	Ce*
U501_60	1749	100	110.806175	#VALUE!	12.990196	5.57895	10.4711	20.392	10.0172	49.148	90.9091	151.181	265.724	442.9	675.2941	1052.35	1547.24	#VALUE!	31.481056	1.20124	#VALUE!
U501_92	1698	90	105.418139	#VALUE!	11.143791	0.54737	1.67024	14.183	3.68966	55.961	112.299	207.087	346.29	554.08	741.9608	1056.47	1361.02	#VALUE!	24.3209	0.44055	#VALUE!
U501_90	1710	92	103.8011696	#VALUE!	9.869281	#VALUE!	#VALUE!	#VALUE!	#VALUE!	54.355	103.476	188.583	321.908	494.86	676.4706	942.941	1241.73	#VALUE!	22.844761	#VALUE!	#VALUE!
U501_97	1591	90	103.1426776	2.10970464	74.183007	#VALUE!	#VALUE!	#VALUE!	#VALUE!	167.88	295.455	533.858	876.325	1407.3	1838.039	2598.82	3476.38	1647.80315	20.707121	#VALUE!	#VALUE!
U501_32	1838	93	102.9379761	#VALUE!	#VALUE!	#VALUE!	#VALUE!	#VALUE!	#VALUE!	#VALUE!	#VALUE!	#VALUE!	#VALUE!	523.26	699.2157	964.706	1251.97	#VALUE!	#VALUE!	#VALUE!	#VALUE!
U501_81	1735	84	101.7867435	#VALUE!	#VALUE!	#VALUE!	#VALUE!	#VALUE!	#VALUE!	#VALUE!	#VALUE!	#VALUE!	#VALUE!	876.74	#VALUE!	1582.35	2019.69	#VALUE!	#VALUE!	#VALUE!	#VALUE!
U501_100	2023	86	101.1863569	#VALUE!	#VALUE!	#VALUE!	#VALUE!	#VALUE!	#VALUE!	#VALUE!	#VALUE!	30.315	52.4735	89.003	131.3725	217.647	333.071	#VALUE!	#VALUE!	#VALUE!	#VALUE!
U501_8	1757	83	101.0813887	#VALUE!	12.663399	#VALUE!	#VALUE!	19.02	#VALUE!	92.165	170.053	321.654	558.834	894.86	1175.294	1647.06	2181.89	#VALUE!	23.673619	#VALUE!	#VALUE!
U501_2	1606	100	100.5603985	0.28270042	49.166667	5.82105	13.5332	31.634	22.931	112.9	197.059	355.512	600.353	991.54	1421.569	2088.82	2960.63	10472.676	26.224545	1.90742	19.9009
U501_51	1861	84	100.2686728	#VALUE!	10.964052	1.4	3.81156	23.856	#VALUE!	89.197	146.257	249.606	398.41	600	769.0196	1052.94	1319.69	#VALUE!	14.79516	#VALUE!	#VALUE!
U501_102	2342	79	99.9146029	20.6751055	34.477124	#VALUE!	#VALUE!	#VALUE!	#VALUE!	#VALUE!	#VALUE!	185.827	297.703	477.95	645.8824	947.059	1230.71	59.5261128	#VALUE!	#VALUE!	#VALUE!
U501_65	1755	90	99.31623932	0.06962025	12.745098	1.52632	3.57602	17.451	5.84483	70.316	134.492	255.906	443.463	693.05	928.2353	1313.53	1717.32	24667.0007	24.422826	0.62389	10.0887
U501_17	2826	73	99.1507431	#VALUE!	31.928105	#VALUE!	#VALUE!	#VALUE!	#VALUE!	101.31	181.551	326.378	542.58	832.63	1103.922	1545.88	1968.9	#VALUE!	19.433644	#VALUE!	#VALUE!
U501_114	1855	90	99.08355795	#VALUE!	#VALUE!	#VALUE!	#VALUE!	#VALUE!	#VALUE!	#VALUE!	172.193	328.74	588.693	954.08	1267.843	1839.41	2326.77	#VALUE!	#VALUE!	#VALUE!	#VALUE!
U501_19	1780	88	98.03370787	#VALUE!	14.232026	#VALUE!	#VALUE!	22.549	#VALUE!	78.735	148.93	268.898	443.286	711.18	942.3529	1329.41	1762.6	#VALUE!	22.386525	#VALUE!	#VALUE!
U501_124	2523	72	97.97859691	#VALUE!	23.137255	#VALUE!	#VALUE!	15.033	#VALUE!	58.491	96.5241	163.386	261.484	391.54	506.6667	730.588	934.646	#VALUE!	15.979175	#VALUE!	#VALUE!
U501_91	1695	97	97.05014749	#VALUE!	21.552288	0.43158	1.67024	10.392	5.98276	46.326	92.7807	168.11	289.576	464.05	636.8627	894.706	1212.6	#VALUE!	26.175313	0.7944	#VALUE!
U501_27	1938	93	95.71723426	0.16033755	12.271242	1.82105	7.00214	39.02	18.1552	129.44	210.695	344.882	532.686	760.73	940.3922	1221.76	1552.36	9681.83796	11.992873	1.39879	8.71773
U501_28	3194	73	95.46023795	0.59915612	17.287582	14.9474	27.8373	83.856	54.4828	290.51	517.914	888.583	1424.03	2079.2	2545.098	3376.47	4133.86	6899.46767	14.229613	2.81585	4.38447
U501_64	1753	82	95.37934969	1.10970464	35.212418	22	34.0471	57.778	28.4483	109.98	174.866	279.528	431.095	661.03	856.4706	1175.88	1506.3	1357.3875	13.696659	2.19644	7.32485
U501_118	1778	98	95.27559055	6.32911392	13.562092	12.3684	28.651	100.72	41.3793	284.67	450.535	710.236	1065.37	1499.7	1811.765	2488.24	3212.6	507.590551	11.285282	2.10782	3.13642
U501_63	1768	90	93.83484163	#VALUE!	#VALUE!	#VALUE!	#VALUE!	#VALUE!	#VALUE!	#VALUE!	#VALUE!	#VALUE!	520.671	791.54	1003.137	1428.82	1857.48	#VALUE!	#VALUE!	#VALUE!	#VALUE!
U501_5	1840	89	93.26086957	0.29535865	13.69281	8.42105	15.2034	35.163	19.1379	101.7	176.738	296.063	454.947	670.09	866.2745	1207.65	1558.66	5277.18223	15.325594	1.63586	4.63793
U501_23	1811	90	92.8216455	#VALUE!	15.04902	#VALUE!	#VALUE!	21.307	9.13793	84.185	162.567	293.307	499.823	784.89	1045.098	1469.41	1914.57	#VALUE!	22.742399	0.88969	#VALUE!
U501_41	1665	90	92.25225225	#VALUE!	#VALUE!	#VALUE!	#VALUE!	#VALUE!	#VALUE!	#VALUE!	#VALUE!	374.016	#VALUE!	999.4	#VALUE!	1992.35	2677.17	#VALUE!	#VALUE!	#VALUE!	#VALUE!
U501_38	1810	80	91.93370166	1.96624473	35.310458	53.2632	79.015	103.14	#VALUE!	183.45	279.679	416.535	642.933	946.22	1227.059	1698.24	2187.4	1112.47677	11.923369	#VALUE!	4.75136
U501_40	1767	84	90.8885116	5.23206751	42.156863	23.5789	36.6167	64.706	46.3793	138.69	226.738	355.512	552.473	847.13	1118.431	1605.88	2181.1	416.871984	15.726896	3.25205	7.85397

Table 53. REE data for concordant data in sample L02 (Hodgson Sandstone) part 1

	Age	Error	Concordance	La	Ce	Pr	Nd	Sm	Eu	Gd	Tb	Dy	Ho	Er	Tm	Yb	Lu	Lu/La	Lu/Gd	Eu*	Ce*
L02_98	4910	130	134.4195519	x9915.611814	7254.902	4473.68	2869.38	1307.2	555.172	583.94	371.658	466.667	464.664	618.13	799.2157	1096.47	1381.5	#VALUE!	2.365812	12.7664	#VALUE!
L02_33	1724	64	109.4547564	#VALUE!	11.993464	0.95789	3.36188	21.83	4.77586	82.871	148.663	322.141	442.756	672.51	891.3725	1217.06	1594.49	#VALUE!	19.240594	0.46674	#VALUE!
L02_80	1710	52	109.2982456	#VALUE!	10.964052	#VALUE!	#VALUE!	12.81	3.62069	57.518	105.348	237.956	333.922	520.24	696.8627	988.235	1293.7	#VALUE!	22.492006	0.43174	#VALUE!
L02_110	1722	57	108.5946574	#VALUE!	12.205882	0.35789	1.67024	10.654	4.15517	52.993	102.674	237.47	331.272	529.91	720.3922	1049.41	1385.83	#VALUE!	26.151277	0.52084	#VALUE!
L02_50	1728	50	107.349537	#VALUE!	20.980392	2.64211	8.41542	44.183	17.0345	153.77	228.61	420.438	499.293	654.98	738.8235	922.941	1094.88	#VALUE!	7.1201971	1.21073	#VALUE!
L02_21	1753	54	107.0735881	0.14345992	58.202614	3.61053	11.1135	44.379	32.5862	142.09	225.668	449.148	584.806	860.42	1106.667	1499.41	1959.45	13658.5109	13.789957	2.38631	30.0397
L02_57	1710	39	106.5497076	0.66666667	34.052288	1.74737	3.57602	13.333	10.3621	44.088	86.0963	201.46	295.76	538.97	825.8824	1361.18	2011.81	3017.71654	45.632137	1.36745	21.9167
L02_71	1682	50	106.0047562	#VALUE!	22.51634	1.16842	4.0257	26.536	7.46552	90.998	160.695	349.392	451.237	679.76	901.1765	1255.88	1633.86	#VALUE!	17.954967	0.68862	#VALUE!
L02_112	1743	57	105.6798623	0.13080169	11.339869	4	13.1692	63.856	28.7931	249.64	423.529	909.002	1197.88	1732.3	2058.431	2680.59	3295.28	25192.9134	13.200373	1.62621	5.57944
L02_75	1738	52	104.8331415	#VALUE!	8.6111111	0.30526	0.85653	8.4967	1.65517	52.311	113.636	285.645	425.618	716.01	1005.098	1470	1944.88	#VALUE!	37.178905	0.21226	#VALUE!
L02_65	1737	52	104.720783	#VALUE!	15.098039	0.50526	2.29122	17.32	4.63793	84.672	166.845	387.348	527.915	858.61	1126.667	1610.59	2062.99	#VALUE!	24.364648	0.45924	#VALUE!
L02_24	1619	58	104.6942557	#VALUE!	#VALUE!	#VALUE!	#VALUE!	#VALUE!	#VALUE!	56.594	103.743	231.63	325.265	511.78	689.0196	988.824	1330.31	#VALUE!	23.506425	#VALUE!	#VALUE!
L02_20	1732	44	104.4457275	#VALUE!	12.53268	0.50526	1.99143	16.144	3.27586	73.528	151.337	358.151	496.996	805.44	1084.706	1534.12	2031.5	#VALUE!	27.628884	0.34594	#VALUE!
L02_22	1761	52	104.3725156	#VALUE!	17.075163	#VALUE!	1.30621	9.8693	1.86207	38.394	81.5508	175.182	241.343	383.08	515.6863	726.471	977.165	#VALUE!	25.450885	0.26803	#VALUE!
L02_111	1728	58	104.1666667	#VALUE!	#VALUE!	#VALUE!	#VALUE!	#VALUE!	#VALUE!	#VALUE!	#VALUE!	374.696	#VALUE!	809.67	#VALUE!	1480	#VALUE!	#VALUE!	#VALUE!	#VALUE!	#VALUE!
L02_56	2445	32	104.1308793	#VALUE!	8.3823529	0.23579	1.26338	16.863	1.84483	78.54	175.401	396.594	520.141	816.92	1103.529	1551.76	1956.69	#VALUE!	24.913283	0.18888	#VALUE!
L02_58	1852	58	104.049676	0.12236287	10.294118	3.05263	9.25054	44.575	40	139.66	203.743	386.861	468.375	643.5	802.3529	1062.94	1389.37	11354.5072	9.948277	2.94696	5.7772
L02_14	1762	56	104.0295119	#VALUE!	6.0784314	#VALUE!	2.52677	23.137	#VALUE!	122.63	254.011	581.509	814.134	1284.6	1678.824	2343.53	3019.69	#VALUE!	24.624813	#VALUE!	#VALUE!
L02_74	1705	49	103.3431085	#VALUE!	10.196078	0.36842	1.58458	12.614	2.2931	56.837	114.439	262.774	379.859	618.73	852.549	1220	1607.48	#VALUE!	28.282295	0.27516	#VALUE!
L02_64	1811	51	103.3130867	0.08860759	15.833333	3.31579	11.0493	51.438	27.7586	156.69	232.888	456.448	563.604	791.54	1018.824	1415.29	1830.71	20660.8549	11.68356	1.92412	8.58128
L02_84	1712	47	103.1542056	0.05274262	55.196078	0.58947	3.3833	23.529	17.6034	87.543	140.909	305.596	401.767	613.9	815.6863	1157.06	1532.68	29059.5591	17.507791	1.6703	68.8759
L02_89	1755	53	103.019943	#VALUE!	13.72549	0.67368	2.54818	16.536	3.94828	85.937	168.449	386.861	546.466	863.44	1132.941	1601.76	2074.8	#VALUE!	24.143378	0.39003	#VALUE!
L02_19	1595	53	103.0094044	5.18987342	47.124183	5.57895	6.63812	15.425	5.98276	63.212	128.877	293.917	416.784	677.95	928.2353	1398.24	1920.87	370.11811	30.387836	0.67467	14.3602
L02_70	1726	52	102.9548088	#VALUE!	37.369281	#VALUE!	4.96788	29.02	17.4138	87.883	151.07	299.757	367.314	540.18	705.098	972.941	1246.06	#VALUE!	14.178624	1.61057	#VALUE!
L02_104	1749	69	102.8016009	0.12658228	7.2385621	1.85263	6.50964	36.732	14.6207	136.25	242.513	513.382	664.488	992.15	1258.039	1667.06	2106.3	16639.7638	15.458732	1.11164	5.14524
L02_81	1784	50	102.690583	#VALUE!	12.647059	1.83158	6.2955	32.876	17.2414	105.11	195.455	445.742	607.774	985.5	1318.039	1861.76	2460.63	#VALUE!	23.41016	1.46776	#VALUE!
L02_34	1754	42	102.6795895	0.05147679	12.320261	1.03158	2.54818	19.542	5.18966	84.623	166.578	403.893	571.025	937.16	1279.608	1852.94	2421.26	47035.9494	28.612358	0.50848	11.8384
L02_96	1705	47	102.3460411	177.21519	189.54248	137.895	124.197	101.31	38.6207	173.24	288.503	541.606	659.894	990.94	1302.745	1798.82	2188.98	12.352081	12.635805	2.33085	10.6776
L02_1	1724	54	102.262181	#VALUE!	#VALUE!	#VALUE!	#VALUE!	#VALUE!	#VALUE!	#VALUE!	#VALUE!	506.083	#VALUE!	913.6	#VALUE!	1505.88	#VALUE!	#VALUE!	#VALUE!	#VALUE!	#VALUE!
L02_93	1747	54	102.1751574	#VALUE!	11.633987	#VALUE!	2.39829	14.706	2.94828	65.937	131.551	300.73	415.548	659.82	883.5294	1272.94	1639.37	#VALUE!	24.862771	0.32831	#VALUE!

Table 54. REE data for concordant data in sample L02 (Hodgson Sandstone) part 2

	Age	Error	Concordance	La	Ce	Pr	Nd	Sm	Eu	Gd	Tb	Dy	Ho	Er	Tm	Yb	Lu	Lu/La	Lu/Gd	Eu*	Ce*
L02_62	1785	52	102.0728291	#VALUE!	11.111111	0.50526	2.35546	13.856	2.46552	63.747	112.834	254.988	348.587	554.08	712.1569	994.118	1255.51	#VALUE!	19.695243	0.27988	#VALUE!
L02_55	1751	45	102.055968	#VALUE!	20.686275	#VALUE!	#VALUE!	16.536	#VALUE!	67.445	129.947	293.431	411.661	636.86	854.902	1200	1570.08	#VALUE!	23.279306	#VALUE!	#VALUE!
L02_41	1762	48	101.7593644	0.1814346	10.310458	0.49474	2.65525	20.719	5.17241	109.15	225.936	535.28	756.36	1209.7	1645.098	2274.12	2940.94	16209.3939	26.944457	0.45388	12.5386
L02_43	2285	34	101.7067834	0.11814346	10.114379	1.57895	4.58244	31.242	14.4828	110.46	195.455	389.781	468.551	696.68	894.902	1214.12	1598.43	13529.5276	14.470325	1.21663	7.76402
L02_45	1758	57	101.5358362	0.3628692	12.598039	1.23158	4.58244	23.922	6.91379	97.324	172.995	363.504	488.869	740.18	975.6863	1330.59	1708.66	4708.75298	17.556496	0.62789	9.97695
L02_88	1658	53	101.2062726	0.08691983	31.503268	1.36842	6.55246	39.281	12.6552	167.4	292.781	644.769	853.357	1288.2	1648.627	2245.88	2881.89	33155.722	17.21594	0.88028	26.114
L02_11	1776	50	101.1261261	0.092827	15.245098	1.66316	4.86081	29.216	8.55172	104.14	187.701	402.92	508.834	772.81	996.0784	1381.18	1744.09	18788.6543	16.748197	0.74055	11.5046
L02_107	2526	34	100.9105305	#VALUE!	31.19281	0.86316	2.76231	17.778	3.37931	75.474	145.187	319.708	439.929	703.32	941.1765	1330.59	1730.71	#VALUE!	22.931053	0.34994	#VALUE!
L02_28	1796	36	100.7238307	0.14345992	13.480392	1.54737	3.91863	25.556	11.5517	118.25	234.225	524.574	724.912	1153.5	1505.098	2156.47	2779.53	19374.9421	23.505881	0.9633	10.367
L02_82	1815	45	100.661157	0.1814346	20.588235	3.21053	9.61456	47.843	27.2414	169.83	330.214	744.039	980.565	1533.5	1964.706	2747.06	3393.7	18704.816	19.982966	1.84641	11.1788
L02_72	1982	41	100.2522704	0.37552743	28.676471	6.81053	14.8608	46.601	34.3103	95.864	140.374	238.929	256.89	343.81	436.0784	580	711.811	1895.49677	7.4252368	2.87456	10.6975
L02_83	1839	52	100	0.11814346	15.473856	0.73684	3.46895	21.83	7.7069	82.141	131.818	280.292	345.23	514.2	659.6078	891.176	1115.35	9440.67773	13.578514	0.75583	16.7347
L02_15	1790	51	99.72067039	#VALUE!	5.375817	0.61053	2.05567	19.412	2.72414	99.319	200	478.832	688.869	1109.4	1457.647	2045.88	2688.98	#VALUE!	27.074211	0.25	#VALUE!
L02_47	1641	49	99.69530774	#VALUE!	106.86275	#VALUE!	14.9893	60.131	54.8276	176.64	302.406	630.657	828.622	1297.3	1819.608	2682.35	3539.37	#VALUE!	20.03693	3.56314	#VALUE!
L02_92	1790	52	99.38547486	7.84810127	18.79085	5.36842	6.38116	20.392	#VALUE!	79.416	158.824	378.589	526.148	842.9	1140.784	1629.41	2153.54	274.403099	27.117227	#VALUE!	5.16878
L02_42	1772	47	99.15349887	0.62447257	14.101307	2.89474	9.16488	46.34	22.4138	169.83	305.882	637.47	830.389	1219.9	1523.529	1977.06	2440.94	3908.81039	14.372899	1.52447	7.51687
L02_2	1740	52	99.08045977	0.06751055	16.176471	1.8	5.91006	39.608	14.0345	156.2	294.385	645.742	845.76	1284.6	1607.451	2243.53	2811.02	41638.2874	17.995805	1.00294	11.8373
L02_5	1748	54	98.91304348	#VALUE!	16.862745	0.6	2.59101	20.196	4.2069	95.085	188.503	433.09	608.304	917.82	1292.549	1830.59	2314.96	#VALUE!	24.346183	0.39182	#VALUE!
L02_6	1967	37	98.52567361	0.63291139	99.836601	14.5263	38.9079	148.37	100.517	318.73	443.316	794.161	931.095	1420.5	1915.294	2829.41	3803.15	6008.97638	11.932019	4.65088	25.642
L02_7	1975	44	98.48101266	0.60759494	#VALUE!	3.67368	9.46467	58.301	25.1724	233.58	416.845	731.387	696.113	796.98	865.098	1035.88	1153.54	1898.54003	4.9386073	1.47341	#VALUE!
L02_94	1813	49	98.23496966	1.72995781	25.310458	8.21053	15.4176	49.02	31.3793	143.55	254.278	535.766	692.58	1081.6	1403.922	1969.41	2393.7	1383.67582	16.674763	2.26124	8.02779
L02_35	1777	47	97.80528981	#VALUE!	#VALUE!	#VALUE!	#VALUE!	#VALUE!	#VALUE!	#VALUE!	#VALUE!	#VALUE!	#VALUE!	700.3	#VALUE!	1343.53	#VALUE!	#VALUE!	#VALUE!	#VALUE!	#VALUE!
L02_103	1787	43	97.36989368	#VALUE!	14.150327	1.55789	7.77302	46.34	15.5172	180.05	315.241	664.234	842.756	1254.4	1572.549	2106.47	2677.17	#VALUE!	14.869121	1.03131	#VALUE!
L02_115	1775	40	96.90140845	#VALUE!	64.836601	2.52632	8.37259	47.386	32.931	160.1	266.845	534.793	676.678	1021.1	1333.333	1839.41	2452.76	#VALUE!	15.320405	2.2862	#VALUE!
L02_67	1767	64	96.77419355	0.05780591	35.816993	1.27368	4.49679	23.072	20.5172	84.185	136.096	292.944	356.714	555.29	712.9412	1041.18	1358.27	23497.0401	16.134336	1.9811	31.0399
L02_59	1717	47	96.33080955	0.10548523	12.287582	4.38947	13.2548	68.497	42.7586	230.17	439.037	908.029	1114.84	1682.8	2239.216	2994.12	3720.47	35270.0787	16.163998	2.47417	5.79567
L02_61	1729	51	95.8935801	#VALUE!	10.882353	1.51579	4.53961	26.536	14.0172	81.995	158.556	311.922	381.449	554.68	740.3922	998.824	1242.13	#VALUE!	15.148777	1.34551	#VALUE!
L02_32	1848	47	95.83333333	0.07172996	1.4803922	1.17895	4.08994	23.987	12.2759	106.57	210.16	447.202	584.099	905.74	1171.373	1607.06	2125.98	29638.7216	19.949304	1.07437	1.32374
L02_53	2359	36	95.63374311	0.27004219	29.934641	2.73684	8.05139	44.51	32.4138	163.99	340.642	709.002	936.396	1481.6	2090.196	3023.53	4043.31	14972.8716	24.655775	2.2448	17.263

Table 55. REE data for concordant data in sample L02 (Hodgson Sandstone) part 3

	Age	Error	Concordance	La	Ce	Pr	Nd	Sm	Eu	Gd	Tb	Dy	Ho	Er	Tm	Yb	Lu	Lu/La	Lu/Gd	Eu*	Ce*
L02_77	1791	57	95.47738693	#VALUE!	#VALUE!	#VALUE!	#VALUE!	#VALUE!	#VALUE!	#VALUE!	#VALUE!	639.903	#VALUE!	1016.3	#VALUE!	1685.29	#VALUE!	#VALUE!	#VALUE!	#VALUE!	#VALUE!
L02_86	1745	37	95.3008596	0.10126582	4.9509804	3.28421	8.8651	55.686	34.6552	193.67	385.027	873.966	1155.48	1828.4	2431.373	3388.24	4299.21	42454.7244	22.198196	2.1946	2.6908
L02_51	1891	43	95.29349551	0.6835443	40.03268	14.3158	39.6146	141.18	86.0345	334.79	462.567	778.589	803.887	1004.2	1133.333	1340.59	1555.12	2275.0802	4.6450112	3.94351	10.3366
L02_108	1753	46	95.15116942	0.07890295	12.728758	1.78947	5.22484	30.523	16.0345	112.46	202.941	416.545	538.869	819.94	1057.255	1454.71	1878.35	23805.7813	16.702735	1.34096	9.31223
L02_73	1978	43	94.53993933	0.05105485	2.1895425	1.13684	4.0257	26.405	8.7931	108.03	232.086	511.436	699.647	1119	1443.137	2052.35	2673.23	52359.9271	24.745425	0.75838	2.00893
L02_66	1927	47	94.49922159	0.16455696	14.101307	1.72632	4.8394	27.647	20.8621	85.255	142.513	281.752	322.968	476.74	595.2941	838.235	1059.45	6438.18898	12.426754	1.96339	10.2548
L02_12	1712	49	94.21728972	0.06075949	7.1078431	2.41053	7.73019	48.301	39.1379	204.38	438.77	940.146	1215.55	1901.5	2529.412	3658.82	4677.17	76978.3465	22.884702	2.46214	4.52144
L02_36	2047	39	93.69809477	0.07890295	5.6535948	1.91579	6.1242	34.052	19.7414	123.41	241.176	494.404	637.633	983.69	1300	1794.12	2334.65	29588.8248	18.918363	1.57324	4.00301
L02_68	1761	59	93.3560477	#VALUE!	46.454248	1.02105	4.0257	29.673	18.4483	95.62	171.925	366.423	476.148	728.7	974.902	1377.65	1791.34	#VALUE!	18.733846	1.64813	#VALUE!
L02_78	1780	42	93.31460674	0.30379747	5.7352941	5.89474	13.2762	56.863	43.9655	173.72	336.898	716.788	1005.3	1581.3	2121.176	2923.53	3712.6	12220.6365	21.37084	2.89532	2.30362
L02_105	1843	42	93.16332067	0.15189873	6.6993464	5.02105	15.4818	83.529	47.069	270.07	443.583	865.693	1054.77	1531.7	1878.431	2500	3188.98	20994.0945	11.807831	2.50309	2.94553
L02_44	1798	54	92.65850945	0.08860759	43.137255	2.54737	7.49465	38.562	40.8621	110.46	189.84	341.606	360.424	496.68	639.2157	847.059	1031.5	11641.1699	9.337993	3.34728	26.5694
L02_116	2385	33	92.41090147	0.09240506	8.251634	0.84211	2.26981	18.039	20.8621	66.472	132.888	260.341	325.972	515.41	707.8431	1055.88	1438.98	15572.4841	21.647851	2.26934	8.53587
L02_46	1705	42	92.14076246	0.55274262	49.019608	9	26.7666	132.68	70.6897	362.53	612.032	1088.08	1254.42	1786.1	2207.843	2964.71	3775.59	6830.64855	10.414548	3.17659	15.8601
L02_25	1835	59	91.28065395	0.1350211	5.9313725	2.14737	9.6788	47.059	19.4828	163.02	275.668	547.932	658.127	951.06	1204.706	1612.35	2086.61	15453.9862	12.799976	1.3442	3.92609
L02_54	1803	58	91.12590128	#VALUE!	#VALUE!	#VALUE!	#VALUE!	#VALUE!	#VALUE!	#VALUE!	#VALUE!	549.878	#VALUE!	1090	#VALUE!	1820.59	#VALUE!	#VALUE!	#VALUE!	#VALUE!	#VALUE!
L02_52	1857	43	91.06085083	#VALUE!	#VALUE!	4.2	9.33619	45.359	34.3103	125.79	247.594	439.416	440.636	524.47	578.0392	685.294	745.669	#VALUE!	5.9278545	2.62263	#VALUE!
L02_99	1718	47	90.86146682	#VALUE!	#VALUE!	#VALUE!	#VALUE!	83.007	66.2069	270.07	489.305	974.696	1162.54	1670.7	2027.451	2658.82	3370.08	#VALUE!	12.4784	3.52344	#VALUE!
L02_17	1744	43	90.30963303	#VALUE!	#VALUE!	#VALUE!	#VALUE!	#VALUE!	#VALUE!	#VALUE!	#VALUE!	454.988	#VALUE!	569.79	#VALUE!	932.941	#VALUE!	#VALUE!	#VALUE!	#VALUE!	#VALUE!
L02_87	1883	44	90.06903877	0.11814346	6.7810458	3.54737	9.87152	53.791	30	209.73	416.043	932.36	1265.02	1995.8	2639.216	3635.29	4688.98	39688.8358	22.356952	1.84804	3.54184

Table 56. REE data for concordant data in sample U507 (Crawford Formation)

	Age	Error	Concordance	La	Ce	Pr	Nd	Sm	Eu	Gd	Tb	Dy	Ho	Er	Tm	Yb	Lu	Lu/La	Lu/Gd	Eu*	Ce*
U507_12	1844	91	104.8806941	#VALUE!	#VALUE!	#VALUE!	#VALUE!	#VALUE!	#VALUE!	#VALUE!	#VALUE!	242.52	362.898	540.18	709.4118	974.706	1266.14	#VALUE!	#VALUE!	#VALUE!	#VALUE!
U507_14	1777	110	102.4198087	#VALUE!	32.924837	2.09474	3.31906	19.02	15.1724	61.168	89.8396	160.236	246.113	387.31	515.6863	710.588	993.307	#VALUE!	16.23903	1.69434	#VALUE!
U507_17	2058	70	101.068999	#VALUE!	61.699346	#VALUE!	#VALUE!	#VALUE!	#VALUE!	#VALUE!	113.636	205.512	320.318	502.11	649.4118	937.647	1211.02	#VALUE!	#VALUE!	#VALUE!	#VALUE!
U507_6	2598	79	100.8468052	0.10548523	33.594771	0.96842	3.61884	23.922	16.7241	91.484	144.118	228.74	361.837	534.14	698.4314	985.882	1287.4	12204.5669	14.072395	1.55679	32.4182
U507_3	4810	160	99.58419958	1476.79325	#VALUE!	#VALUE!	#VALUE!	#VALUE!	#VALUE!	#VALUE!	#VALUE!	#VALUE!	#VALUE!	#VALUE!	#VALUE!	#VALUE!	#VALUE!	#VALUE!	#VALUE!	#VALUE!	#VALUE!
U507_13	1840	87	97.93478261	0.42616034	65.359477	11.0526	25.0535	69.02	56.3793	189.78	297.594	478.74	730.919	1132.3	1467.059	2082.35	2799.21	6568.44936	14.749697	3.50459	19.2913
U507_5	1810	95	97.40331492	#VALUE!	#VALUE!	#VALUE!	#VALUE!	#VALUE!	#VALUE!	#VALUE!	#VALUE!	#VALUE!	584.276	797.58	950.1961	1221.18	1511.42	#VALUE!	#VALUE!	#VALUE!	#VALUE!
U507_16	1926	110	97.1443406	#VALUE!	#VALUE!	#VALUE!	#VALUE!	#VALUE!	#VALUE!	152.31	224.599	352.362	522.968	740.79	910.1961	1216.47	1500	#VALUE!	9.8482428	#VALUE!	#VALUE!
U507_14	2855	56	96.56742557	#VALUE!	18.267974	0.81053	2.69807	15.621	3.89655	68.905	127.005	229.921	398.233	619.34	827.451	1144.12	1483.07	#VALUE!	21.52338	0.42382	#VALUE!
U507_13	1911	71	96.49398221	0.1	14.362745	0.1	2	15.294	6.10345	63.358	114.439	206.693	336.926	524.47	689.8039	958.235	1248.82	12488.189	19.710621	0.68821	32.1161
U507_1	1786	63	95.07278835	#VALUE!	#VALUE!	#VALUE!	#VALUE!	#VALUE!	#VALUE!	410.71	#VALUE!	755.906	#VALUE!	1478.5	#VALUE!	2588.24	3350.39	#VALUE!	8.1576529	#VALUE!	#VALUE!
U507_6	1843	71	93.54313619	0.24050633	8.0718954	2.11579	5.1606	21.438	13.7586	80.779	139.572	229.134	367.845	560.73	714.1176	1011.18	1396.06	5804.68297	17.282587	1.36086	5.25848
U507_5	2601	64	91.65705498	1.37974684	92.647059	13.5789	26.3597	96.601	100.172	276.89	423.262	626.378	957.597	1381.9	1737.647	2405.88	3137.8	2274.1819	11.332459	5.18335	23.9544

Table 57. REE data for concordant data in sample U503 (Jalboi Formation)

	Age	Error	Concordance	La	Ce	Pr	Nd	Sm	Eu	Gd	Tb	Dy	Ho	Er	Tm	Yb	Lu	Lu/La	Lu/Gd	Eu*	Ce*
U503_46	1955	89	103.887468	0.47257384	26.879085	10.0316	27.6874	92.288	36.7241	251.09	370.856	543.307	793.286	1100.9	1384.314	1841.18	2389.76	5056.91085	9.5173732	1.98181	8.29343
U503_16	1858	97	102.3143165	#VALUE!	8.1045752	0.6	1.75589	12.418	1.2931	49.002	84.492	155.512	259.011	384.89	516.8627	720	937.008	#VALUE!	19.12166	0.165	#VALUE!
U503_43	2451	85	101.3871889	#VALUE!	14.558824	#VALUE!	#VALUE!	#VALUE!	#VALUE!	118.25	181.283	278.74	408.127	551.06	698.8235	898.235	1125.98	#VALUE!	9.5222125	#VALUE!	#VALUE!
U503_19	1699	88	101.0594467	#VALUE!	13.594771	0.42105	2.07709	13.856	3.60345	58.978	110.16	203.543	370.141	585.5	800.7843	1130.59	1523.62	#VALUE!	25.833691	0.42223	#VALUE!
U503_34	1633	89	100.3061849	2.82700422	28.447712	1.50526	3.27623	17.712	9.72414	69.1	132.086	234.646	408.127	655.59	870.5882	1223.53	1610.24	569.591021	23.303066	1.04366	13.6675
U503_23	1715	92	100.1166181	0.09704641	13.70915	0.8	2.33405	15.229	2.51724	55.328	95.7219	157.48	270.141	408.46	558.0392	756.471	993.701	10239.4385	17.960027	0.29968	14.4745
U503_25	1774	110	100.0563698	0.10970464	5.620915	2.28421	7.73019	39.281	19.5172	123.6	179.947	280.709	434.982	612.69	773.3333	1081.76	1477.56	13468.5191	11.954267	1.52926	3.63289
U503_47	1754	95	99.31584949	#VALUE!	12.369281	0.72632	2.05567	15.686	4.24138	72.457	146.524	255.906	447.173	682.18	916.4706	1268.24	1654.72	#VALUE!	22.837197	0.45176	#VALUE!
U503_44	2562	78	98.04839969	#VALUE!	20.620915	4.34737	13.6831	62.68	#VALUE!	202.92	329.144	521.26	862.721	1240.5	1544.706	1975.29	2582.68	#VALUE!	12.727582	#VALUE!	#VALUE!
U503_8	1785	87	97.87114846	#VALUE!	10.310458	#VALUE!	#VALUE!	15.686	4.98276	62.774	117.647	222.047	410.424	655.59	936.8627	1299.41	1724.41	#VALUE!	27.470244	0.56253	#VALUE!
U503_38	2007	96	97.15994021	#VALUE!	17.238562	#VALUE!	5.09636	28.758	18.2759	82.92	140.374	228.346	374.735	563.75	747.451	1019.41	1340.94	#VALUE!	16.171606	1.7294	#VALUE!
U503_51	1785	84	96.91876751	7.67932489	24.754902	#VALUE!	#VALUE!	#VALUE!	#VALUE!	148.42	256.15	443.307	727.562	1059.2	1388.627	1835.88	2358.27	307.093104	15.889312	#VALUE!	#VALUE!
U503_50	1738	89	96.54775604	#VALUE!	#VALUE!	#VALUE!	#VALUE!	#VALUE!	#VALUE!	#VALUE!	#VALUE!	274.803	438.163	653.17	858.4314	1176.47	1515.75	#VALUE!	#VALUE!	#VALUE!	#VALUE!
U503_5	1819	87	96.26168224	#VALUE!	#VALUE!	#VALUE!	#VALUE!	#VALUE!	#VALUE!	#VALUE!	#VALUE!	#VALUE!	#VALUE!	526.28	#VALUE!	981.765	#VALUE!	#VALUE!	#VALUE!	#VALUE!	#VALUE!
U503_22	1810	98	95.13812155	#VALUE!	10.931373	#VALUE!	#VALUE!	48.17	#VALUE!	163.99	248.663	396.457	631.095	902.72	1196.863	1582.35	2142.52	#VALUE!	13.06492	#VALUE!	#VALUE!
U503_10	2536	80	94.24290221	#VALUE!	#VALUE!	#VALUE!	#VALUE!	#VALUE!	#VALUE!	86.521	141.444	227.953	387.102	615.11	871.3725	1290	1877.95	#VALUE!	21.705247	#VALUE!	#VALUE!
U503_45	1845	98	93.71273713	0.26582278	14.003268	3.85263	6.85225	32.092	19.1379	81.8	140.107	251.575	412.898	646.53	849.0196	1190.59	1539.37	5790.96363	18.818593	1.79328	6.90021
U503_26	1984	90	93.64919355	0.66666667	64.542484	8.87368	20.9208	96.732	66.0345	231.63	335.829	477.559	690.813	916.01	1125.49	1498.24	1874.02	2811.02362	8.0905512	3.64413	20.896
U503_2	1862	86	92.42749731	1.05485232	21.944444	10.3684	18.2441	61.503	37.069	124.57	187.433	286.22	441.343	636.25	848.2353	1185.88	1437.01	1362.28346	11.535356	2.71746	6.49276
U503_6	1771	83	91.5866742	1.32489451	29.803922	11.7895	19.2505	69.281	45.5172	138.69	215.508	330.709	500	703.32	913.3333	1204.71	1539.37	1161.88124	11.099668	3.1563	8.23
U503_52	1961	83	91.43294238	#VALUE!	3.9869281	2.04211	5.1606	34.444	6.55172	121.65	221.658	386.614	653.71	966.16	1263.529	1714.12	2216.54	#VALUE!	18.219921	0.52439	#VALUE!
U503_15	1842	82	90.39087948	6.03375527	56.372549	58.9474	81.7987	208.5	150	349.39	481.283	714.961	1102.47	1563.1	1996.078	2611.76	3283.46	544.182589	9.3976597	6.35064	6.99317
U503_32	2426	88	90.27205276	#VALUE!	#VALUE!	#VALUE!	#VALUE!	#VALUE!	#VALUE!	#VALUE!	95.1872	162.598	260.247	397.58	565.4902	837.647	1240.16	#VALUE!	#VALUE!	#VALUE!	#VALUE!

Table 58. REE data for concordant data in sample U506 (Arnold Sandstone)

	Age	Error	Concordance	La	Ce	Pr	Nd	Sm	Eu	Gd	Tb	Dy	Ho	Er	Tm	Yb	Lu	Lu/La	Lu/Gd	Eu*	Ce*
U506_19	1732	94	106.9861432	#VALUE!	13.611111	1.05263	3.79015	15.882	3.82759	68.175	136.898	249.213	422.438	687.01	934.1176	1279.41	1728.35	#VALUE!	25.351549	0.41748	#VALUE!
U506_34	1743	94	105.9093517	#VALUE!	9.6732026	0.4	1.39186	11.961	3.01724	64.282	144.652	283.858	513.074	860.42	1227.451	1723.53	2346.46	#VALUE!	36.502411	0.34555	#VALUE!
U506_5	1728	90	104.8611111	#VALUE!	11.323529	0.76842	1.37045	14.248	3.01724	73.966	172.995	333.465	605.83	961.93	1346.667	1930.59	2555.12	#VALUE!	34.544524	0.32125	#VALUE!
U506_3	1749	89	103.3161807	#VALUE!	9.6405229	0.46316	1.30621	10.915	2.67241	45.839	98.6631	205.512	366.078	580.06	847.8431	1177.65	1643.7	#VALUE!	35.857804	0.35473	#VALUE!
U506_39	1727	92	101.5634047	0.55696203	17.45098	7.68421	11.0707	30.98	26.7241	59.854	104.011	154.724	256.184	382.48	559.6078	825.294	1244.09	2233.7151	20.785481	2.804	6.0789
U506_28	1712	92	101.5186916	#VALUE!	11.911765	0.54737	2.18415	16.144	3.32759	77.859	171.123	329.921	583.039	932.93	1309.804	1811.76	2437.01	#VALUE!	31.30032	0.34321	#VALUE!
U506_27	1738	98	100.6904488	#VALUE!	17.205882	0.50526	1.84154	16.144	4.67241	76.886	150.535	262.992	438.163	687.01	937.2549	1258.82	1696.85	#VALUE!	22.069795	0.48443	#VALUE!
U506_7	1807	93	100.6087438	#VALUE!	4.4117647	0.76842	3.7045	24.51	12.4483	111.44	186.096	324.803	535.336	773.41	1007.843	1376.47	1850.39	#VALUE!	16.605061	1.06765	#VALUE!
U506_11	1696	100	100.4716981	0.21518987	14.558824	3.09474	4.90364	20.327	10.7069	63.601	123.797	214.173	359.717	544.41	776.8627	1091.76	1456.69	6769.33766	22.903626	1.16872	8.00234
U506_44	2521	95	99.08766363	#VALUE!	44.934641	#VALUE!	#VALUE!	22.68	#VALUE!	66.229	105.882	174.016	262.014	387.92	529.4118	729.412	980.315	#VALUE!	14.801964	#VALUE!	#VALUE!
U506_4	1725	100	97.62318841	0.23206751	18.120915	3.15789	7.53747	36.34	15.6897	127.98	260.16	454.331	756.184	1155.3	1563.922	2047.06	2657.48	11451.3243	20.764723	1.22396	9.84198
U506_30	1769	93	97.17354438	#VALUE!	#VALUE!	#VALUE!	#VALUE!	#VALUE!	#VALUE!	#VALUE!	#VALUE!	404.331	#VALUE!	991.54	#VALUE!	1847.65	#VALUE!	#VALUE!	#VALUE!	#VALUE!	#VALUE!
U506_14	1851	96	96.27228525	0.16877637	10.947712	2.88421	8.45824	47.255	11.9138	176.16	326.738	570.866	927.562	1363.1	1764.706	2310	2976.38	17635.0394	16.896289	0.79707	6.26557
U506_6	1757	93	95.21912351	0.57805907	15.996732	10	18.4154	49.15	37.931	117.27	193.583	305.906	471.025	692.45	950.9804	1317.65	1717.72	2971.52423	14.646919	2.94026	4.91845
U506_12	1795	100	94.20612813	0.30801688	10.392157	9.15789	15.2034	60.784	40.1724	165.45	289.305	456.693	713.781	1031.4	1372.549	1864.71	2440.94	7924.71147	14.753358	2.67084	3.37773
U506_33	1746	97	93.87170676	0.27004219	32.156863	4.74737	10.4497	38.235	24.3103	113.38	188.503	295.276	447.703	627.79	819.6078	1074.12	1382.68	5120.22638	12.194857	1.97432	14.356
U506_1	1724	97	107.6566125	#VALUE!	#VALUE!	#VALUE!	#VALUE!	#VALUE!	#VALUE!	#VALUE!	#VALUE!	#VALUE!	#VALUE!	852.57	#VALUE!	1661.76	#VALUE!	#VALUE!	#VALUE!	#VALUE!	#VALUE!

Table 59. REE data for concordant data in sample GSD302 (Limmen Sandstone)

	Age	Error	Concordance	La	Ce	Pr	Nd	Sm	Eu	Gd	Tb	Dy	Ho	Er	Tm	Yb	Lu	Lu/La	Lu/Gd	Eu*	Ce*
GSD302_32	1752	78	105.9360731	0	67.48366	0	81.3704	134.64	89.6552	201.46	286.096	382.283	581.272	850.15	1161.569	1676.47	2255.91	#DIV/0!	11.197792	4.89036	#DIV/0!
GSD302_87	2078	76	101.9249278	25.0632911	354.57516	372.632	770.878	1248.4	850	1464.7	1550.8	1692.91	1918.73	2235.6	2501.961	3023.53	3716.54	148.28601	2.5373689	16.3188	17.7801
GSD302_33	2075	72	101.7831325	0.3164557	23.77451	5.47368	8.99358	21.503	15	48.273	87.4332	150	251.06	392.15	556.8627	799.412	1170.08	3697.44882	24.23903	1.79572	9.88023
GSD302_171	1813	79	101.7098731	34.5991561	606.20915	622.105	1291.22	1921.6	1431.03	2384.4	2299.47	2263.78	2243.82	2404.8	2611.765	3100	3712.6	107.30315	1.5570183	21.8079	23.6558
GSD302_69	2547	64	101.6882607	290.7173	3946.0784	4463.16	8650.96	13438	9155.17	15766	16310.2	15511.8	14470	13680	12784.31	13464.7	13543.3	46.5858313	0.8589968	53.5726	57.2324
GSD302_74	1851	76	100.8643976	402.109705	3464.0523	4768.42	9914.35	16863	9396.55	18248	18609.6	17244.1	15936.4	15287	14588.24	16411.8	15944.9	39.6530641	0.8737795	50.1473	48.1745
GSD302_43	1784	73	99.60762332	107.172996	1655.2288	1810.53	3597.43	5019.6	3258.62	5450.1	5481.28	4913.39	4469.96	4271.9	4215.686	4647.06	4968.5	46.3596627	0.9116317	31.8468	37.7979
GSD302_53	1898	81	99.20969442	39.6624473	374.18301	492.632	910.064	1490.2	1043.1	1742.1	1818.18	1649.61	1837.46	2060.4	2227.451	2711.76	3212.6	80.9984922	1.8441033	18.3473	16.2184
GSD302_128	1768	91	99.15158371	202.109705	3529.4118	3473.68	6980.73	11046	7948.28	13528	13850.3	13503.9	12932.9	12145	12078.43	13705.9	13622	67.3992734	1.0069535	50.7034	58.2139
GSD302_35	1795	86	98.99721448	91.9831224	1973.8562	1957.89	4132.76	6189.5	4258.62	7206.8	7005.35	6429.13	6219.08	5994	6039.216	6558.82	7141.73	77.6417684	0.9909696	36.7939	43.5965
GSD302_22	1803	80	98.11425402	6.32911392	57.843137	49.4737	0	177.78	0	243.31	288.77	358.268	510.601	700.3	886.2745	1188.24	1527.56	241.354331	6.2782677	0	7.74326
GSD302_64	1840	68	98.09782609	125.738397	2723.8562	2663.16	5331.91	7692.8	5034.48	8666.7	8021.39	7039.37	6501.77	6151.1	5874.51	6276.47	6704.72	53.3228082	0.773622	39.3614	51.5784
GSD302_54	2543	66	97.99449469	0	68.627451	0	0	0	150	243.31	291.444	307.087	330.389	395.77	521.5686	670.588	775.591	#DIV/0!	3.1876772	9.61639	#DIV/0!
GSD302_118	2560	65	97.8125	104.219409	1486.9281	1610.53	3190.58	4902	3293.1	5790.8	6042.78	6062.99	5671.38	5679.8	5843.137	6647.06	7165.35	68.7525901	1.2373784	31.8465	35.9079
GSD302_6	1972	70	96.75456389	0	0	0	0	0	0	0	0	0	0	0	0	0	0	#DIV/0!	#DIV/0!	#DIV/0!	#DIV/0!
GSD302_105	2567	67	95.79275419	114.345992	1553.9216	1620	3355.46	6019.6	4379.31	6910	6780.75	6007.87	5565.37	5196.4	4972.549	5117.65	5145.67	45.0008717	0.7446726	38.5135	37.3131
GSD302_163	1745	78	95.35816619	25.6962025	280.39216	378.947	676.66	1015.7	687.931	1168.9	1141.71	1165.35	1206.71	1348.6	1471.373	1882.35	2192.91	85.3399791	1.8761187	14.7185	13.9389
GSD302_66	1800	83	95.11111111	18.5232068	290.84967	274.737	582.441	856.21	515.517	919.71	954.545	948.819	1038.87	1160.1	1364.706	1735.29	2224.41	120.087708	2.4186039	12.233	16.9841
GSD302_134	1880	81	94.84042553	6.83544304	135.62092	108.421	214.133	339.87	231.034	413.63	451.872	503.937	600.707	779.46	905.8824	1247.06	1622.05	237.299504	3.9215377	8.4166	12.6326
GSD302_94	1855	75	94.44743935	109.957806	2058.8235	2069.47	4074.95	5947.7	3810.34	6681.3	6847.59	6385.83	5913.43	5824.8	5682.353	6423.53	7055.12	64.1620488	1.0559554	33.9063	44.1009
GSD302_136	1820	91	94.17582418	110.126582	1665.0327	2010.53	3640.26	5019.6	3258.62	5284.7	5401.07	4944.88	4699.65	4664.7	5019.608	5735.29	6098.43	55.3765047	1.1539838	32.1015	36.1566
GSD302_31	1726	81	93.68482039	30.3797468	0	0	0	0	0	0	0	507.874	650.177	881.57	1082.353	1429.41	1881.89	61.9455381	#DIV/0!	#DIV/0!	0
GSD302_75	1841	82	92.93862032	1	1	1	1	1	1	1	1	1	1	1	1411.765	1900	2500	2500	2500	0.70711	0.70711
GSD302_49	1831	72	92.73620972	36.0759494	446.07843	454.737	858.672	1541.2	1039.66	1824.8	1927.81	2059.06	2291.52	2652.6	3141.176	3982.35	4830.71	133.903854	2.6472283	17.9198	20.1351
GSD302_143	2506	66	92.09896249	#VALUE!	3508.1699	3621.05	7451.82	12542	8482.76	14793	14492	13228.3	11819.8	10937	10274.51	11047.1	10669.3	#VALUE!	0.7212301	51.3065	#VALUE!
GSD302_126	1922	73	91.88345473	47.6793249	748.36601	763.158	1520.34	2444.4	1672.41	2919.7	3155.08	3043.31	3056.54	3178.2	3219.608	3847.06	4330.71	90.8299073	1.4832677	22.8346	26.2813
GSD302_131	1859	84	91.23184508	18.3544304	194.28105	233.789	427.195	679.08	437.931	770.8	844.92	918.11	1084.81	1293.7	1476.078	1852.94	2216.54	120.762965	2.8756189	11.5011	12.2351

Table 60. REE data for concordant data in sample U602 and U603 (Limmen Sandstone)

	Age	Error	Concordance	La	Ce	Pr	Nd	Sm	Eu	Gd	Tb	Dy	Ho	Er	Tm	Yb	Lu	Lu/La	Lu/Gd	Eu*	Ce*
U602_32	3.40E+03	2.00E+03	217.6470588	79324.8945	40849.673	46315.8	32976.4	#VALUE!	11206.9	#VALUE!	#VALUE!	#VALUE!	#VALUE!	#VALUE!	#VALUE!	#VALUE!	#VALUE!	#VALUE!	#VALUE!	#VALUE!	115.245
U602_39	1692	43	103.8416076	#VALUE!	27.48366	#VALUE!	#VALUE!	#VALUE!	#VALUE!	53.917	97.5936	229.197	321.731	541.99	724.7059	1044.71	1403.94	#VALUE!	26.038723	#VALUE!	#VALUE!
U602_37	2010	55	103.5820896	#VALUE!	25.457516	#VALUE!	#VALUE!	9.9346	6.63793	32.555	53.2086	106.764	133.039	196.25	264.3137	386.471	504.724	#VALUE!	15.503866	1.01834	#VALUE!
U602_20	2914	36	103.4660261	0.66666667	42.875817	#VALUE!	#VALUE!	16.013	7.72414	62.822	119.519	251.582	350.707	528.7	708.2353	988.824	1279.92	1919.88189	20.37365	0.86994	#VALUE!
U602_35	2285	35	101.8818381	#VALUE!	13.153595	#VALUE!	6.25268	30.719	15.569	130.51	242.781	570.803	826.855	1415.1	1952.941	2811.76	3830.71	#VALUE!	29.351627	1.22613	#VALUE!
U602_2	3378	31	100.9177028	2.02531646	34.395425	9.89474	16.0171	41.242	14.1207	121.17	214.171	475.426	627.032	975.23	1282.745	1725.29	2204.72	1088.58268	18.195617	1.10803	9.96235
U602_11	2042	43	99.31439765	#VALUE!	26.960784	23.2632	32.9764	53.595	21.3793	92.944	145.187	292.944	370.671	575.83	765.4902	1084.12	1385.83	#VALUE!	14.910335	1.76611	#VALUE!
U602_4	1834	47	97.76444929	0.92405063	13.071895	12.8421	22.9122	54.902	17.5862	165.94	343.048	775.182	1049.47	1561.9	2037.255	2743.53	3350.39	3625.76853	20.190789	1.18341	3.52316
U602_25	1794	48	96.48829431	#VALUE!	#VALUE!	#VALUE!	#VALUE!	#VALUE!	#VALUE!	342.09	#VALUE!	1072.51	1326.86	1891.2	#VALUE!	2911.76	3566.93	#VALUE!	10.426799	#VALUE!	#VALUE!
	Age	Error	Concordance	La	Ce	Pr	Nd	Sm	Eu	Gd	Tb	Dy	Ho	Er	Tm	Yb	Lu	Lu/La	Lu/Gd	Eu*	Ce*
U603_11	1756	78	517.8571429	455.696203	472.22222	330.526	310.493	183.01	66.2069	166.91	201.337	273.622	422.085	594.56	790.9804	1090	1422.83	3.12233158	8.5245633	3.53933	16.8412
U603_43	1822	93	128.1690141	15.0632911	24.019608	13.5789	21.4347	51.046	19.1379	129.93	202.674	291.732	448.233	622.96	798.8235	1026.47	1350.79	89.6741216	10.39651	1.42262	4.4881
U603_25	1915	67	127.5568182	2.83966245	41.993464	53.2632	96.1456	230.07	154.483	333.33	435.294	565.354	793.286	1100.9	1396.078	1865.29	2397.64	844.339016	7.1929134	6.50837	5.60647
U603_26	1780	67	121.7171717	1.80590717	14.836601	28.3158	51.606	129.41	79.6552	236.5	314.171	340.945	380.035	410.27	428.2353	492.941	547.638	303.248031	2.3156289	4.16417	2.7033
U603_12	2135	64	121.1180124	#VALUE!	90.849673	78.7368	125.268	315.69	224.828	478.35	650.535	753.937	916.961	1181.3	1600	2274.12	2905.51	#VALUE!	6.0740862	7.97867	#VALUE!
U603_30	1863	77	117.3913043	1.82700422	21.094771	35.8947	69.379	180.39	127.414	308.03	444.118	598.031	872.792	1216.3	1585.49	2147.65	2795.28	1529.97763	9.0747099	5.76526	3.43462
U603_4	1887	71	115.4727794	2.73417722	36.111111	46	86.2955	228.1	135.172	411.19	610.695	829.921	1139.58	1526.9	1847.059	2364.71	2811.02	1028.10586	6.8362764	5.3461	5.17278
U603_2	1816	71	114.8	1.81012658	23.366013	33.0526	61.4561	163.4	96.3793	277.37	410.963	572.441	833.922	1098.5	1407.059	1782.35	2228.35	1231.04455	8.0337754	4.59068	3.95734
U603_31	2399	66	113.3462282	3.45991561	40.522876	70.1053	125.482	337.91	267.759	574.7	823.529	870.079	1021.2	1238.1	1462.745	1882.35	2334.65	674.769541	4.0624021	8.86344	4.72459
U603_33	2448	62	104.743083	4.72151899	57.679739	92.9474	170.236	496.08	360.172	794.16	1037.43	1166.54	1353.36	1602.4	1908.627	2388.82	2834.65	600.367313	3.5693608	10.0271	5.8364
U603_34	2425	66	104.1800643	2.02531646	33.660131	35.1579	69.379	203.27	151.897	355.23	497.326	606.299	772.085	1035	1305.882	1817.65	2251.97	1111.90945	6.3394456	6.42742	5.52004
U603_3	1834	70	97.78067885	#VALUE!	9.9183007	16	32.0771	100.13	68.4483	183.45	290.909	443.307	663.604	966.77	1318.039	1797.06	2271.65	#VALUE!	12.382621	4.06462	#VALUE!
U603_14	2412	57	97.31682147	3.85232068	69.771242	95.0526	201.927	633.33	434.655	872.51	1077.54	1161.81	1265.02	1477.9	1713.725	2148.24	2500	648.959474	2.8653095	11.201	7.01564
U603_7	1810	70	95.88785047	#VALUE!	15	5.41053	10.985	34.967	25	93.382	151.337	231.102	368.905	548.04	759.2157	1050	1417.32	#VALUE!	15.177689	2.2067	#VALUE!
U603_39	1908	76	95.69648924	0.60759494	10.996732	9.24211	18.0942	57.712	27.4138	120.68	182.353	262.992	383.746	536.56	680	867.647	1102.36	1814.30446	9.1344933	2.05248	3.5039
U603_37	1898	70	94.3452381	1.43037975	29.542484	31.2632	67.8801	219.61	158.103	321.65	431.818	515.354	663.251	873.11	1083.922	1457.65	1889.76	1321.16229	5.8751355	6.79575	5.16673
U603_15	1874	65	91.47609148	28.2700422	250.65359	490.526	942.184	3143.8	2603.45	6666.7	8395.72	7834.65	7526.5	7383.7	7627.451	8717.65	8708.66	308.05265	1.3062992	26.2848	11.0046

Table 61. REE data for concordant data in sample GSD301 (Limmen Sandstone)

	Age	Error	Concordance	La	Ce	Pr	Nd	Sm	Eu	Gd	Tb	Dy	Ho	Er	Tm	Yb	Lu	Lu/La	Lu/Gd	Eu*	Ce*
GSD301_31	1676	82	103.8186158	13.1223629	#VALUE!	#VALUE!	#VALUE!	#VALUE!	#VALUE!	#VALUE!	#VALUE!	#VALUE!	#VALUE!	603.63	788.6275	1064.12	1401.57	106.808112	#VALUE!	#VALUE!	#VALUE!
GSD301_21	1706	69	95.83821805	68.7763713	251.63399	230.526	357.602	745.1	506.897	958.64	1139.04	1330.71	1625.44	2114.8	2733.333	3852.94	4606.3	66.9750254	4.8050482	12.2806	14.545
GSD301_38	1735	80	102.9971182	#VALUE!	#VALUE!	#VALUE!	#VALUE!	#VALUE!	#VALUE!	#VALUE!	#VALUE!	#VALUE!	#VALUE!	#VALUE!	#VALUE!	884.118	1083.86	#VALUE!	#VALUE!	#VALUE!	#VALUE!
GSD301_58	1776	78	89.35810811	1012.65823	#VALUE!	#VALUE!	#VALUE!	#VALUE!	#VALUE!	#VALUE!	#VALUE!	#VALUE!	#VALUE!	#VALUE!	#VALUE!	#VALUE!	#VALUE!	#VALUE!	#VALUE!	#VALUE!	#VALUE!
GSD301_8	1779	82	93.70432827	#VALUE!	14.084967	#VALUE!	#VALUE!	#VALUE!	#VALUE!	88.078	156.15	258.661	434.099	635.65	837.2549	1154.71	1476.77	#VALUE!	16.766662	#VALUE!	#VALUE!
GSD301_26	1793	75	93.92080312	2.01265823	25.490196	19.2632	32.5482	90.196	62.5862	223.36	345.989	515.748	786.219	1091.2	1345.098	1776.47	2263.78	1124.77096	10.135222	3.53446	5.52624
GSD301_25	1808	90	94.69026549	#VALUE!	19.444444	#VALUE!	#VALUE!	#VALUE!	#VALUE!	94.404	143.85	233.465	381.625	557.7	760.7843	1045.88	1385.83	#VALUE!	14.679763	#VALUE!	#VALUE!
GSD301_66	1829	92	99.2345544	#VALUE!	#VALUE!	#VALUE!	#VALUE!	#VALUE!	#VALUE!	#VALUE!	#VALUE!	#VALUE!	#VALUE!	#VALUE!	747.451	1005.88	1246.06	#VALUE!	#VALUE!	#VALUE!	#VALUE!
GSD301_44	1831	74	100.1092299	4.39240506	48.039216	42.2105	74.0899	171.24	140.345	344.53	499.465	694.882	975.265	1340.8	1707.059	2262.94	2933.07	667.75965	8.5133625	6.17973	7.03703
GSD301_12	1841	71	95.16567083	#VALUE!	#VALUE!	#VALUE!	#VALUE!	#VALUE!	#VALUE!	#VALUE!	344.92	509.843	759.717	1077.9	1384.314	1862.35	2389.76	#VALUE!	#VALUE!	#VALUE!	#VALUE!
GSD301_28	1876	73	97.97441365	#VALUE!	38.888889	#VALUE!	#VALUE!	#VALUE!	#VALUE!	#VALUE!	#VALUE!	#VALUE!	249.117	343.81	444.3137	624.706	838.976	#VALUE!	#VALUE!	#VALUE!	#VALUE!
GSD301_52	1901	72	96.58074698	629.113924	4506.5359	5778.95	10342.6	20314	15551.7	29781	36363.6	35354.3	32473.5	30163	27254.9	28752.9	27480.3	43.6809835	0.9227459	69.4836	56.2963
GSD301_59	1915	88	89.45169713	140.506329	1339.8693	1646.32	2832.98	5006.5	3862.07	6481.8	6925.13	6133.86	5653.71	5202.4	5015.686	5205.88	5240.16	37.2948145	0.8084477	36.0323	31.6973
GSD301_63	2401	68	90.83715119	133.755274	1516.3399	1578.95	2749.46	5209.2	4293.1	7250.6	8262.03	7952.76	7226.15	6948.6	6862.745	7588.24	7401.57	55.3366949	1.0208212	38.4606	36.64
GSD301_45	2622	65	97.78794813	0.98312236	30.571895	11.4947	20.621	48.562	32.2414	98.783	131.283	178.74	242.756	335.35	428.6275	580	757.087	770.083809	7.6641034	2.6561	8.65471

APPENDIX B: EXTENDED METHODS

Appendix Ba: GEOCHRONOLOGY

Mineral Separation
Crushing

1. Cut rocks using rock saw to ensure rocks are clean and fresh.
2. Clean jaw crusher prior to use
    a. This is achieved with compressed air, metal brush and ethanol.
3. Line the collection tray with butcher paper to minimise contamination between samples.
4. Transfer chips from jaw crusher to disc mill to achieve zircon and glauconite fraction. Similar to jaw crusher, clean disc mill with compressed air and ethanol.
5. Adjust discs until desired gap between the two is achieved. Start at 1mm.
6. Run this through sieve using <79µm and >479µm mesh. Place sieve into the Endcotts EPL2000 Super Shaker and allow for the fractions to separate.
7. Take the >479 µm fraction and run it though the disc mill again, ensuring to change the spacing between the disc mills to approximately 0.7mm.
8. Repeat process, this time adjusting disc mill to 0.4mm.
9. Place each fraction into sample bags, ensuring to label either '>479 µm', 'Zircon fraction' and <79 µm.

Separating zircons from zircon fraction

Separation was undertaken in the Mawson Building lab B29 at The University of Adelaide. Prior to the usage of the lab, the room was thoroughly cleaned. Benches were wiped down and floors were vacuumed. Sample was panned removing the lights of the fraction. The lights were placed into a funnel with filter paper and later dried in the oven. The heavies extracted by this method are then placed on the hotplate to dry at 50^0C. The heavies were then checked under microscope to see if sufficient zircons were present. Zircons were transferred into a tube for picking.

Picking zircon

10. Clean a glass petri dish with ethanol.
11. Transfer the zircon sample into the glass petri dish and place under a binocular microscope in room G36 in the Mawson building.
12. Using a fine tipped pick, select zircons from the petri dish and place on to a Teflon mount base with double sided tape applied to the bottom (this allows the zircons to stick).
13. The process of mounting was repeated until a sufficient number of zircons were mounted, or until all visible zircons were mounted (~100).

Epoxy resin zircon mounts

14. The base of the mount was coupled with a tube like teflon closing form. This was coated in Vaseline to allow removal of the mount after setting.
15. Expoxy resin was prepared using a two part expoxy resin; one part epoxy (5g) and one part hardner (1.2g). These were carefully mixed in a disposable cup for 2-3 minutes, ensuring to mix slowly to prevent air pockets forming. The resin was then heated for 1-2minutes at 50^{o}C on a hotplate, allowing any bubbles to rise to the top.
16. The heated resin was carefully poured into the Teflon mount holder and left for 24 hours to set. The epoxy mount was then removed from the Teflon holder and cleaned with ethanol to remove the Vaseline.
17. This process was used in the preparation of all mounts.

Appendix Bb: GEOCHEMISTRY

Cleaning the 7 and 15ml Teflon Vials

1. Collect sufficient (36) 7 and (12) 15ml PFA Teflon vials from the recycling container for a batch of samples.
2. Remove labels from the vials with an ethanol moistened tissue in the fume cupboard.
3. Fill with about 5mm of recycled 6M HCl.
4. Place on hot plate at 140^{0}C for 30 minutes with cap on.
5. Discard acid to original container using a funnel under fume cupboard and mark with the number of uses.
6. Transfer vials and caps into large beaker of deionized (DI) water and then drain.
7. Transfer rinsed vials and caps into Savillex Teflon 4.5L Container cover with 6M HNO_3 ensuring to label vessel with name and acid in fume cupboard FCAMA024.
8. Set hotplate to 170^{o}C and leave container on hotplate for 48 hours.
9. Remove cleaning vessel from hotplate and allow to cool.
10. When cool enough to touch, drain acid into appropriate nitric acid container ensuring to label number of uses.

11. Rinse Savillex Teflon 4.5L container with deionised (DI) water under fume cupboard, ensuring to swirl and rinse all of the vials and caps. Empty container via the spout.
12. Repeat a further two times.
13. Fill container with 6M HCl, ensuring to cover all vials and caps.
14. Fill out appropriate label and leave on hotplate at 170^0C for 48 hours.
15. Remove from hotplate after 48 hours and allow to cool for ease of handling.
16. Transfer 6M HCl back into original container via the spout and label number of uses.
17. Rinse container with DI water under fume cupboard.
18. Swirl and drain the water.
19. Fill Savillex Teflon container with DI water and leave on hotplate over night at 170^0C.
20. Swirl and drain the following morning.
21. Rinse three times with DI water.
22. Carefully remove caps and vials, ensuring not to touch rims and insides.
23. Add 5ml of single distilled (SD) 6M HCl to vials and cap them.
24. Leave on hotplate in fume cupboard FCAMA022 for 2 hours allowing the vials to reflux.
25. Remove from hotplate and allow to cool before transferring the acid into the "recycled 6M HCl" container.
26. Recap the vials and store in a clean plastic container with name clearly labelled.

Sample preparation for vials

27. Calculate the necessary sample powder weight in grams on the basis of a nominal 2μg of Nd (this is the optimum Isotopx Pheonix thermal ionization mass spectrometer (TIMS) accuracy and recovery value). This was found to be approximately 0.05g of sample.
28. Weighing is carried out on the Mettler Toledo AT201 balance in airlock room b13.
29. A 15ml vial was labelled with sample number on both the side and cap.
30. The long and short term balance stability is monitored during all weigh sessions by recording the weight of a 100g weight from the weight box at the beginning and end of each session, ensuring to record the exact weight in the ISOTOPE LAB weighing record.
31. Holding the uncapped vial with balance tweezers, shoot inside the vial using the Zerostat gun from a distance of roughly 3cm by squeezing and releasing the trigger over a period of 5 seconds. This neutralises any static charges.
32. Place vial on a balance using tweezers and tare to zero.
33. Weigh in the required amount of spike; in this case approximately 0.5g for every 2μg of Nd per sample.
34. Next, weigh in sample with spatul9ha.
35. Record sample name, powder weight (g) and spike name and weight (g) in the ISOTOPE LAB weighing record.

36. Remove vial with sample from balance using balance tweezers and add a nominal 2ml of 7M HNO_3 to reduce static build up. Recap the vial.

Dissolution of vials

37. Add 4ml of HF to the uncapped vials, ensuring to wear appropriate HF protection.
38. Heat capped vials on a hotplate at 140^0C overnight in fume cupboard FCAMA022.
39. Allow samples to cool and place on an angle to allow any acid drops to fall to bottom of vial prior to the removal of the cap.
40. Allow vials to evaporate to almost dryness on the same hotplate at 140^0C. This step removies silicon as silicon tetrafluoride (Si_2F_4) Prior to total evaporation add a nominal 2ml of 7M HNO_3, this prevents the Formation of insoluble flurorides which can lead to issues in the fractionation of Sm and Nd and inhomogeneity problems if sample splitting is necessary for ID analysis.
41. Allow to evaporate to complete dryness and then add 4ml of HF and 2ml of 7M HNO_3
42. Recap and heat overnight as outlined in step 2.
43. Similarly, to the first dissolution allow samples to cool the following morning and tap vial gently on its side to collect any acid drops that may be present on cap or side of vials.
44. Uncap vial and evaporate to complete dryness at 140^0C in fume cupboard. To reduce the likelihood of insoluble fluorides forming add a nominal 2ml of HNO_3 prior to sample drying.
45. Allow sample to cool and add 6ml of 6M HCl to solid residue.
46. Cap the vials and heat overnight to allow sample to dissolve.

Centrifuge

47. Uncap the vials and leave on hotplate to evaporate to complete dryness
48. Allow the sample to cool and add 1.5ml of .16M HCl to the vial. Swirl the acid in the vial to allow the sample to dissolve.
49. Rinse the outside and inside of a 2ml centrifuge tube that is stored in 6M HCl with deionised water.
50. Repeat this rinsing a further two times.
51. Transfer dissolved sample into the centrifuge tube, ensuring to close lid tightly.
52. Place into centrifuge in room B14, proceed to centrifuge samples at 13200rpm for 5 minutes.

Columns

FIRST RB SR AND/OR SM ND COLUMN PROCEDURE

Precean

53. Remove columns from reservoir, place in rack and allow acid to drain.
54. Add 10ml 6M HCl single distilled (sd) into columns, allow acid to filter through into waste beaker.
55. Add 5ml of deionised (DI) water into columns, allow water to filter into waste beaker.
56. Add 10ml 6M HCl sd into columns, allow acid to filter through into waste beaker.
57. Add 5ml of deionised (DI) water into columns, allow water to filter into waste beaker.
58. Rinse tip of column with 6M HCl sd.

Load sample – 6M HCl

59. Equilibrate column with 6ml of 2M HCl sd, allow acid to filter into waste beaker.
60. Take centrifuge tube with sample in it and load the top 1ml of the tube into the column using a 1000µg pipette.
61. Add 1ml 2M HCl sd into columns, allow acid to filter through into waste beaker.
62. Add 1ml 2M HCl sd into columns, allow acid to filter through into waste beaker.

No Rb or Sr required

63. Add 8ml 2M HCl sd into columns, allow acid to filter through into waste beaker.
64. Add 4ml 3M HCl sd into columns, allow acid to filter through into waste beaker.

Sm Nd collection

65. Add 1ml 6M HCl sd into columns, allow acid to filter through into waste beaker.
66. Replace waste beaker with a 7ml Teflon vial with sample name and "Sm/Nd" clearly labelled on cap and side of vial.
67. Add 5ml of 6M HCl sd into columns, allow acid to collect into labelled Teflon vial.
68. Cap the vials and put aside for Sm Nd separation column procedure.

Post clean

69. Add 10ml 6M HCl sd to columns, allow to filter into waste beaker.
70. Add 5ml DI H_2O, allow water to filter into waste beaker.
71. Add 10ml 6M HCl sd to columns, allow to filter into waste beaker.
72. Add 5ml DI H_2O, allow water to filter into waste beaker.
73. Rinse lower section of column and return into new 6M acid into cleaned tube in rack. Replace cap.

SM ND COLUMN PROCEDURE

Preclean

74. Remove columns from the reservoir, place in numbered racks and allow the acid to drain
75. Add 10ml of 6M HCl sd into columns, allow acid to filter through into waste beaker
76. Add 5ml of 0.5M HCl sd into columns, allow acid to filter through into waste beaker.
77. Add 10ml of 6M HCl sd into columns, allow acid to filter through into waste beaker.
78. Add 5ml of 0.5M HCl sd into columns, allow acid to filter through into waste beaker.

Load sample – 0.16M HCl sd.

79. Equilibrate the column by transferring 4ml 0.16M HCl into columns.
80. Load 0.5ml of sample in 0.16M HCl from centrifuge tubes into columns. Ensuring to avoid any solid material.
81. Add 1ml of 0.16M HCl sd into columns, allow to drip into waste beaker.
82. Add 1ml of 0.16M HCl sd into columns, allow to drip into waste beaker.
83. Add 13ml of 0.16M HCl sd into columns.

Collecting Nd – 0.27m HCl sd.

84. Add 0.5ml of 0.27M HCl sd into columns, allow to drip into waste beaker.
85. Replace waste beaker with a clean, labelled 7ml Teflon vial
86. Add 3.5ml of 0.27M HCl sd into columns, allow to drip into Nd labelled vial.
87. Add 1 drop of phosophorous acid (H_3PO_4) to vial containing Nd and place on hot plate at 140^0C. Once evaporated, cap the vial and allow to cool.
88. Place waste beaker back under columns.
89. Add 2.5ml of 0.27M HCl sd into columns and allow acid to drip through into waste beaker.

Collecting Sm – 0.5M HCl sd.

90. Take originl Sm Nd vials that were used in the first columns and clean them by heating the vials on a hotplace with 6M HCl allowing them to reflux for an hour. Replace the waste ebaker with newly cleaned vial.
91. Add 3ml of 0.5M HCl sd to the columns and collect the acid in vial.
92. Add 1 drop of phosophorous acid (H_3PO_4) to vial containing Sm and place on hot plate at 140^0C. Once evaporated, cap the vial and allow to cool.

Post Clean

93. Add 10ml of 6M HCl single distilled (sd) into columns, allow acid to filter through into waste beaker
94. Add 5ml of 0.5M HCl sd into columns, allow acid to filter through into waste beaker.
95. Add 10ml of 6M HCl sd into columns, allow acid to filter through into waste beaker.
96. Add 5ml of 0.5M HCl sd into columns, allow acid to filter through into waste beaker.
97. Add 1-2ml 0.5M HCl, rinse column stem, replace column into its numbered tube of 0.5M HCl.